UNIVERSITY OF OKLAHOMA

GRADUATE COLLEGE

HIGH RESOLUTION SEQUENCE STRATIGRAPHY AND SEISMIC STRATIGRAPHY OF THE LEONARDIAN BONE SPRING FORMATION DELAWARE BASIN, SOUTHEAST NEW MEXICO

A THESIS

SUBMITTED TO THE GRADUATE FACULTY

in partial fulfillment of the requirements for the

Degree of

MASTER OF SCIENCE

By

TYLER BICKLEY
Norman, Oklahoma
2019

HIGH RESOLUTION SEQUENCE STRATIGRAPHY AND SEISMIC STRATIGRAPHY OF THE LEONARDIAN BONE SPRING FORMATION DELAWARE BASIN, SOUTHEAST NEW MEXICO

A THESIS APPROVED FOR THE
SCHOOL OF GEOSCIENCES

BY

Dr. John D. Pigott, Chair

Dr. Heather Bedle

Dr. Kulwadee L. Pigott

For my family and friends who support me in all of life's pursuits.

Acknowledgements

First and foremost, I would like to thank my parents Jay and Karla Bickley and my brother Justin Bickley for their love and support over the years. They have always been my rock and have supported me in all of my undertakings. My amazing girlfriend and other half Carsyn Cunningham has supported me unwaveringly and kept me sane throughout this entire process. I can't thank her enough for the time and effort she has put into helping me and without her this process would have been impossible. She makes me a better person and I cannot wait to continue to share our lives together. I'd also like to thank all of the other friends and family members who have been there for me through this process.

I cannot thank Dr. Pigott enough for everything he has done for me. Thank you for putting up with my work schedule over the years and for continuing to make sure I had everything I needed to be successful. You have made me a better geologist and a better person and there is no doubt that your impact will help me to further my career. Additionally, a big thank you to the other members of my committee Dr. Bedle and Dr. Kulwadee Pigott. Your technical insights and support have helped greatly throughout this process.

Finally, thank you to the members of the McCoy research group for all of their technical insights. The discussion around the ideas in this thesis helped to bring all of the ideas presented here to maturity. I must make a special shout out to Rui Zhai. Without his help with the seismic data much of this thesis would have been impossible. Thank you also to Devon energy for the access to the data.

Table of Contents

List of Figures

Abstract

A high-resolution sequence stratigraphic investigation integrating 3D seismic with petrophysics of the Leonardian Bone Spring Formation, Northern Delaware Basin, New Mexico reveals the sedimentologic process-response interplay between allocyclic (relative sea level) and autocyclic (depositionally controlled) changes. The Bone Spring formation has a complex deep water, mass transport style of deposition in which unconventional reservoir potential varies greatly both vertically and laterally over relatively short distances. Data for analysis include a proprietary 215 square mile 3D seismic survey, 138 digital well logs, and two cores.

Fundamentally, this study is based upon the integration of three main pillars: high-resolution sequence stratigraphy using a lithology corrected, adapted Galloway approach, facies analysis using high resolution core photos, and seismic stratigraphy using the methods defined by Vail. Based on these three pillars, sixteen fourth order sequences are identified and mapped across the study area and reveal substantial changes in Bone Spring deposition and reservoir quality. While third order cycles in the Bone Spring express reciprocal sedimentation with dominantly carbonate deposition during highstand intervals and dominantly clastic deposition during lowstand intervals, higher frequency, fourth order cycles also have a significant impact on sedimentation and reservoir quality. Within the 2nd Bone Spring Sand (the focus of this study), carbonate intervals with reduced porosity and reservoir quality are shown to correlate with fourth order lowstands where incision and erosion of the carbonate shelf moved more carbonate content into the basin. Overlying the adapted Galloway motifs upon the seismic stratigraphic models provide additional insight into the lateral continuity of these low-quality reservoir intervals. In the era of drilling extended lateral wells, it is essential to

know the lateral extents of the highest quality reservoir. The detailed stratigraphic models created in this study will have far reaching implications not only for well planning and execution in the immediate study area, but also for reservoir facies prediction within the Bone Spring Formation across the Delaware Basin

Chapter 1: Introduction

The Permian Basin, of West Texas and Southeast New Mexico, is a vast oil and gas producing region that has been producing from conventional reservoirs for nearly a century (Keller et al., 1980). Consequently, the geology of the Permian basin has been studied for over 100 years with almost a library of contributions, resting largely upon the pioneering work of P. B. King (1948). Indeed, the volume of research has led many to postulate that the outcrops surrounding the Permian Basin are some of the best understood depositional systems in the world (Kocurek and Kirkland, 1998). However, with respect to petroleum exploration, many of these studies focus on the more proximal depositional systems because the first production from Leonardian units came from up dip conventional reservoirs in sand pinchouts and carbonate flows that developed diagenetic porosity (Hart, 1997). These conventional targets had high porosity and permeability and could flow oil and gas with minimal stimulation while their tighter basinal equivalents were uneconomic to produce until technological advancements in drilling and completion came around decades later. Therefore, while the proximal equivalents of many of the basinal sediments being drilled today are very well understood, the depositional processes that led to the basinal sediments themselves are much more poorly understood and can still be refined.

The Delaware Basin, a sub basin of the greater Permian Basin, has seen a resurgence in recent years with the development of horizontal drilling and fracturing technologies that allow for production from unconventional resources. These technologies caused a shift in focus from up dip conventional targets to basinal unconventional targets. In fact, the combined Wolfcamp and Bone Spring formations in the Delaware Basin surpassed the Bakken to become the largest unconventional oil field

in the U.S. in 2017 (EIA, 2017). In 2018 the U.S. Geologic Survey (USGS) estimated the total reserves of the Delaware Basin at over 46.3 billion barrels of oil, 281 trillion cubic feet of gas, and 20 billion barrels of natural gas liquids in the Wolfcamp and Bone Spring formations alone. This analysis represents one of the largest continuous oil assessments ever conducted by the USGS (USGS, 2018). By providing additional insight to the impact of depositional systems upon reservoir quality, this investigation will have immediate relevance to hydrocarbon exploration strategies.

Owing to its reciprocal sedimentation, the Bone Spring is a complex formation made up of multiple members of alternating siliciclastic and carbonate rich deposition during times of alternating sea levels (Crosby, 2015). The Bone Spring formation contains conventional targets, unconventional targets, and the potential for self-sourcing hydrocarbon generation. Such a complex petroleum system must be understood at its most fundamental depositional and stratigraphic level before being expanded into more complex analysis. Previous work has been conducted by Charlie Crosby (2015) in this area to define the sequence stratigraphy of the Bone Spring Formation and relate it to reservoir quality using multiple cores. This study will extend the boundaries of his work while also integrating the petrophysical and core interpretations to a 3D seismic volume.

Specifically, this investigation attempts to use high quality seismic logs, core data, and optimally acquired and processed seismic data in order to delineate the complex depositional processes and responses on a high resolution stratigraphic scale that led to the Bone Spring's geometries observed in the subsurface in the Northern Delaware Basin and associated reservoir seal qualities. Such a depositional understanding is essential for defining the extents, quality, and thickness of reservoir targets, organic rich source rocks, seals, and frac barriers within the Bone Spring.

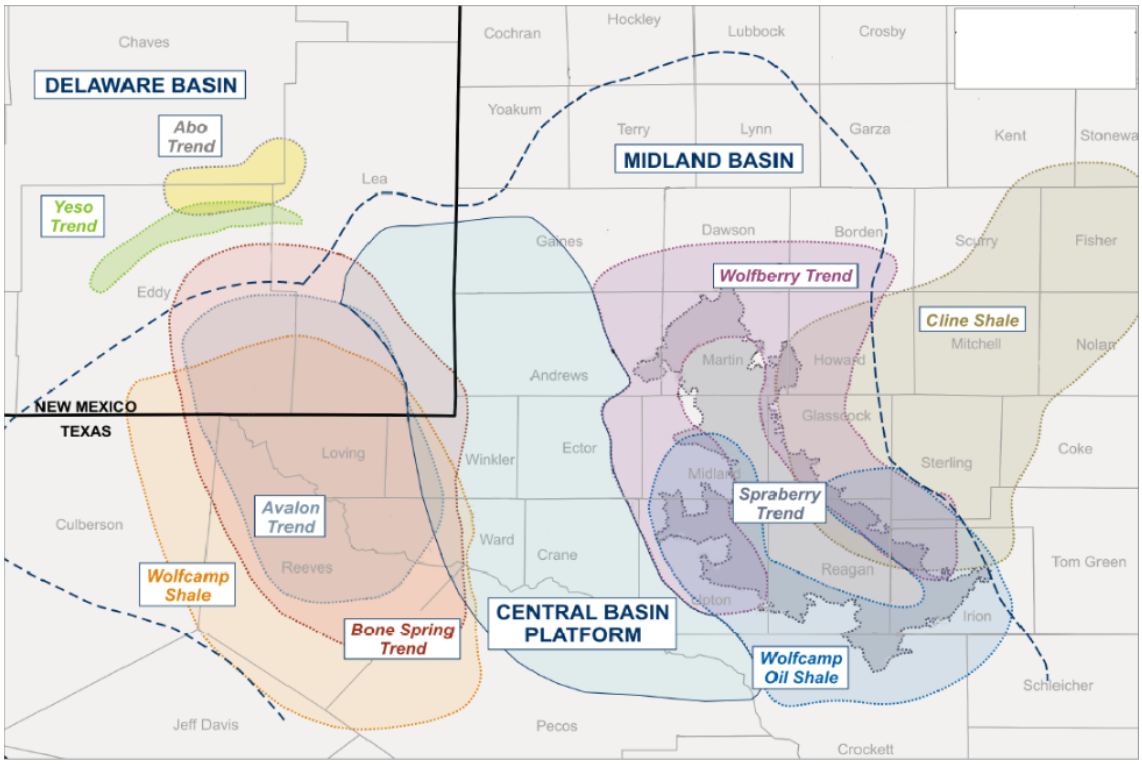

Figure 1: Overview of play trends in the Permian Basin. Highlights the overlapping Bone Spring, Wolfcamp, and Avalon trends in the Delaware Basin.

Study Location

Figure 2 is an annotated figure from Ruppel and Ward (2013) showing the approximate location of the study area which lies within the Northern Delaware Basin. All the data used in this study were provided by Devon Energy. Because the study is located in an active drilling area with current drilling projects being executed or planned for Bone Spring intervals, exact locations of the 3D survey and included well logs will not be provided. All of the data used in this study lies within the limits of the provided 3D survey allowing for direct correlation to the seismic using synthetic well ties. The survey covers an area of approximately 215 square miles with a N-S length of ~18 miles and an E-W width of ~16 miles. Based on industry analysis by Scotiabank, the study

area is proximal to the Northern Delaware Basin Core Bone Spring area (Bachmann et al., 2014).

Geologically, the survey is located along the northern portion of the Delaware Basin and thus depositionally lies at the slope to basin transition of the Delaware Basin during the time of Bone Spring deposition. The slope to basin transition is a preferred location for a detailed seismic stratigraphic study because it best displays multiple potential energy surfaces along depositional facies tracts (Pigott, 2016). More basinward facies typically lack the terminations necessary to define sequence boundaries within the system. The survey also sits in a unique position at a curve in the shoreline of the basin meaning that it is proximal to sediment sources to the west and north.

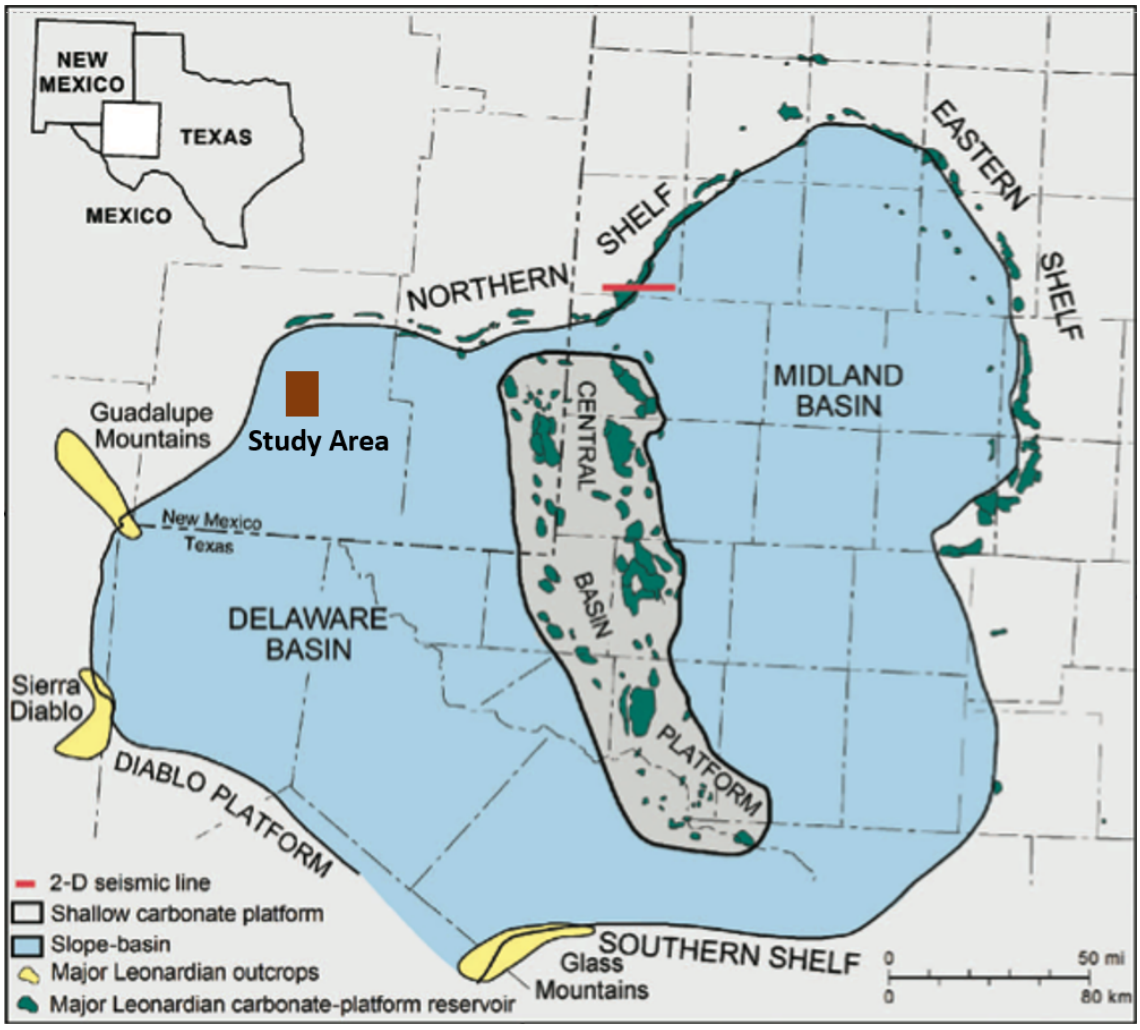

Figure 2: Generalized map of the Delaware and Midland Basins separated by the Central Basin Platform. The approximate study area is highlighted in red. The study area sits on the Bone Spring slope to basin transition of the Delaware Basin. Modified from Ruppel and Ward, 2013

Previous Work

While many studies in the past focused on outcrop data and shallow well logs, in the past few decades more studies have begun to emerge on the basinal facies of the Bone Spring formation. These previous studies have laid the foundation for the understanding the structural and depositional processes that controlled sedimentation in the Delaware Basin and without that insight, this study would be impossible. The previous work will not be detailed here but instead will be discussed when summarizing the Delaware Basin's structural and depositional history.

However, there is one study that is immediately relevant to and offsetting the location of the current study that should be referenced and summarized here: that of Charlie Crosby's thesis titled, "Depositional History and High Resolution Sequence Stratigraphy of the Leonardian Bone Spring Formation, Northern Delaware Basin, Eddy and Lea Counties, New Mexico" which is an important recent study that was done also in the Northern Delaware Basin but to the Northeast of the current study (Crosby, 2015). Using well logs, cores, and chemostratigraphic interpretations, Crosby created a depositional history and sequence stratigraphic framework for the Bone Spring formation in the Northern portion of the Delaware Basin. His conclusions included:

- Events ranging from 1st order stratigraphic cycles down to small sea level changes have direct and critical implications on the depositional history of a basin and therefore the petroleum system elements
- Eight parasequences (i.e. 1st Bone Spring Sand) were distinguished within the four identified 3rd order sequences of the Leonardian

- The primary depositional controls of these units are sea level fluctuations, basin physiography such as reciprocal sedimentation and compensational stacking patterns, and subaqueous erosion of carbonate units
- 3rd order lowstands correlated with siliciclastic deposits while 3rd order highstands correlated to dominantly carbonate deposits
- Within 3rd order sequences, higher cyclicity 4th order sequence stratigraphic cycles were also identified from well logs and core data
- Terrigenous, detrital proxies are concentrated in lowstand intervals while highstands correlate to higher carbonate concentrations
- Times of anoxic basin conditions correlated more with lowstand turbidites than highstand carbonates
- Anoxic events leading to TOC preservation suggest that many reservoirs could be self-sourced

Crosby's work agrees with previous studies conducted in the Bone Spring formation and expands on the overall understanding of the depositional processes that led to the cyclic deposition of the Bone Spring. The quality and proximity of Crosby's work to the current study area make it an ideal launching point for the current study which attempts to expand on Crosby's initial work.

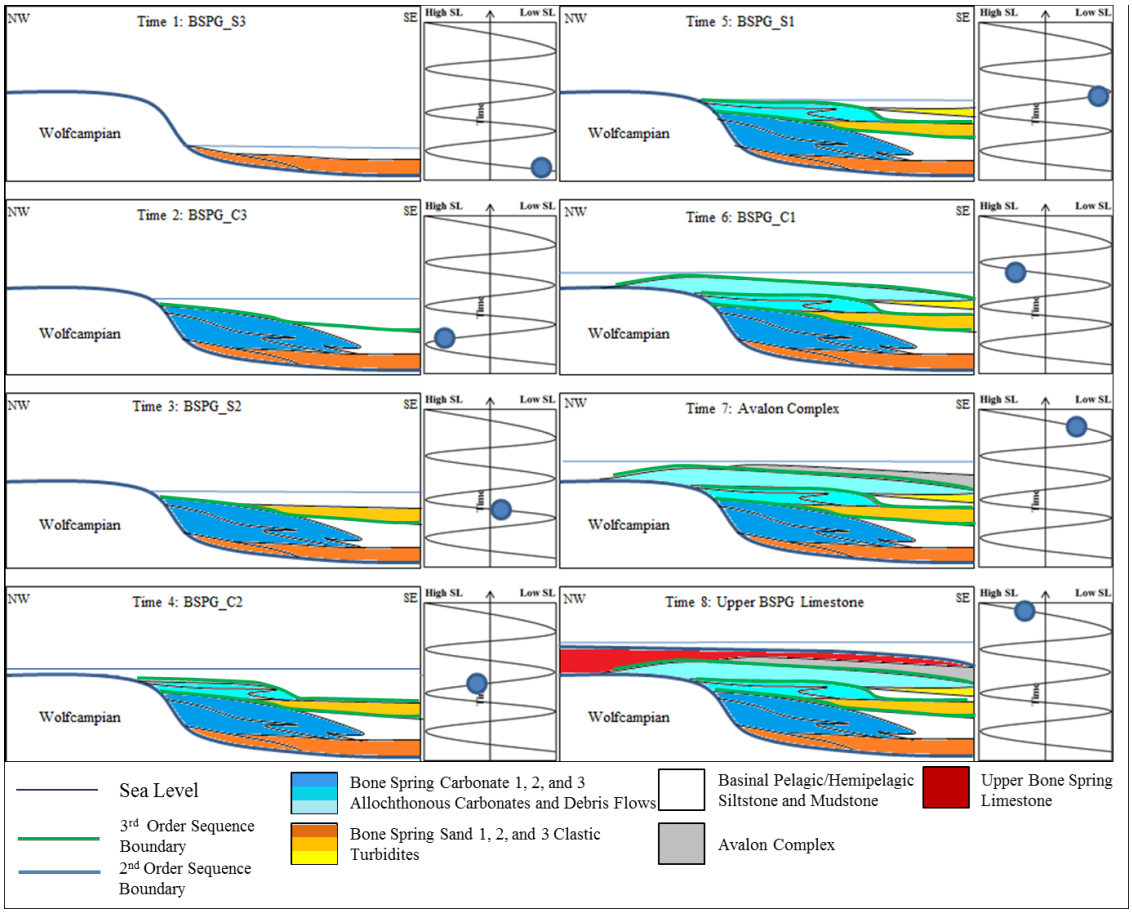

Figure 3: Illustration of the impact of 3rd order sea level fluctuations on Bone Spring deposition (Crosby, 2015). 3rd Order highstands correlate with carbonate intervals while lowstands correlate with siliciclatic intervals.

Objectives

The overall objective of this study is to further define the sequence stratigraphy of the Bone Spring and its complete depositional history. Using well logs and a few cores for facies verification, this study will expand on Crosby's sequence stratigraphic model of the Bone Spring. The proximity of the study area to Crosby's will allow for direct application of Crosby's concepts and having more well logs should help to refine his proposed sequence stratigraphic history. Furthermore, this study will then build a seismic stratigraphic model of the Bone Spring by adapting a Galloway approach to the Vail approach (Pigott and Bradley, 2014). Using synthetic well ties, the well log sequence

stratigraphy can be directly compared with the seismic stratigraphy. With the vertical resolution of well log sequence stratigraphy and the horizontal resolution of seismic stratigraphy, this study hopes to create a more complete and detailed depositional history of the Bone Spring.

The Bone Spring is thousands of feet thick and has a complex depositional history (Crosby, 2015). While this investigation goes into some depth on certain specific intervals within the Bone Spring, the overall focus is on creating a depositional history for the entire Bone Spring interval and therefore has a broad scope. However, enough data have been supplied for this study that it is entirely possible to conduct deeper analyses on the specific formations and unconventional landing zones in the Bone Spring and further refine the stratigraphic impacts on reservoir quality, source quality, and the existence of potential frac barriers. Therefore, a secondary objective is to create a broad stratigraphic depositional model that lends itself to further in-depth studies and lays the groundwork for a Delaware Basin multidisciplinary research group. Much of this work including basin modelling, petroleum generation and migration analysis, decline curve analysis, and statistical review of reservoir quality using well logs and seismic attributes has already begun. However, the focus of this study will remain on crafting a high-level Bone Spring sequence stratigraphic and depositional model.

Chapter 2: Geologic Background

Before embarking on an in-depth study on a small portion of the Delaware Basin it is essential to take a step back and fully understand the geologic development of the Permian basin and the Delaware Basin within it. The Leonardian Bone Spring formation is bounded at its base by Wolfcampian sediments and at the top by the progradation of the Guadalupian Brushy Canyon formation meaning it was deposited over a relatively short period of time when compared to the overall history of the Permian Basin. However, the tectonic and depositional histories of the Permian Basin have direct impacts on the stratigraphy of the Bone Spring formation. Only by understanding the overall basin history and merging it with a detailed understanding of the stratigraphy of the Bone Spring can one hope to form a firm understanding of the petroleum systems present and optimize oil and gas production from the basin.

The Delaware is a north-south elongate basin with an average length of about 200 miles and an average width of about 100 miles (Adams, 1965). The Permian Basin is made up of multiple smaller basins including the Delaware Basin and the Midland Basin. The Delaware and Midland Basins are relatively isolated from each other with the Central Basin Platform creating a divide between the two basins. The Hovey Channel in the southwestern portion of the Delaware basin connected the basin to the Panthalassic Ocean while the Sheffield and San Simon Channels to the east connected the Delaware Basin to the Midland Basin (Figure 4). The bounding features of the Delaware Basin also include the Diablo Platform to the west, the Central Basin Platform to the east, the Northwest Shelf to the north, and the Marathon Ouachita thrust belt to the south (Yang and Dorobek, 1995).

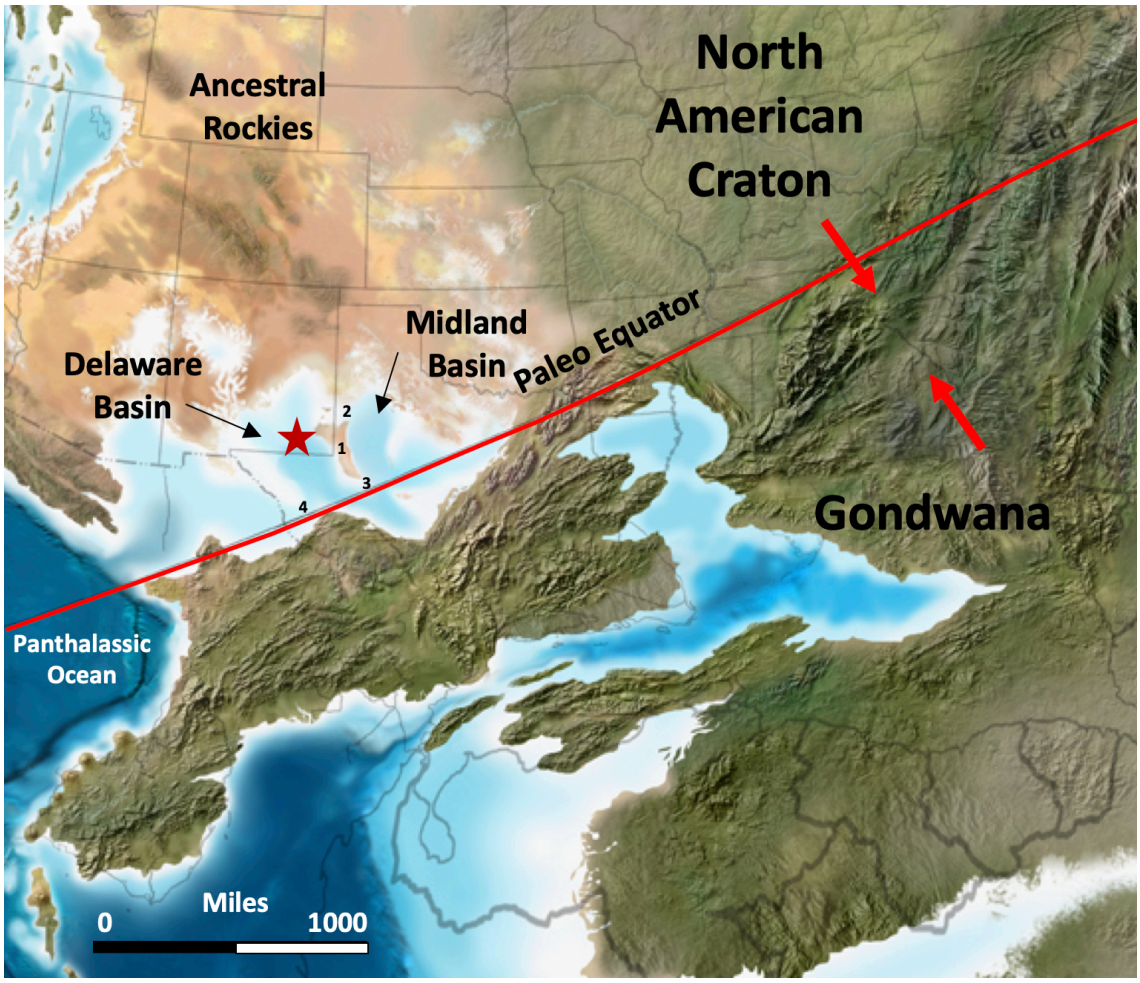

Figure 4: Modified Blakey map during the Leonardian (~282-275 Ma) showing the approximate location of the study area with a red star. Also annotated are the major continents colliding to form Pangea forming the Ouachita Marathon thrust belt. 1 – Central Basin Platform, 2 – San Simon Channel, 3 – Sheffield Channel, 4 – Hovey Channel

Tectonic History

Tectonic events that eventually lead to the formation of the Delaware Basin stretch back all the way to the formation and breaking up of the supercontinent Rodinia (Schumaker, 1992). The Grenville Orogeny associated with the creation of Rodinia and the subsequent breaking up of the supercontinent caused Proterozoic zones of weakness that eventually defined the location of the Central Basin Platform and therefore partially caused the rapid subsidence of the Delaware Basin leading to the thick, rapidly deposited

Permian sediments that are observed today (Schumaker, 1992). The Variscan orogeny, which was part of the formation of Pangea, was responsible for reactivating these existing Proterozoic lines of weakness. This orogeny lead to the creation of the Marathon Ouachita thrust belt which bounds the Delaware Basin to the South and also led to the uplift of the Central Basin Platform which bound the basin to the east (Schumaker, 1992).

From the Pre-Cambrian to the Devonian, the tectonic development of the basin was tied to passive margin tectonism. A peninsular protrusion off the Transcontinental Arch formed a positive relief feature in the area (Adams, 1965). As underlying basement rocks and the mantle cooled, the positive relief feature began to subside forming a shallow negative relief feature along the axis of the later Permian Basin (Keller et al., 1980). This shallow feature had not yet formed into a basin but was rather a coastal plain onto which a shallow ocean transgressed during the early Ordovician (Adams, 1965).

Following the shallow coastal plain phase of development, the area saw the formation of the ancestral Tobosa Basin (Figure 5) during the middle Ordovician which was a broad basin encompassing what would later become the separated Delaware, Midland, and Val Verde Basins (Adams, 1965). The Tobosa Basin was formed due to continued crustal sagging along the aforementioned negative relief feature and was bounded on the west by the Diablo Arch and on the east by the Texas arch that separated the Tobosa Basin from the Ft. Worth Basin (Adams, 1965). Figure 5 shows the outline of the Tobosa Basin, its bounding features, and the relative positions of the Delaware, Midland, and Val Verde basins that would form later due to tectonic forces acting on the Tobosa Basin (Adams, 1965).

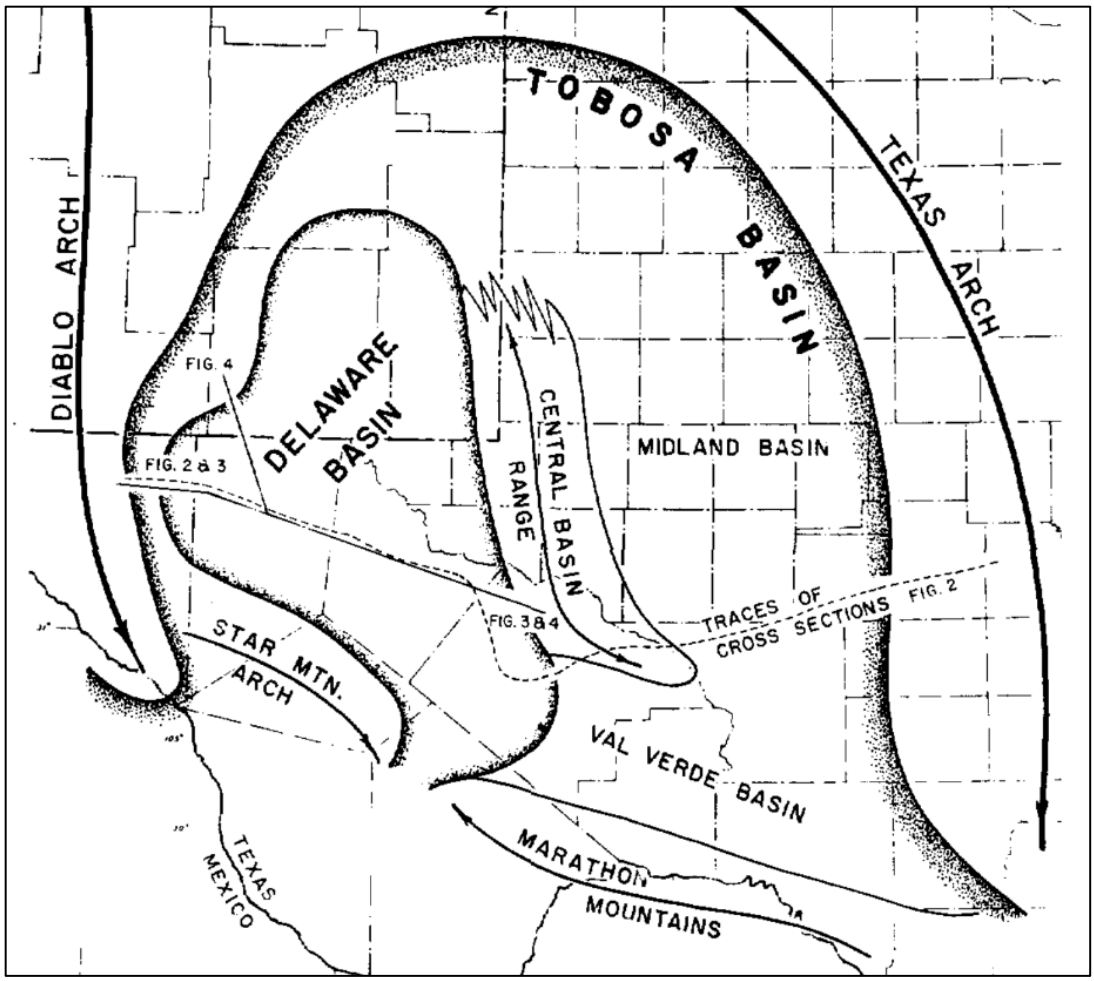

Figure 5: Outline of the Tobosa Basin and its bounding features in relation to the Delaware, Midland, and Val Verde Basins. Proterozoic zones of weakness along the axis of the Tobosa Basin were reactivated by the Variscan Orogeny leading to the uplift of the Central Basin Platform (Adams, 1965).

As the Variscan Orogeny began in the Early to Middle Mississippian, minor uplift began along the Proterozoic zones of weakness that existed at the axis of the Tobosa Basin. The Variscan Orogeny formed the Ouachita Marathon Thrust Belt to the south and created overall compressional forces within the Tobosa Basin. These compressional forces caused movement to occur along steeply dipping faults associated with the Proterozoic zones of weakness (Hills, 1984). Uplift of these fault blocks occurred creating the Central Basin platform and effectively split the Tobosa Basin into the

Delaware and Midland Basins (Yang and Dorobek, 1995). Up until this point in the rock record, the Midland and Delaware basins have continued to share very similar stratigraphic histories. However, with the uplift of the Central Basin platform, the two basin stratigraphic histories began to diverge. While they maintain similarities due to their proximity to each other, increased subduction along the western side of the Central Basin Platform caused the Delaware basin to be deeper and more sediment starved than the adjacent Midland Basin and caused Permian sedimentation to be much more rapid in the Delaware Basin than the Midland Basin and created the unique, thick Permian sequence that is observed in the Delaware Basin today (Adams, 1965).

Studies by Schumaker (1992) and Yang and Dorobek (1995) suggest that the Central Basin Platform is really made up of multiple fault blocks. Schumaker suggests that there are two major blocks, the Fort Stockton and Andector blocks, while Yang and Dorobek split it up into 6 major blocks (Schumaker, 1992; Yang and Dorobek, 1995). They both agree that the blocks show clockwise rotational movement which is supportive of the uplift being caused by the Variscan Orogeny. Figure 6 shows Schumaker's interpretation of the Central Basin Platform and the bounding faults and thrusts associated with its uplift. In addition to splitting the Tobosa Basin into the Midland and Delware Basins, the uplift of the Central Basin Platform was also important in causing the rapid subsidence necessary to make the Delaware Basin such a deep, sediment starved basin. As the fault blocks of the Central Basin Platform were uplifted, the blocks were forced out over the newly formed Delaware Basin (Schumaker, 1992). Flexural loading of the platform (Pigott et al., 2016) onto the Delaware Basin coupled with rapid sediment loading caused subsidence of the basin along the N-S trending faults along the western edge of the Central Basin Platform (Figure 7).

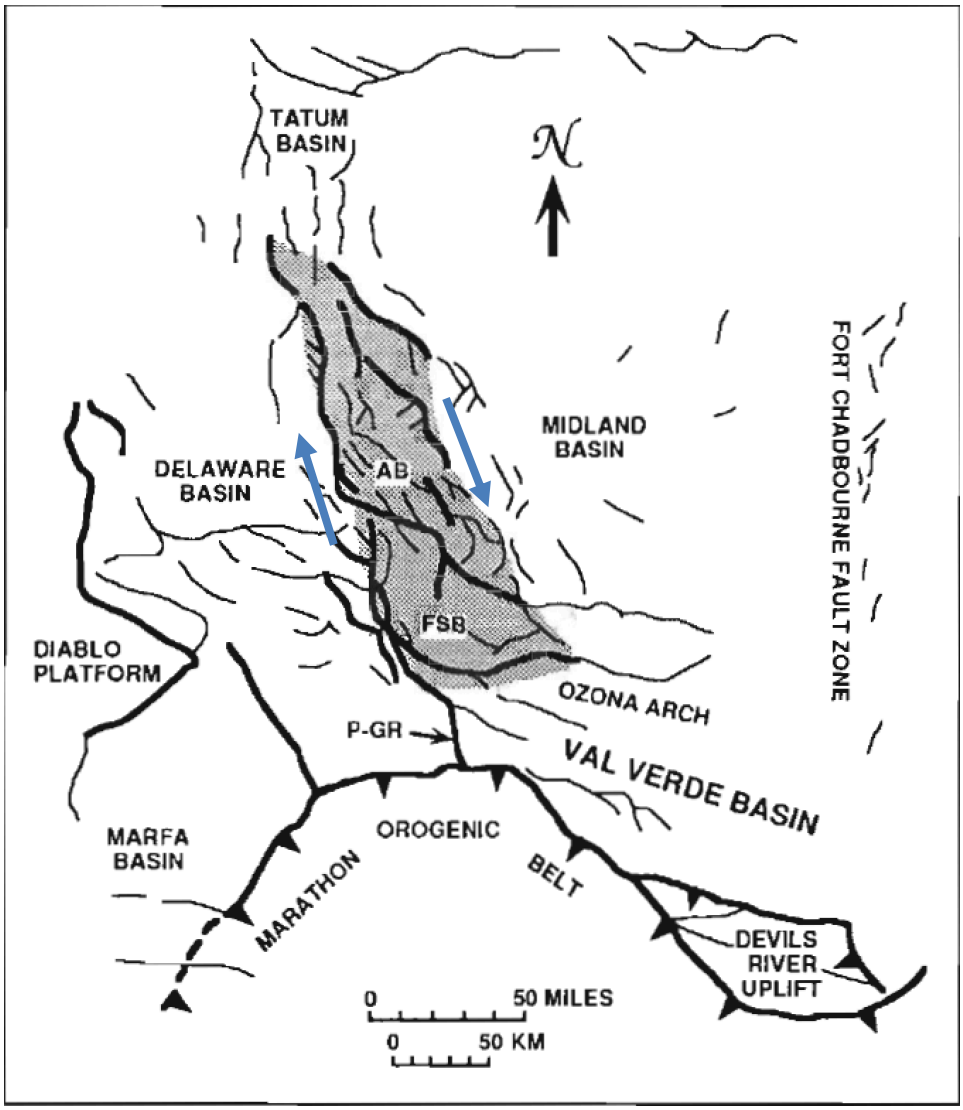

Figure 6: Schumaker's (1992) interpretation of the Central Basin Platform splitting in into two major fault bounded uplift blocks (Ft. Stockton and Andector blocks) showing clockwise rotation. Notice the Marathon Thrust Belt to the south which caused the uplift and the vertical faults along the western side of the platform that accommodated rapid subsidence of the Delaware Basin.

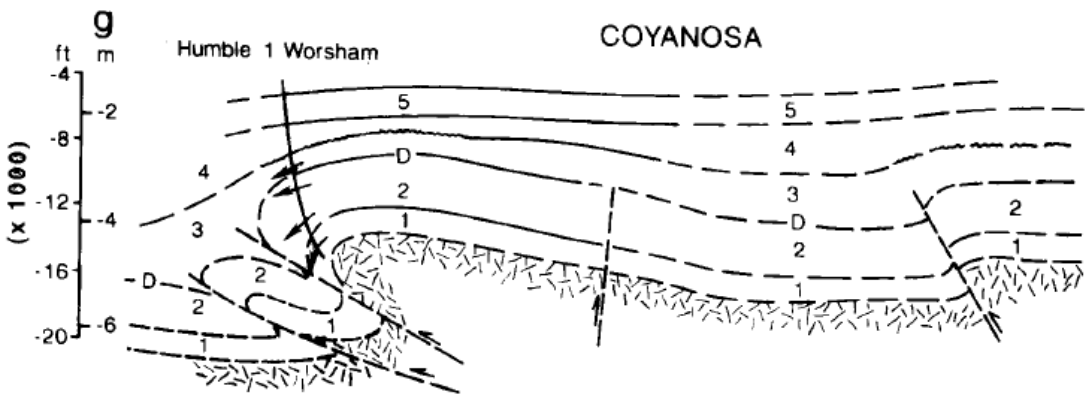

Figure 7: Coyanosa faulted fold interpretation done by Shumaker (1992) showing the thrusting of Central Basin Platform sediments out over the Delaware Basin leading to rapid subsidence along the eastern side of the basin.

By the Permian, tectonics in the Delaware Basin are mostly associated with waning, short pulses of tectonic activity at the tail end of the Variscan Orogeny and rapid subduction due to sediment loading (Adams, 1965). As tectonics associated with the Variscan Orogeny faded, subsidence due to sediment loading took over as the major driver of basin subsidence (Hills, 1984). Subsidence also caused thousands of feet more of uplift on the Central Basin Platform and began to form ridges around the basin (Adams, 1965). Subsidence during the Wolfcampian and Leonardian created a massive relief from shelf to basin floor in the Delaware Basin creating the accommodation space necessary for massive sediment packages to be deposited, including the Bone Spring. In addition, the massive (>1000 ft) relief also lead to a separation between the oxygen rich productive surface waters in the basin and anoxic bottom water (Hill, 1984). Toward the end of the Permian, basin subsidence had slowed and tilting and deepening of the basin eastward was left as the only tectonic activity in the basin (Keller, et al., 1980).

By the end of the Permian (approximately Ochoan time) the Delaware Basin was mostly tectonically stable and was no longer an actively subsiding basin leading to slower

sedimentation rates (Mazzullo, 1995). With the exception of the Laramide Orogeny during the Late Cretaceous which caused further eastward tilting of the basin and the uplift of the Guadalupe Mountains, Delaware Mountains, and Sierra Diablos, the Delaware Basin is relatively similar today to how it would have looked at the end of the Permian (Yang and Dorobek, 1995).

Depositional History

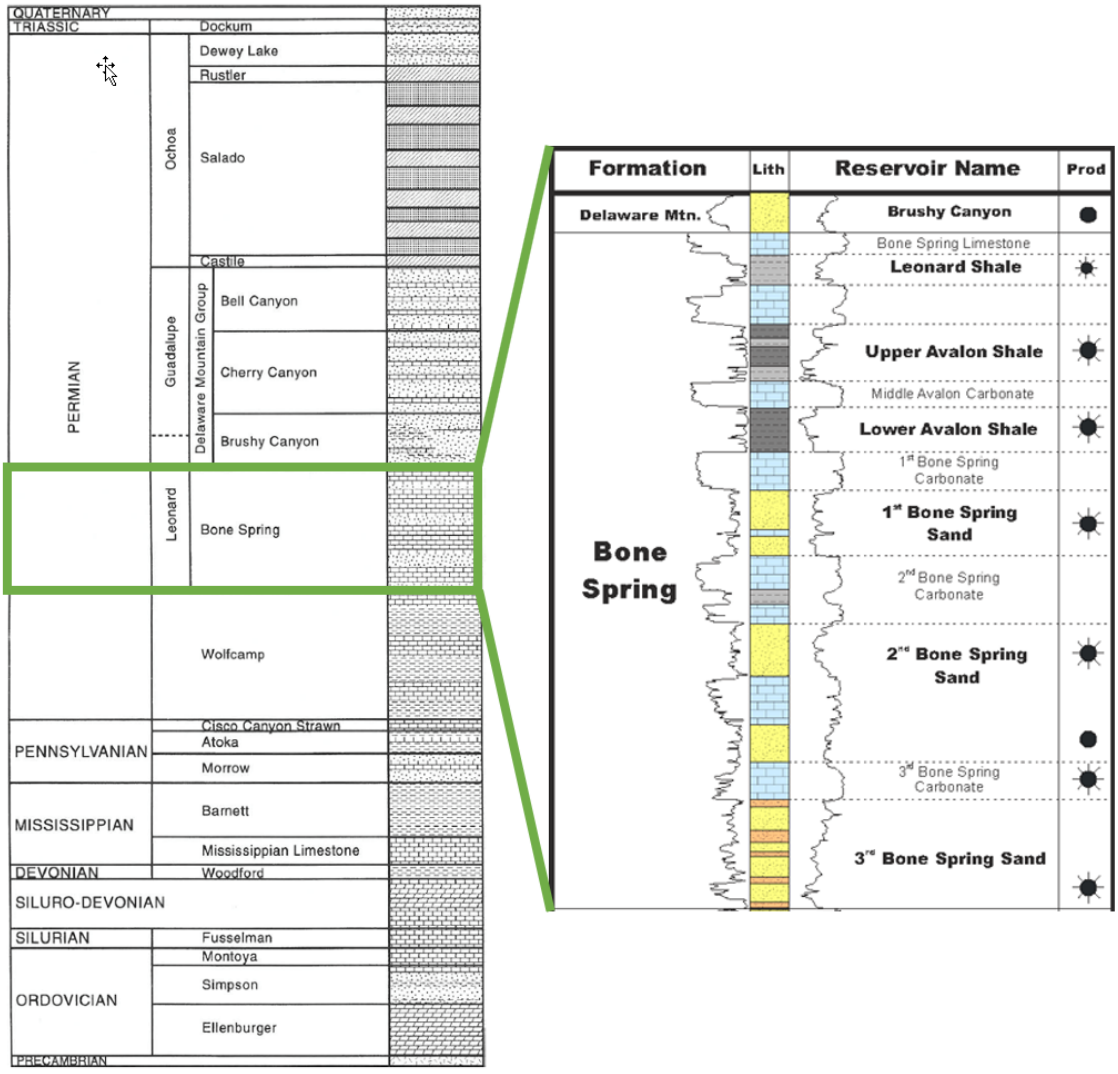

Figure 8: Stratigraphic column of the Delaware Basin modified from Hardage et al., 1998. The Bone Spring formation is broken up into further detail showing the additional formations that exist within the Bone Spring and their variety of lithologies. Oil and gas producing targets are annotated to the right. (Core Laboratory, 2014)

Pre-Bone Spring Deposition

The earliest sediments observed in the Delaware basin began with the Cambrian Sands that were shed off Precambrian uplifts (Hills, 1984). These sands were deposited prior to the formation of the Tobosa Basin into the slight negative depression that had

formed. The slight bathymetric low acted as a shallow coastal plain onto which a shallow sea transgressed during the Ordovician. The shallow, warm sea created an ideal environment for the deposition of the broad, shallow water carbonates of the Ellenberger Formation (Adams, 1965). During the early creation of the Tobosa Basin, the Simpson group of interbedded shales and limestones were deposited in a wedge that thickened to the south and lapped out to the north, east, and west (Hills, 1984).

Carbonate deposition dominated throughout the remainder of the Ordovician, Silurian, and Early Devonian. However, thin siliciclastic beds are also present and are thought to have been deposited at relative lowstands in sea level embedded within a larger highstand (Hills, 1984). Formations during this time included the Thirtyone, Fusselman, and Montoya carbonates. According to Adams (1965), this period of the Tobosa Basin was also marked by the formation of seaward forestepping carbonate shelves.

The late Devonian and Mississippian marked a shift away from the earlier, dominantly carbonate deposition as thick, organic rich, black shales began to be deposited. These shales were deposited over a very large area and are known today as the Woodford and Barnett Shales (Hills, 1984). These world class source rocks and unconventional drilling targets are an important source of hydrocarbons in many of the most prolific U.S. onshore basins. Intermittent carbonate dominated intervals were also deposited during the Mississippian including the broad Mississippi Lime formation (Hills, 1984). The shift from dominantly carbonate deposition to dominantly siliciclastic deposition is marked by the onset of the Marathon-Ouachita Orogeny. These compressive forces caused uplift along Proterozoic lines of weakness including the uplift

of the Central Basin Platform and increased the sourcing of siliciclastic sediments into the basin (Hills, 1984).

By the Pennsylvanian, tectonic activity had picked up substantially in the area. The basin was rapidly subsiding at the time leading to thick, dominantly clastic formations such as the Atoka and Morrow formations (Adams, 1965). Adams (1965) also argues that there was some carbonate shelf development in the Pennsylvanian and these carbonates can be observed in the study area as the Cisco formation that the Wolfcamp was deposited on top of. Formations from the Ordovician to the Pennsylvanian in the Delaware Basin show relatively consistent thickness with a slight thickening of sediments toward the Central Basin Platform likely due to flexural subsidence near the platform during the beginning of the Marathon-Ouachita Orogeny (Yang and Dorobek, 1995).

By the early Wolfcampian, clastic deposition in the form of mass transport deposits shed off of shelves in the northwest, west, and southwest dominated. Carbonate deposition increased throughout Wolfcampian time as clastic influx decreased (Adams, 1965). The increase in carbonate content led to the deposition of carbonate rich debris flows and turbidites that are characteristic of the Wolfcamp formation. These carbonate rich debris flows were separated by periods of relative quiescence and the deposition of pelagic, organic rich mudstones that draped the former debris flows (Silver and Todd, 1969). Because of its high organic content, the Wolfcamp has become a prolific unconventional target over the past decade.

The first shelf carbonate buildups in the Delaware Basin occurred during the Wolfcamp (Hills, 1984). These buildups are characterized by isolated mounds of skeletal hash that also contain shale beds (Silver and Todd, 1969). However, according to Hills

(1984) these carbonate buildups were not developed enough for complete restriction of the basin though they probably led to some restriction and therefore would have helped to preserve organic material. Adams (1965) argues that waters were very nutrient rich in the Wolfcampian because the water column was constantly reworked by debris flows and mass transport deposits. The Wolfcampian was therefore a time of extensive organic material preservation as is made obvious by the prolific well results produced in the Wolfcamp formation in just the last few years.

Figure 9: Summary of deposition prior to the Bone Spring in the Delaware Basin with formation locations on the stratigraphic column. Modified from Hardage et al., 1998.

Bone Spring Deposition

The Bone Spring formation was deposited during the Leonardian which occurred during the Early to Middle Permian and the basinal sediments are interpreted as being an amalgamation of deep-water sediment gravity flows largely sourced from the Northwest Shelf. The duration of deposition of the Bone Spring continues to be refined but recent work has shown that it was likely deposited between ~282.5 – 272.3 Ma, or a duration of approximately ten million years (Henderson et al. 2012).

Generally, the Bone Spring is split up into approximately six stratigraphic units that alternate between carbonate and siliciclastic dominated depositional systems. This sedimentation pattern is tied to relative sea level changes with carbonates being deposited at relative highstands and siliciclastics being deposited at relative lowstands (Montgomery, 1998; Crosby, 2015). The average thickness of the Bone Spring varies between ~3000 – 4500 feet (Hart, 1997) and the six stratigraphic units that compose it are generally split into three major groups namely the 1st, 2nd, and 3rd Bone Spring intervals with the 1st being the youngest and 3rd being the oldest (Bachman et al., 2014).

During Bone Spring deposition, reef buildups on the shelf expanded and the basin became partially restricted. Partial restriction led to anoxic bottom waters while the shallow waters remained nutrient rich and productive because of reworking of the water column and movement of surface waters through the San Simon, Hovey, and Sheffield channels (Hills, 1984; Crosby, 2015). Figure 4 shows the locations of these channels as they relate to the Delaware Basin. This combination of productive surface waters and anoxic bottom waters led to high TOC preservation within the Bone Spring like the underlying Wolfcamp formation. High TOC preservation led to self-sourcing of

hydrocarbons within the Bone Spring and helped to make it the prolific, stacked pay interval that it is today (Hills, 1984).

That the Bone Spring is a massive (3000 – 4500') column of sediment that was deposited over a relatively short ten million years has been attributed to rapid subsidence of the basin during the Leonardian from both sediment loading and tectonic activity associated with the uplift of the Central Basin Platform (Montgomery, 1998). Active uplift of the platform also implies that the basin had at least a small amount of tectonic activity during the deposition of the Bone Spring (Hart, 1998). Given that the Bone Spring is an amalgamation of deep-water sediment flows, it is not out of the question to postulate that some of these flows could have been triggered by tectonic activity in the area. There is one major fault zone, oriented N-S that runs through the study area that looks to have been active during early Bone Spring deposition. The inherited topography from this structure may have influenced the direction and ponding of flows within the basin and early movement along that fault could have potentially triggered debris flows.

It has been observed that inherited topography from the more tectonically active Pennsylvanian and Wolfcamp time had a significant impact on the deep water flows of the Bone Spring (Hart, 1998). Hart (1998) observed that inherited topography, specifically paleo bathymetric lows, acted as conduits for the deep-water flows moving across the shelf. Relative lows on the basin floor created more accommodation space for the Bone Spring and created sediment traps leading to thickness trends that correlate with inherited topography and compensational stacking patterns.

Rimmed shelf carbonates continued to develop during Bone Spring deposition (Silver and Todd, 1969). Silver and Todd (1969) contend that these prograding carbonate reefs were made possible by the inherited topography from shelf and slope carbonates

that were deposited during Wolfcampian time. On the Northern Shelf of the Delaware Basin these reefs are not thought to have acted as major barriers which allowed for the creation and preservation of channels and incised valleys that acted as highways for the transport of siliciclastic sediments out into the basin (Adams, 1965). It has also been argued that these channels and incised valleys could have preferentially formed in the groves of carbonate spur and groove topography that developed on the shelf (Crosby, 2015).

The major formations of the Bone Spring (Figure 20) in order from bottom to top or oldest to youngest are the 3rd Bone Spring Sand, 3rd Bone Spring Carbonate, 2nd Bone Spring Sand, 2nd Bone Spring Carbonate, 1st Bone Spring Sand, Lower 1st Bone Spring Carbonate, Avalon Sand/Shale, and the Upper 1st Bone Spring Carbonate (Crosby, 2015). These alternating lithologies have been described as a reciprocal sedimentation model where variations in relative sea level control the lithology of deposition. The reciprocal sedimentation model leads to the widely accepted theory that carbonate deposition in the Bone Spring occurred at relative highstand and sand deposition occurred at relative lowstand. (Hart, 1998). During relative highstands, subaqueous erosion of the carbonate shelf triggered carbonate debris flows that transported reworked carbonate sediments into the basin. At relative lowstands, a classic channel/turbidite system is observed with siliciclastic sediments moving into the basin through channels and incised valleys that pass through the established shelf reefs (Montgomery, 1998). Studies tend to agree that the slope to basin floor transition zone of the Bone Spring is dominated by four major facies: meggabreccias (debris flows), allochthonous packstones, fine to very fine-grained sandstone turbidites, and dark laminated mudstones (Saller et al., 1989).

Figure 10 below shows a one-dimensional basin model created for a well within the study area to verify subsidence history and determine thermal maturity windows for hydrocarbon generation. For the model, depths, thicknesses, porosity, TOC, and temperature were all determined from logs or core data when available. Facies, organofacies, and paleobathymetry were all estimated based on the inferred depositional environment. A temperature log was used to calculate a current heat flow of 1.1 HFU which agrees with regional heat flow maps. The model shows the subsidence profile for this portion of the Delaware Basin highlighting the change from slow subsidence of the Tobosa Basin to the rapid subsidence that occurred during the Permian. Additionally, maturity windows are highlighted in yellow, green, and red highlighting early mature, mid mature, and late mature windows respectively. The entire Bone Spring is shown to lie within the oil maturity windows suggesting that some of the hydrocarbons within the Bone Spring could have been self-sourced because of the high preserved TOC content that is observed. However, other organic carbon rich formations like the Wolfcamp, Barnett, and Woodford shales are in the late maturity window suggesting that most of the gas produced in the region is migrated up from those formations. Early oil generation from these formations could have also migrated upwards and been trapped within the Bone Spring.

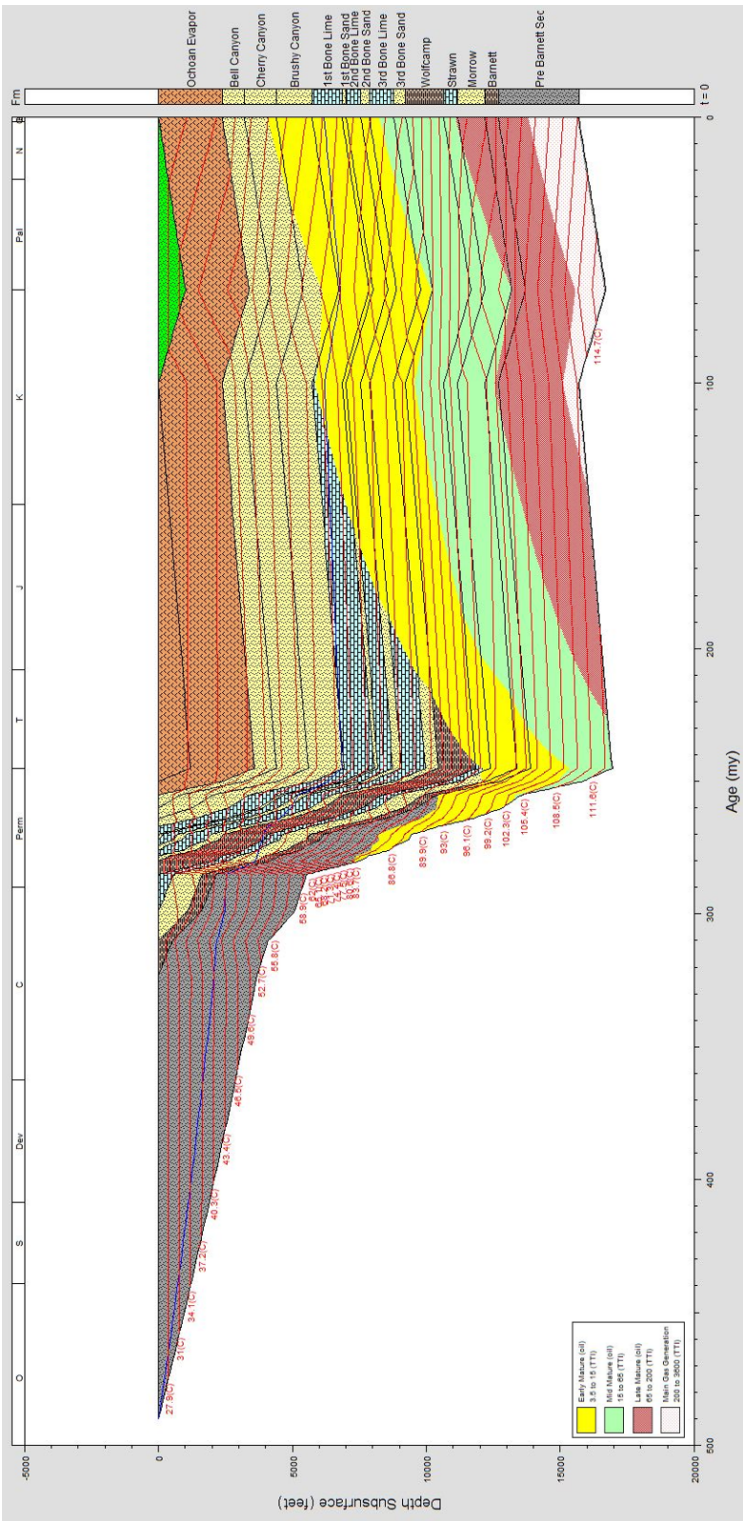

Figure 10: One dimensional basin model showing the study area's subsidence profile highlighting the rapid subsidence occurring during the Permian. The entire Bone Spring is in the oil maturity window and could be self-sourcing.

Figure 11: Summary of Wolfcamp and Bone Spring deposition and their position in the stratigraphic column. Modified from Hardage et al, 1998, and Core Laboratory, 2014.

Post-Bone Spring Deposition

Deposition during the Guadalupian immediately following the deposition of the Bone Spring consists of the Brushy Canyon, Cherry Canyon, and Bell Canyon formations (Silver and Todd, 1969). These formations mark a shift in the basin away from the cyclic, reciprocal carbonate and siliciclastic deposition of the Bone Spring to a much more siliciclastic dominant system (Ross and Ross, 1995). Carbonate development during this time is much more confined to the shelf margin with more reef development during this time than at any other time during the Permian (Adams, 1965). Eventually, this reef development completely restricted the basin which marks the end of the Guadalupian series (Adams, 1965).

By Ochoa time the Delaware Basin had transitioned to dominantly evaporitic deposition (Adams, 1965). These evaporite formations are the Rustler, Salado, and Castile formations and they act as a widespread seal over the Delaware Basin leading to extensive trapping of hydrocarbons over time. They also acted as the top seal for many shallow conventional targets.

Following the Ochoa, sedimentation in the Delaware Basin is largely nonexistent. Terrestrial red beds prograded into the basin at the very end of the Permian and then there was an extended depositional hiatus (Hills, 1984). Small pulses of sedimentation occurred during the Late Triassic, depositing thin red beds (Keller et al., 1980). The rest of the basin's history is marked by erosion of Permian sediments and deposition of Pliocene-Pleistocene alluvium (Hills, 1984).

Figure 12: Summary of post Bone Spring deposition. Modified from Hardage et al., 1998.

Chapter 3: Stratigraphy Introduction

Given that this study will combine elements of both well log sequence stratigraphy and seismic stratigraphy, it is essential to introduce the concepts that will be discussed and the assumptions that are made. Different stratigraphic models define terms slightly differently, so it is important to have a unified definition before applying concepts from different authors.

Sequence stratigraphy attempts to explain the many processes that impact sedimentation such as relative sea level fluctuations, tectonic subsidence, and sedimentation rate by tracking regionally correlatable time surfaces or unconformities, namely sequence boundaries and maximum flooding surfaces, through the rock record (Slatt, 2006). These surfaces split the sedimentary column into packages called parasequences and sequences which relate to the environment that they were deposited in (Slatt, 2006). Correlation of these surfaces and identification of the sedimentary packages that they bound can then lead to more accurate depositional interpretations and better lateral prediction of facies (Slatt, 2006).

Below are definitions of some key stratigraphic terms as they will be used in this study (Crosby, 2015; Catuneanu et al., 2011; McCullough, 2014; Zhou, 2014):

- Parasequence – A genetically related, conformable succession of beds or bedsets bounded by sub-regional correlative surfaces
- Sequence – A succession of genetically related strata during a full cycle of change in accommodation or sediment supply bounded by sequence boundaries
- Sequence Boundary – A regional surface that denotes the transition from one sequence to another. Vail and Galloway define sequence boundaries

differently based on what is easily correlatable on seismic or well logs respectively. This study attempts to compare well log and seismic stratigraphy and it is therefore essential to use a common definition of the sequence boundary. This investigation adopts the Vail sequence boundary which places sequence boundaries on the top of highstand systems tracts (Vail, 1987; Galloway, 1989).

- Maximum Flooding Surface – Interpretation of highest relative sea level. Marked by widespread silt/shale deposition in clastic sediments and can also be marked by blocky carbonate deposition in carbonates (May, 2018).
- Lowstand Systems Tract (LST) – A systems tract deposited at a relative lowstand in sea level usually associated with increased process energy and progradation of coarser grained sediments into the basin. In the Bone Spring, 3rd order LSTs correlate with the dominantly siliciclastic 1st, 2nd, and 3rd Bone Spring Sands as well as the Avalon Sand/Shale.
- Highstand Systems Tract (HST) – A systems tract associated with a relative highstand in sea level usually marked by progradation onto the maximum flooding surface. The HST is capped by the Vail sequence boundary (Vail, 1987). In the Bone Spring, HSTs are associated with the dominantly carbonate deposition of the 1st, 2nd, and 3rd Bone Spring carbonates.
- Transgressive Systems Tract (TST) – Sediments deposited during the onset of sea level rise usually following an LST. The TST is then caped by the maximum flooding surface.

- Falling Stage Systems Tract (FSST or RST) – Sediments associated with the onset of a drop in sea level deposited on top of the HST. In the Bone Spring this is associated with incision and erosion and the beginning of siliciclastic sediments being transported into the basin. At a higher order within relative LSTs, FSSTs can also be associated with carbonate erosion and slumping moving more carbonate sediment into the basin (Li, 2015; Pigott and Bradley, 2014).

Slatt (2006, 2013) visualizes these terms over one full cycle of sea level change. Figure 13 lays out this visual representation of the different systems tracts and where they fall on the relative sea level curve. In a mixed carbonate/siliciclastic basin like the Delaware Basin, eustatic and relative sea level changes seem to have a significant impact on the makeup of sediments and depositional processes occurring within the Bone Spring. It is important to note that other factors such as subsidence, tectonics, climate, depositional process energy, and basin paleo bathymetry also impact the deposition of sediments. However, with all these controls in mind, it is possible to map out high order changes in sea level within the Bone Spring which seem to have a very strong impact on reservoir and source quality in the formation.

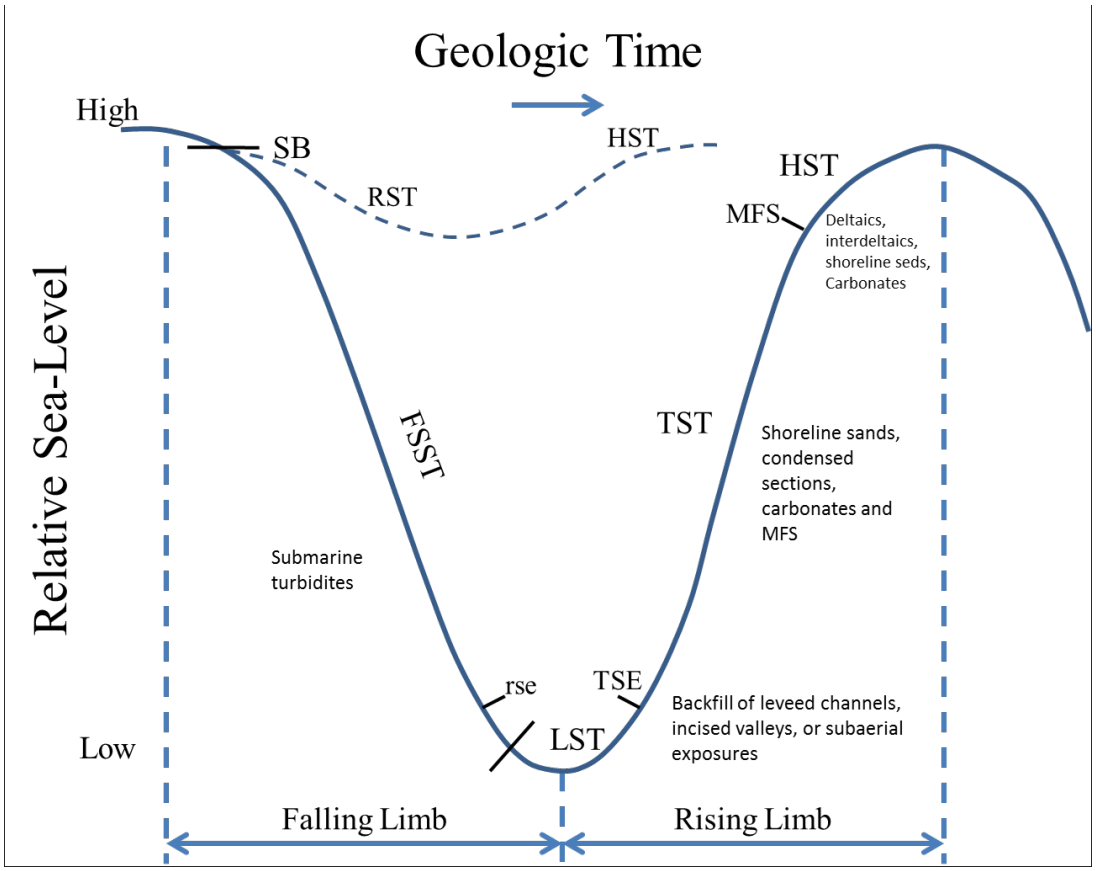

Figure 13: Model of one full relative sea level cycle highlighting the positions of important sequence stratigraphic systems tracts and markers within the falling limb and rising limb of sea level change (Slatt, 2006; Slatt, 2013; Crosby, 2015).

Reciprocal Sedimentation

Reciprocal sedimentation is based on the theory that mixed carbonate and siliciclastic depositional environments alternate over time (Catuneanu et al., 2009). In the Bone Spring, this reciprocal sedimentation is marked by carbonate fan deposition during highstand systems tracts and classic turbidite sand deposition during lowstand systems tracts (Mullins and Cook, 1986). Carbonate flows are deposited in a carbonate apron according to Mullins and Cook (1986). The carbonate flows in the study area are made up of mud supported debris flows and allochthonous packstones and are therefore interpreted as being deposited on the inner apron of these carbonate fans. The deposition

of carbonate fan aprons is interrupted during relative lowstands because the drop in sea level decreases carbonate production and siliciclastic input increases. Classic channel and turbidite sands incise valleys into the established carbonate shelf allowing for transport of siliciclastic sediments out into the basin. In the study area, siliciclastic sediments are made up of fine grained to silt sized sand and show Bouma sequence patterns (Slatt, 2006). The reciprocal sedimentation model for the Bone Spring is shown in Figure 14.

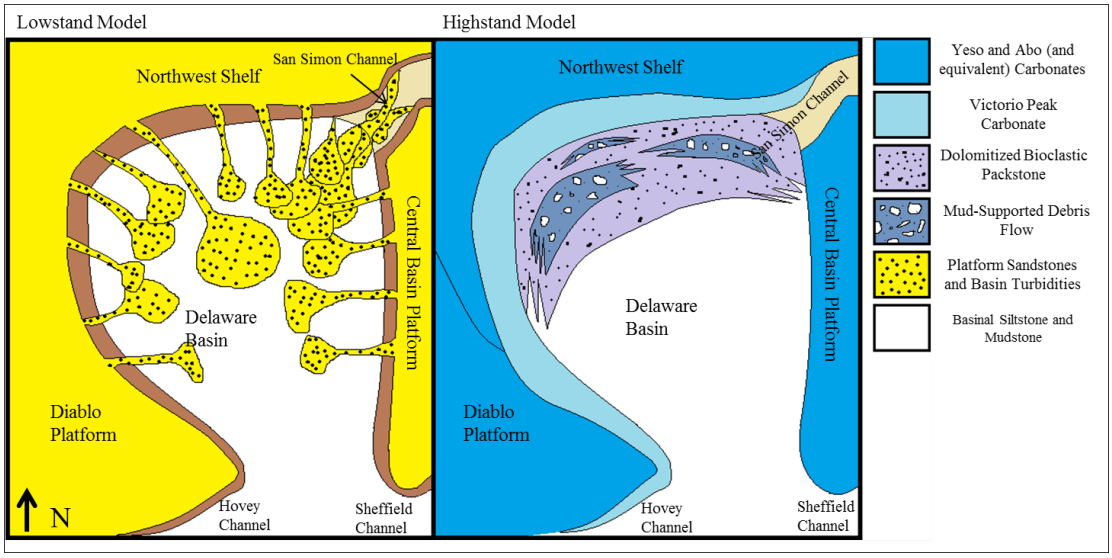

Figure 14: Reciprocal sedimentation model of the Bone Spring highlighting the deposition of siliciclastic turbite fans and channel systems at relative lowstands and carbonate apron deposition at relative highstands (Crosby, 2015; Scholle, 2002).

Adapted Galloway Motif Sequence Stratigraphy

Well log sequence stratigraphy relies on the assumption that the gamma ray curve acts as a proxy for grain size and therefore can be an indicator of depositional process energy with coarser sediments being deposited at lowstand times under higher process energy and finer grained sediments being deposited at highstand times with lower process energy (Slatt, 2006). The arrows alongside the gamma ray (GR) curve in Figure 15 show traditional clastic Galloway sequence stratigraphic motifs with increasing gamma

representing transgression and highstand deposits and decreasing gamma representing regression and lowstand intervals (Galloway, 1989; Pigott, 2016). This model is very effective at predicting sequence stratigraphic changes in deposition in purely siliciclastic environments.

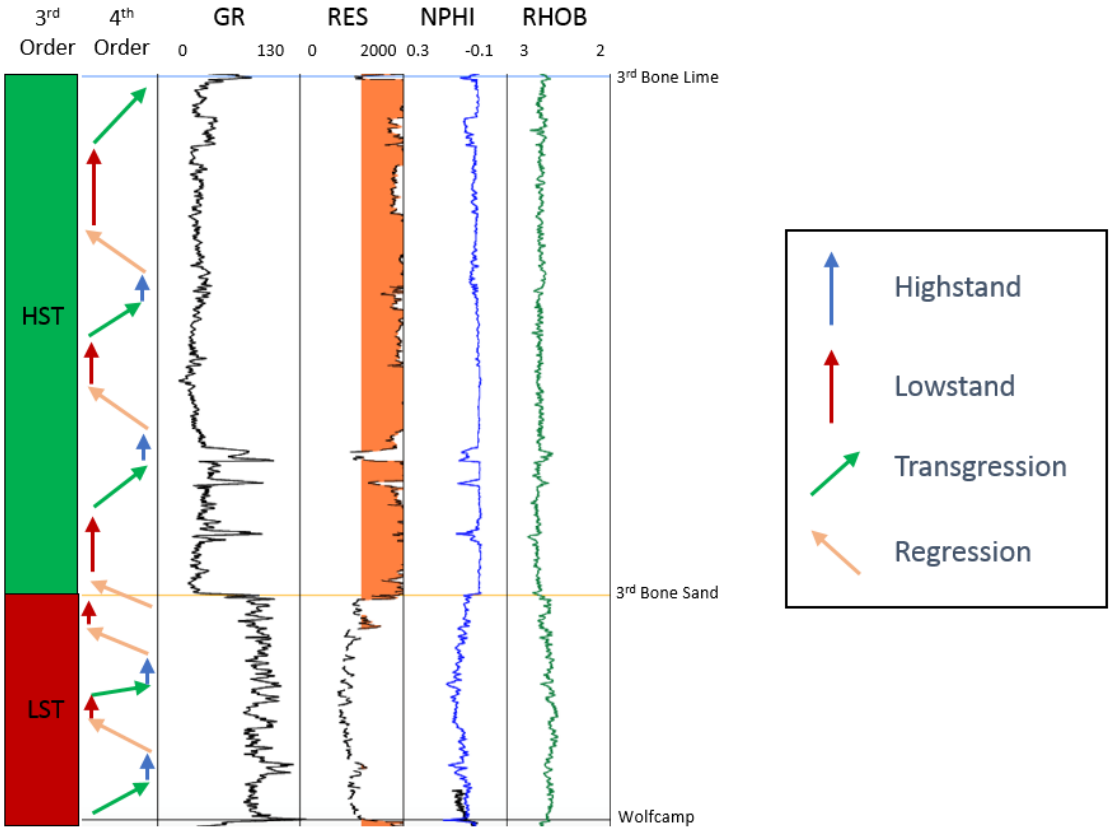

Figure 15: Classic Galloway based sequence stratigraphic motifs illustrated in the 3rd Bone Spring. The model works well in the lowstand 3rd Bone Spring Sand with highstands consisting of finer grained siltstones and lowstands consisting of coarser grained sandstones. The model breaks down in the highstand carbonates with the suggestion that these facies were deposited during a relative lowstand when they are known to be deposited during relative highstands. Resistivity (RES), Neutron Porosity (NPHI), and Density (RHOB) logs are also shown.

However, the analysis breaks down when dealing with mixed siliciclastic and carbonate environments due to the changes in depositional processes observed in siliciclastic vs carbonate depositional environments. While finer grained siliciclastic muds and shales are deposited at relative highstands in deep water, muddy, high gamma

carbonates are associated more with carbonate mud that is more abundant at relative lowstand times and likely to be mixed with siliciclastic material in the Bone Spring (Pigott, 2016). On the other end of the spectrum, lower gamma ray clean sands are expected at relative lowstands while in a carbonate system, low gamma ray readings are indicative of cleaner, "blocky" carbonates that more closely resemble highstand carbonate growth (Pigott, 2015).

Therefore, this study contends that an adapted Galloway approach is the most accurate way to represent cyclic relative sea level changes in the Bone Spring formation. As is shown in Figure 16, the adapted Galloway approach essentially flips the interpretation of Galloway petrophysical motifs in carbonate dominated intervals. This approach more closely aligns with the idea that blocky carbonates are more widespread during relative highstand times. Increasing gamma is tied to regression in carbonate intervals while decreasing gamma is tied to transgression and highstand and the growth (and subsequent transport to the basin) of cleaner, low gamma carbonate intervals. In addition, due to reciprocal sedimentation, this method better accounts for the fact that relative 4th order lowstands within a 3rd order highstand could lead to increased siliciclastic deposition.

Figure 17 shows the adapted Galloway technique as applied to the 3rd Bone Spring. The adapted motifs tell a more coherent story and better represent the changes in relative sea level that were happening over the course of deposition. As was stated before, this study also diverges from classical Galloway interpretation in the fact that sequence boundaries are defined at the top of HSTs rather than at maximum flooding surfaces (Galloway, 1989). This technique works very well for general trends, but the presence of shale dominated maximum flooding surfaces within carbonate intervals must

also be noted during times when sea level is high enough to flood the reef and blanket underlying sediments in a shale drape.

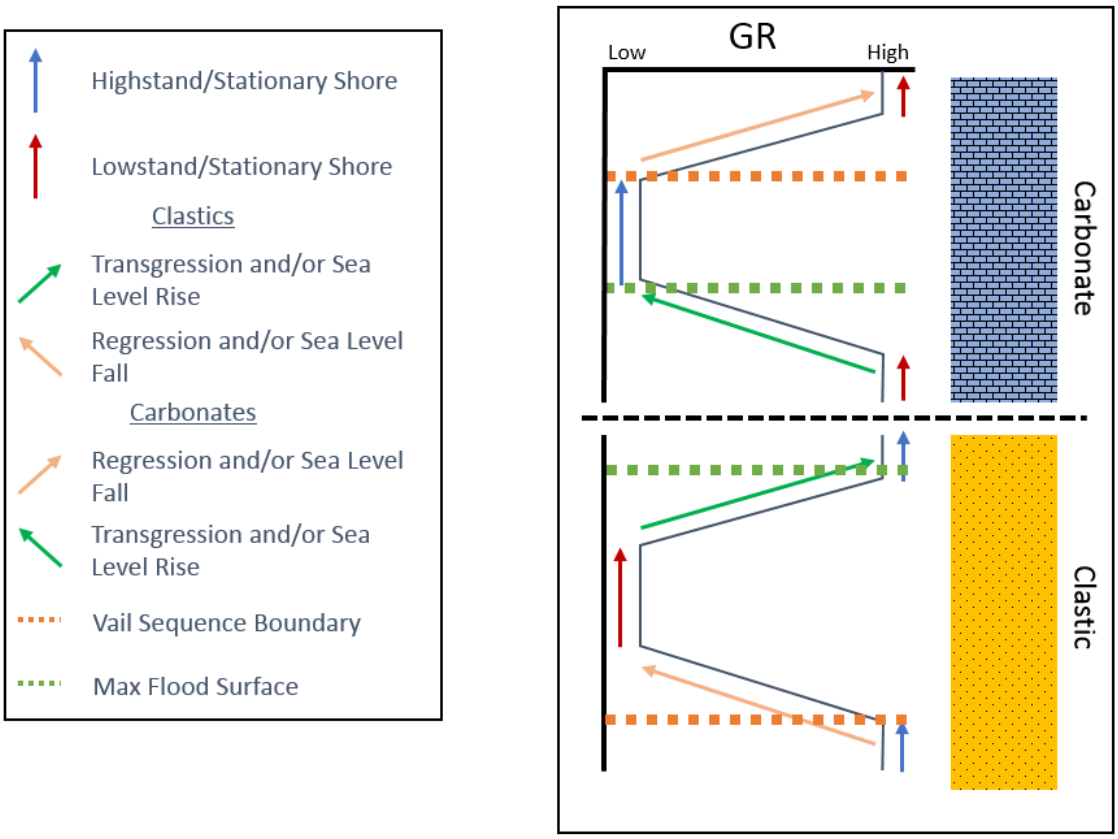

Figure 16: Idealized representation of the proposed adapted Galloway sequence stratigraphic motifs. The clastic model agrees with a classic Galloway school of thought other than placing sequence boundaries at the top of HSTs as is done by Vail. In carbonates, the motifs are reversed to better represent deposition of clean, blocky carbonates at highstand times (Galloway, 1989).

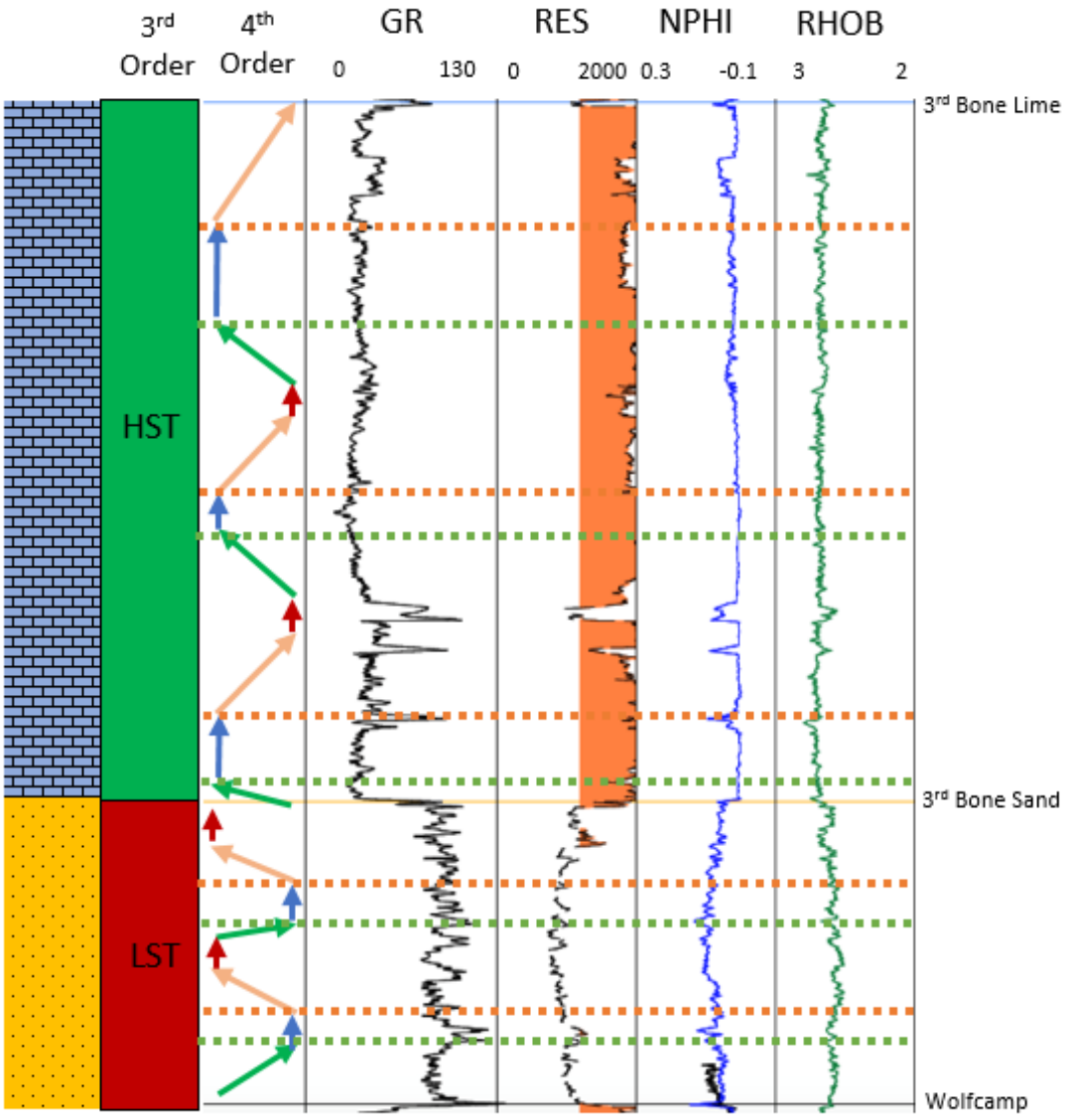

Figure 17: 3rd Bone Spring interpreted using 4th order adapted Galloway technique. 3rd order highstand and lowstand are marked along with dominant lithology shown on the left. In the lowstand clastic system of the 3rd bone sand the interpretation remains unchanged. In the highstand carbonates of the 3rd Bone Lime, motifs are reversed. This interpretation better fits transgression into clean carbonates and regression into sandier and more carbonate mud rich sediments.

Overall, the adapted Galloway method considers lithology when determining sequence stratigraphic trends. In a formation such as the Bone Spring where reciprocal sedimentation leads to a complex intermingling of carbonates and clastics, this method is

essential to account for changes in lithology rather than blindly relying on trends in the gamma ray curve.

Seismic Stratigraphy

Seismic stratigraphic theory utilized in this investigation is based on the original model proposed by Vail in 1987. Seismic stratigraphy is based on the fundamental assumption that the reflectors observed in a seismic volume represent bedding planes and can therefore be interpreted as time surfaces that are chronostratigraphically significant (Pigott, 2016). Therefore, terminations of these reflectors into other reflectors represent termination into operational sequence boundaries which are interpreted as unconformities or correlative conformities. Major termination types include erosional truncation and toplap at upper boundaries and onlap and downlap at bottom boundaries. Figure 18 adapted from Vail (1987) illustrates how this study represents these terminations and sequence boundaries.

Vail sequence boundaries occur at the top of HSTs (Vail, 1987). This study interprets well log sequence boundaries also at the top of HSTs allowing for a more accurate comparison of the two methods. Using synthetic well ties to tie logs to the seismic data, this study attempts to compare the seismic stratigraphic model with the high vertical resolution of well log sequence stratigraphy. In the complex Bone Spring interval, the nature of individual reflectors can be hard to determine due to their chaotic nature which is inherent to a mass transport style of deposition. However, using a merged Galloway/Vail approach, this investigation attempts to better define these chaotic reflectors leading to better lateral facies prediction.

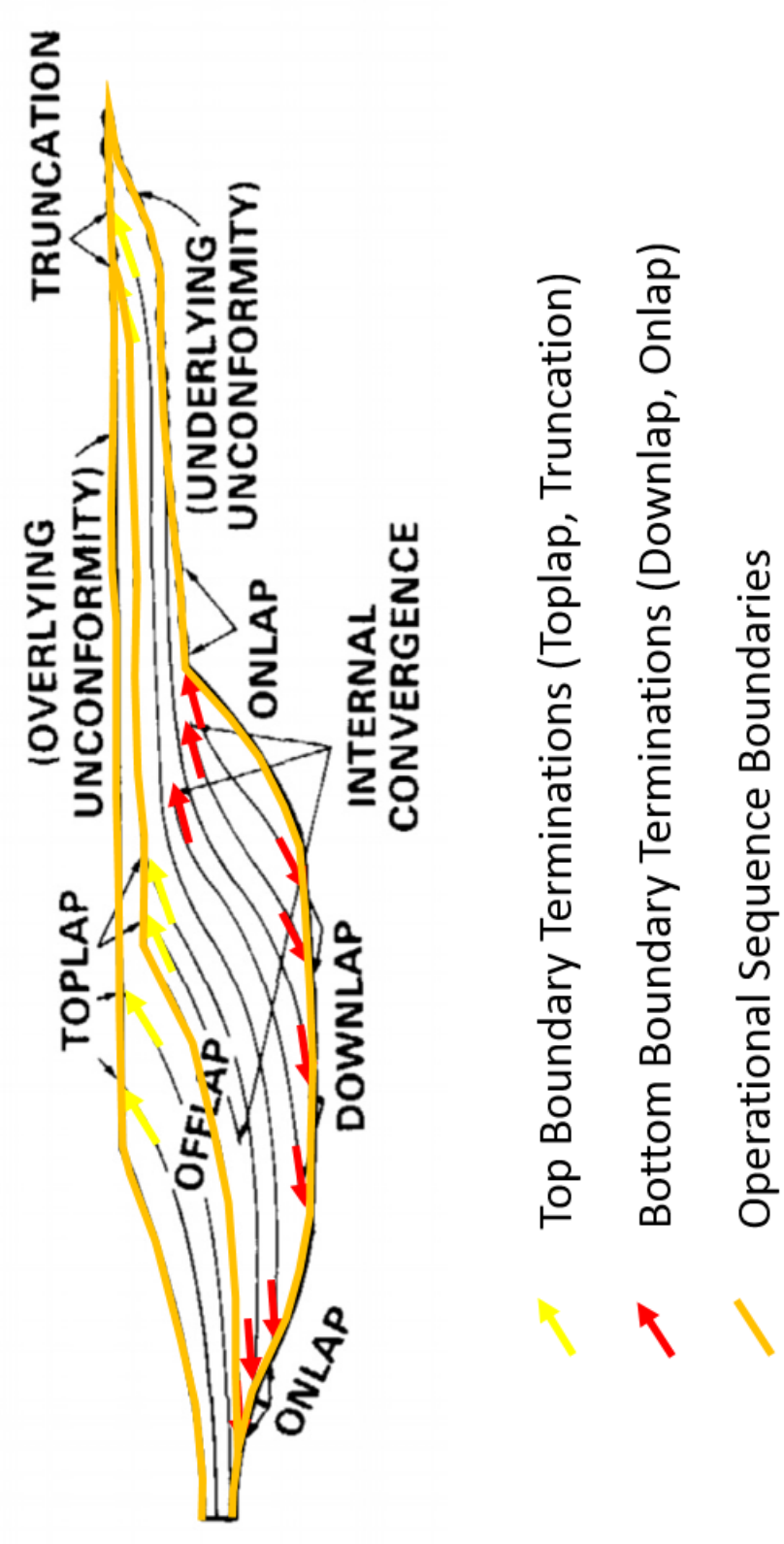

Figure 18: Diagram illustrating the symbols used to define terminations and operational sequence boundaries in this study (Vail, 1987).

Permian Sequence Stratigraphy

According to Sloss's early definitive work on sequences (1963), the Permian falls within the Absaroka Sequence or Supercycle of the North American Craton. More specifically, the Permian falls within the Lower Absaroka II (Sloss, 1988). The Absaroka II is known within the greater Absaroka Supercycle as a period with lower frequency and amplitude sea level fluctuations than the Absaroka I but higher than the underlying Absaroka III (Ross and Ross, 1995). Ross and Ross (1995) also contend that the Permian is deposited at a 1st or 2nd order eustatic regression and that the four stages within the Permian, the Wolfcampian, Leonardian, Guadalupian, and Ochoan, are cyclic sea level fluctuations within this 1st – 2nd order regression. These stages have 3rd order and higher sea level fluctuations imprinted on them that partially control deposition of the specific formations in those intervals. This study will focus on identifying those 3rd and 4th order sequences and the impact they had on Bone Spring deposition.

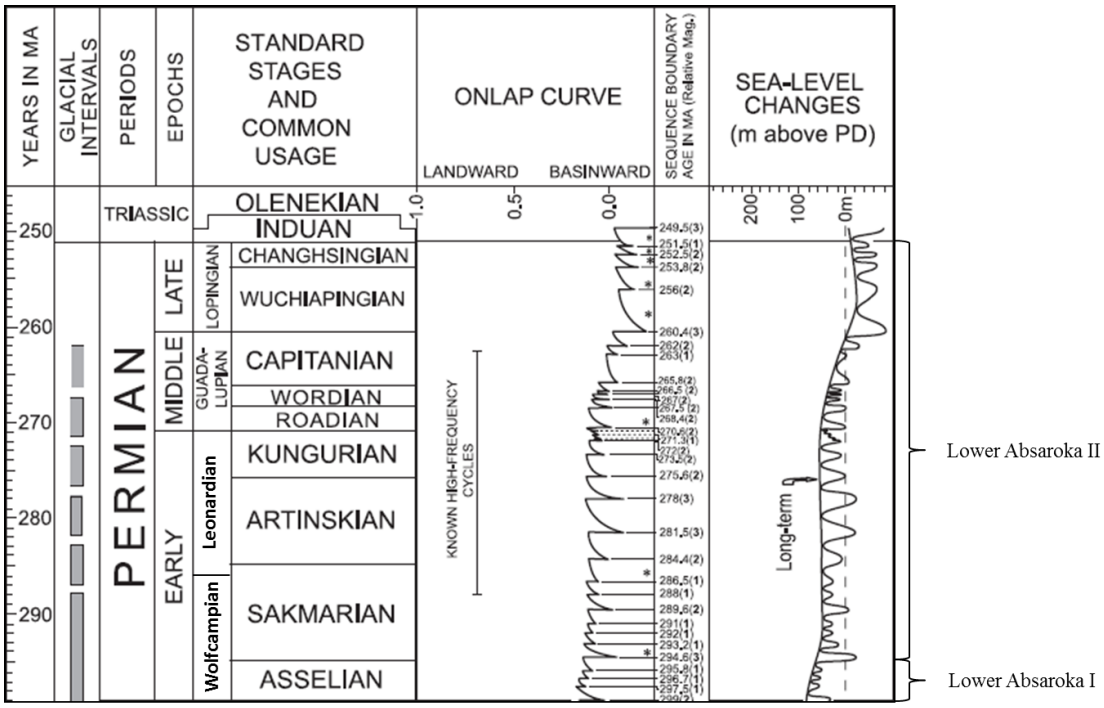

Figure 19: Geologic time scale highlighting the Permian period. Note the Leonardian is located in the Lower Absaroka II with respect to supercycles on the

North American Craton (Sloss, 1963). The onlap curve shows that there are multiple higher order cycles within the Leonardian (Haq and Schutter, 2008; Crosby, 2015).

According to Ross and Ross (1994), the Wolfcamp formation which immediately underlies the Bone Spring formation is made up of four to five 3rd order sequence stratigraphic cycles. These 3rd order cycles in the Wolfcamp as well as the later 3rd order cycles in the Bone Spring formation are thought to be caused by glacioeustacy relating to ice sheet volumes on Gondwana (Veevers and Powell, 1987). A second order unconformity caps the Wolfcamp on top of which the Bone Spring was deposited. The Wolfcampian second order unconformity along with the 2nd order unconformity at the top of the Bone Spring underlying deposition of the Brushy Canyon Formation are 2nd order sequences boundaries bounding the Bone Spring (Silver and Todd, 1969).

The Leonardian has been postulated to have anywhere from four to eight 3rd order sequences (Ross and Ross, 1994; Montgomery, 1998). This investigation identifies four 3rd order sequences within the Bone Spring formation. Third order sequences in the Bone Spring appear to last longer than those in the Wolfcamp likely because of increased carbonate production in the Leonardian (Ross and Ross, 1995; Crosby, 2015). These 3rd order cycles also show internal complexity related to 4th order cycles. This study identifies 16 4th order cycles within the Bone Spring interval and attempts to correlate those cycles and associated systems tracts across the study area. Figure 20 below is a type log that identifies the 3rd order highstands and lowstands associated with the Bone Spring and shows the industry accepted formation tops that were picked across the entire study area. While these tops are picked largely based on lithologic boundaries, the theory of reciprocal sedimentation gives the formation tops stratigraphic significance.

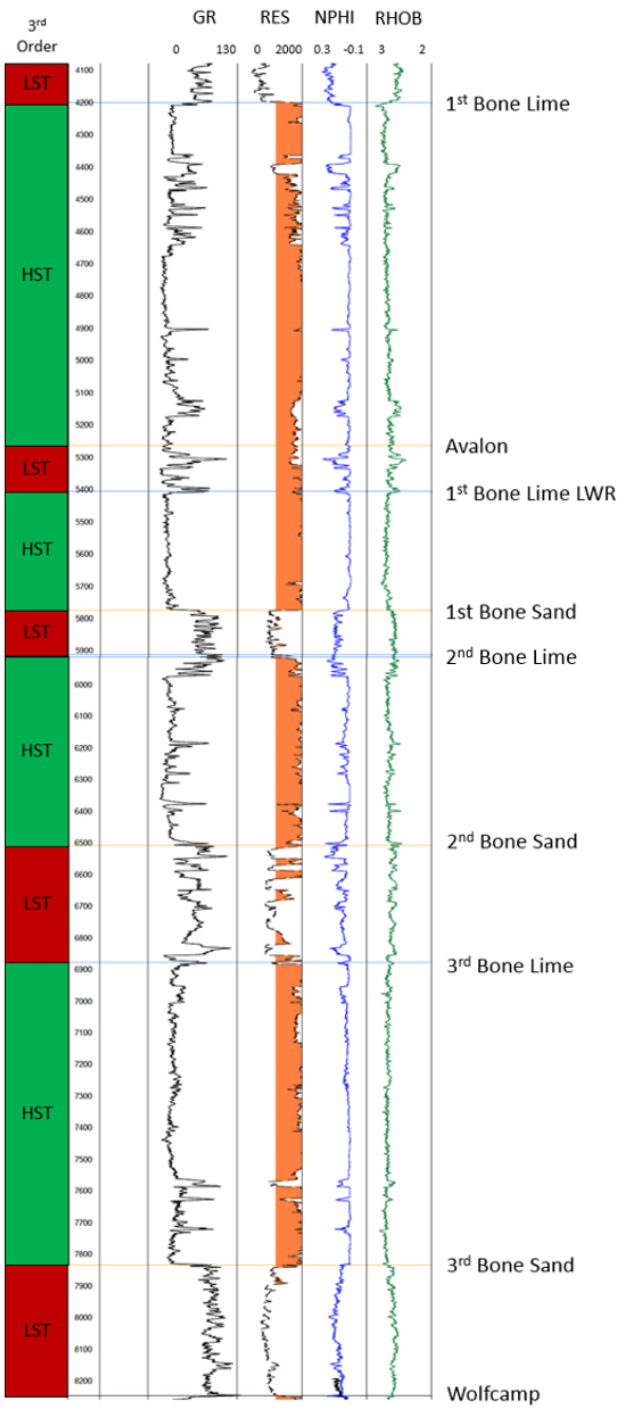

Figure 20: Type log from the study area defining the internal Bone Spring tops picked over the study area. These tops agree with the oil and gas industry accepted, lithologically based standards. Also shown at the left are the 3rd order sequences identified which, due to reciprocal sedimentation, drive this alternation in lithology from highstand carbonates to lowstand siliciclastics. This log is centrally located in the study area and will be discussed in more detail later.

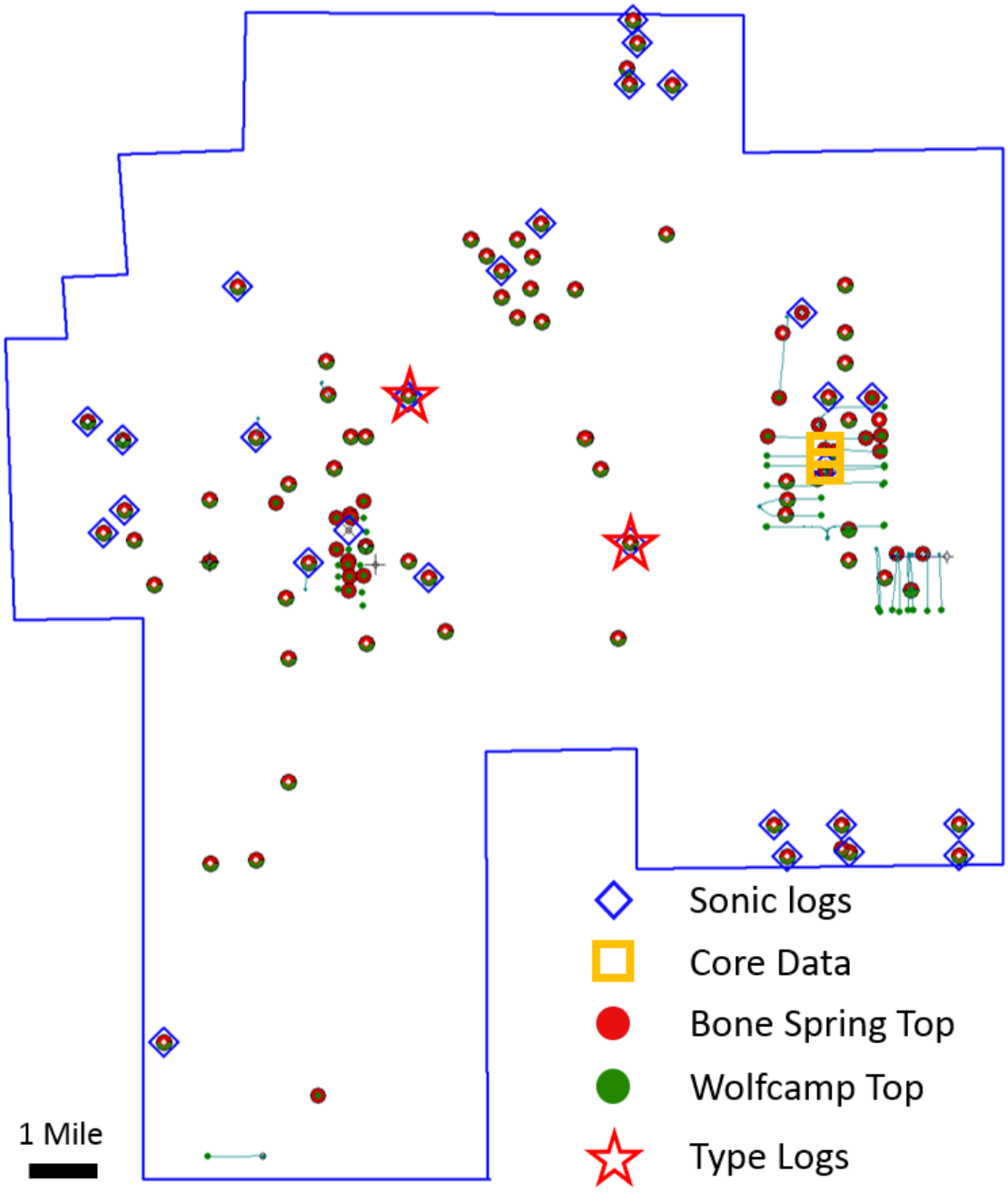

Figure 21: Data availability map showing the outline of the 3D survey provided for the study along with the relative positions of the wells that data was provided for within the survey.

All the data in this study was generously provided by Devon Energy, an active player in the Delaware Basin. Devon provided a proprietary 3D survey, digital well logs for 138 wells within the survey, and core photos and descriptions from two cores also taken within the survey area. The data is from an area that is currently being explored and developed and therefore, for the sake of confidentiality, all exact locations and well names are excluded from the study. Figure 2 shows the approximate location of the study area within the basin. All subsequent maps will show the outline of the 3D survey and relative position of the Devon well logs and cores that were provided for the study within the survey.

Log Data

Digital well logs were provided for 138 wells within the study area which included high quality triple combo logs on all vertical wells and 24 sonic logs that covered the Bone Spring that were used to create synthetic well ties. Of the logs, 99 penetrated at least the top of the Bone Spring and 73 logs passed at least through the top of the Wolfcamp. The other logs included GRMWD logs on 33 horizontal wells and shallow logs on 13 Brushy Canyon vertical producing wells. The GRMWD and shallow data was not used in this study but lends itself to further analysis for other future studies. Two type logs were chosen for the area which are named type logs one and two for the case of this study. The positions of these type logs as well as all the other log data provided are shown in Figure 21. Formation tops across the area were picked using these well logs and patterns in log character were used to identify stratigraphic trends.

Core Data

High resolution core photos and core descriptions were provided on two wells in the study area. Core 1 cored and interval of 6455’ – 6638’ covering most of the 1st Bone

Spring Sand. Core 2 cored 7185' – 7665' covering the 2nd Bone Spring Sand and the top ~20 feet of the 3rd Bone Spring Lime. For the purposes of this study, the cores were used to verify the lithologies assumed from log data and ensure that they agreed depostionally with the identified fourth order systems tracts. Figure 22 shows examples of the high-resolution core photos that were provided. The depths of these cores and their position in the stratigraphic column will be explored in more detail in the results chapter of this study.

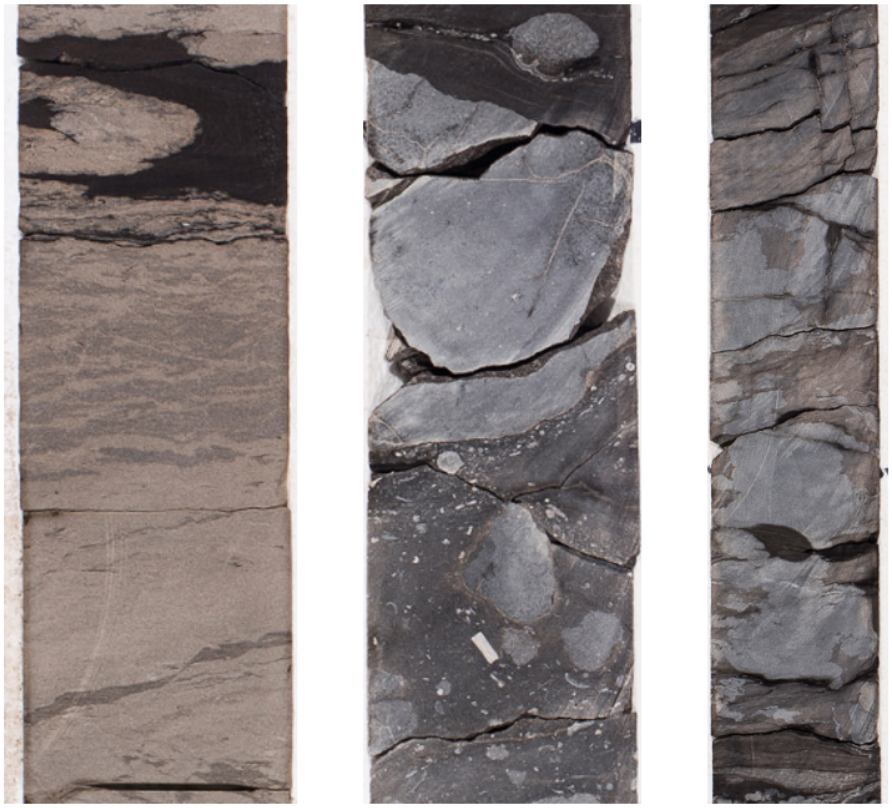

Figure 22: Example core photos showing the high resolution of the core photography that was done. Core depths and position within the stratigraphic column will be discussed later.

Seismic Data

The provided 3D survey covers an area of ~215 square miles and was shot by Dawson and processed by Sterling in 2015. Seismic data acquisition in the Delaware

Basin is known to be difficult due to the shallow anhydrites that are detrimental to seismic data quality. However, the bin size and high CDP fold of this survey allow it to better image below the anhydrites than older vintage 3D surveys. Higher quality seismic data allows for the identification of reflector terminations that can then be used for stratigraphic interpretation. Internal reflectors can also be identified within most of the major formations within the Bone Spring, but these reflectors appear chaotic in some areas due to the mass transport nature of the Bone Spring. Overlying well log sequence stratigraphy with the seismic allows for better geologic interpretations to be made about those internal reflectors. Note that the polarity of the data is European standard convention with peaks displayed in blue and troughs in red (Brown, 2011). An example of the seismic data quality can be seen in Figure 23. Important acquisition parameters for the survey are as follows:

- Record Length: 6000 ms
- Sample Rate: 2 ms
- Bin Size: 82.5 ft
- CDP fold up to 470
- Inlines: 1001 – 2207
- Xlines: 5001 – 6020

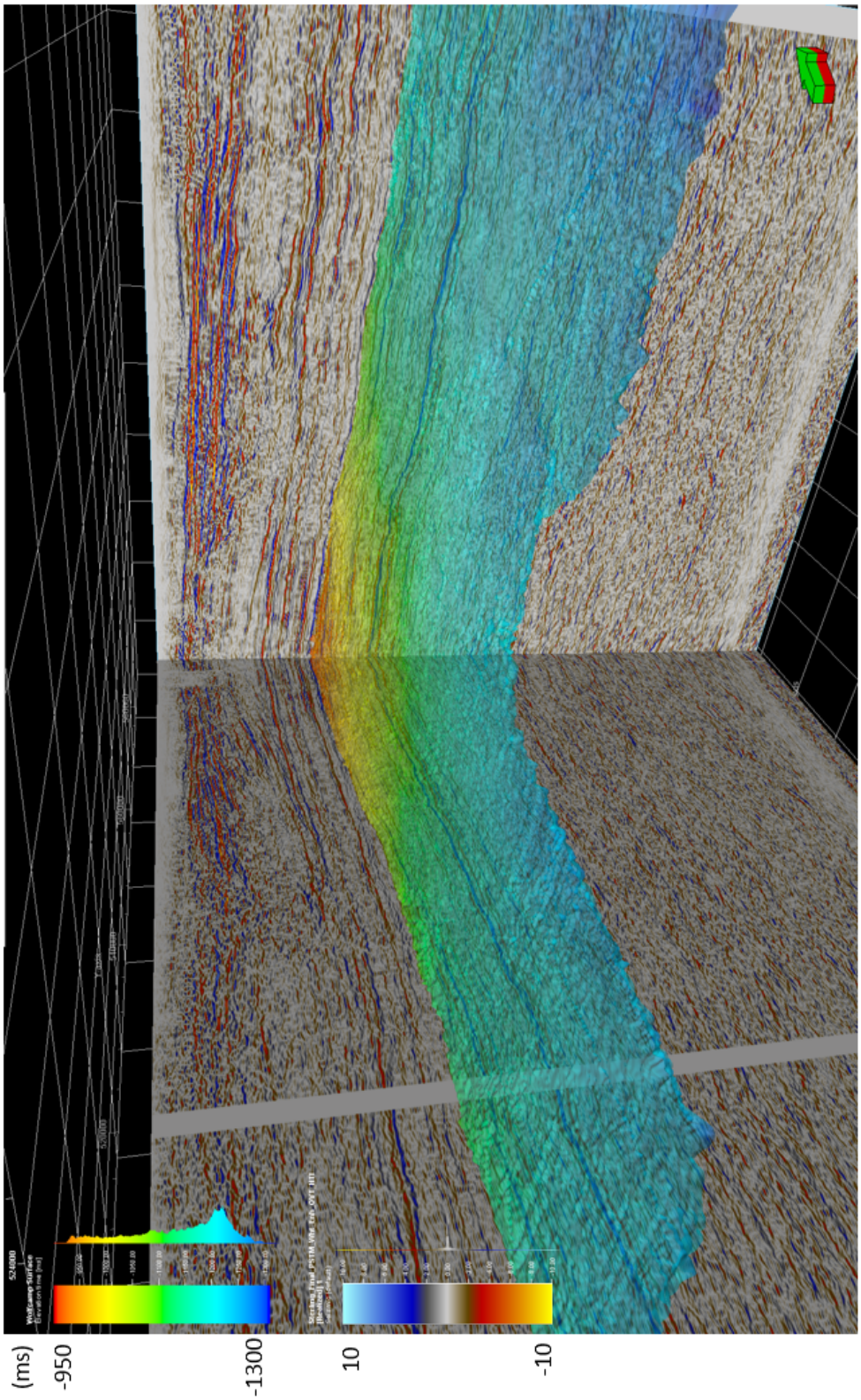

Figure 23: Example of the high-quality seismic data used in this study. The shown horizon is the top of the Wolfcamp immediately underlying the Bone Spring.

Chapter 5: Methods

Figuratively, this study stands on three pillars: well log sequence stratigraphy, core analysis, and seismic stratigraphy. All three of these methods of assessing the depositional environment of a formation have their strengths and weaknesses but only through utilization of all three pillars can one attempt to fully understand the depositional controls on a system. This chapter breaks down the methods carried out within each of these three pillars before starting to assess the results of these studies in chapter 6.

Well Log Analysis

The well logs utilized in this investigation (Chapter 4) were first used to identify important formation boundaries. These industry accepted boundaries from oldest to youngest include the Wolfcamp, 3rd Bone Spring Sand, 3rd Bone Spring Lime, 2nd Bone Spring Sand, 2nd Bone Spring Lime, 1st Bone Spring Sand, 1st Bone Spring Lime Lower, Avalon, and 1st Bone Spring Lime. As was stated earlier, these industry accepted tops are largely lithologically picked but have stratigraphic significance due to reciprocal sedimentation. Picking these tops allowed for structure and isopach maps to be constructed over the study area that acted as a guideline when picking wells and cross sections for sequence stratigraphic analysis.

Following the initial assessment, a sequence stratigraphic framework was interpreted and correlated across the study area which consisted of defining adapted Galloway motifs and identifying sequence boundaries and maximum flooding surfaces as described earlier (see Chapter 3: Adapted Galloway Sequence Stratigraphy). The primary log curve used to identify these sequences is the gamma ray (GR) curve. Resistivity, porosity, density, and sonic logs were also valuable especially in determining

lithologic trends within a well. For example, increased carbonate content was observed to correlate with increased resistivity readings, decreased porosity, and increased bulk density. These general observations were verified when comparing to the available core data. These trends are not univocal in their interpretation as they can be impacted by other factors than just lithology. Nonetheless, in general terms the log responses do a good job of differentiating carbonate and siliciclastic intervals. Therefore, this method was employed in splitting out the lithology of the formations in order to apply the lithologically dependent, adapted Galloway motifs discussed in Chapter 3.

Core Analysis

The core data provided for this study were mainly used for verification of the facies that were predicted from the well logs. Well log sequence stratigraphy identified 4th order parasequences within the 3rd order high and lowstands associated with reciprocal sedimentation. It can then be hypothesized what facies would be expected within these 4th order parasequences but only using core data can a more detailed analysis be done to verify those facies. Therefore, within the cored 1st and 2nd Bone Spring sands, high resolution core photos and core descriptions done by Devon energy were used to verify that the facies observed in core agreed with the depositional environment interpreted using adapted Galloway motifs.

Seismic Analysis

To identify important horizons and eventually compare the seismic stratigraphy to the well log sequence stratigraphy, the first step was to create synthetic well ties throughout the survey using the wells that had sonic and density logs. After tying those wells into the seismic, important horizons were mapped across the survey including the

base Wolfcamp unconformity, the Wolfcamp top, and the internal horizons within the Bone Spring. These horizons were used to make time structure maps and isochron maps. These maps gave a more detailed picture of the thickness and structural trends within the Bone Spring than the well log-based mapping and helped to identify stacking trends and potential sediment supply pathways into the basin.

After mapping these horizons, seismic terminations were picked using a Vail seismic stratigraphy model. After picking these horizons, 3rd order sequence boundaries could be identified breaking the Bone Spring into four 3rd order sequences which agreed with the well log sequence stratigraphy done in this study. Between these sequence boundaries it becomes difficult to identify trends in the reflectors. The Bone Spring basinal deposits represent a variety of sediment gravity flows with discrete flow times being often below seismic resolution. This study attempts to overlay 4th order adapted Galloway motifs with the seismic in an attempt to interpret the stratigraphic meaning of these internal reflectors.

Chapter 6: Results

Well Log Analysis

As was described in Chapter 5, all the available logging tools were used to help to identify formation tops across the entire study area and separate the carbonate dominated Bone Spring Carbonate members from the siliciclastic Bone Spring Sand members. Figure 20 shows an example of the formation tops picked across the area. After mapping out all these formations, structural cross sections, structure maps, and isopach maps were created in Petra™. Figure 21 shows the locations of all the well logs used in this study and identifies wells that logged part of the Bone Spring and wells that logged the entire Bone Spring interval down to the Wolfcamp.

This section will walk through a summary of the mapping results. On the following maps, the wells within the survey are displayed using gas or oil well producing symbols. All data points available were used for the created maps. Overall, this section will introduce the structure and thickness trends of the Bone Spring across the area. For sequence stratigraphic purposes, the 1st Bone Spring Lime is broken out into an upper and lower member separated by the Avalon Sand. However, this study focuses on the Bone Spring 1st, 2nd, and 3rd Sands. Therefore, these maps treat the 1st Bone Spring Lime as a combined interval. Subsequent sequence stratigraphic analysis breaks this out into multiple sequences but this 1st Bone Spring Lime interval and the transition into the overlying Brushy Canyon formation lends itself to more detailed study in the future.

Structure Maps

Present day structure maps across the area generally shallow to the northwest and deepen to the southeast as is expected from the location of the study area within the basin shown in Figure 2. A structure map of the top of the Wolfcamp, and therefore the

approximate paleo bathymetric profile that the Bone Spring would be deposited on is shown in Figure 24. The basin strike trends north to south along the western side of the survey area and curves to the east in the northern portion of the study area. From a depositional standpoint, this means that sediment input should be coming from both the west and north. This should mean that carbonate formations deposited in a carbonate apron style of deposition should thicken with proximity to the slope in the northwest. Siliciclastic sediments deposited in a channel – fan system should generally thicken downdip to the southeast but are expected to also be influenced by paleo bathymetry and ponding of flows in inherited lows. Structure maps of the internal Bone Spring intervals are shown in Figure 25 and show the same general trends observed in the Wolfcamp structure map. Evolution of the shoreline over time seems to be highlighted on the maps with depositional strike wrapping around more tightly to the east as the carbonate shelf prograded into the basin from the northwest. Additionally, structure contours along the eastern side of the study area seem to show ridge and valley like features that could be associated with submarine channels and valleys that fed sediments into the basin. However, limited well density makes it difficult to confirm these structures. Seismic time structure maps will confirm this hypothesis and will be discussed in more detail later.

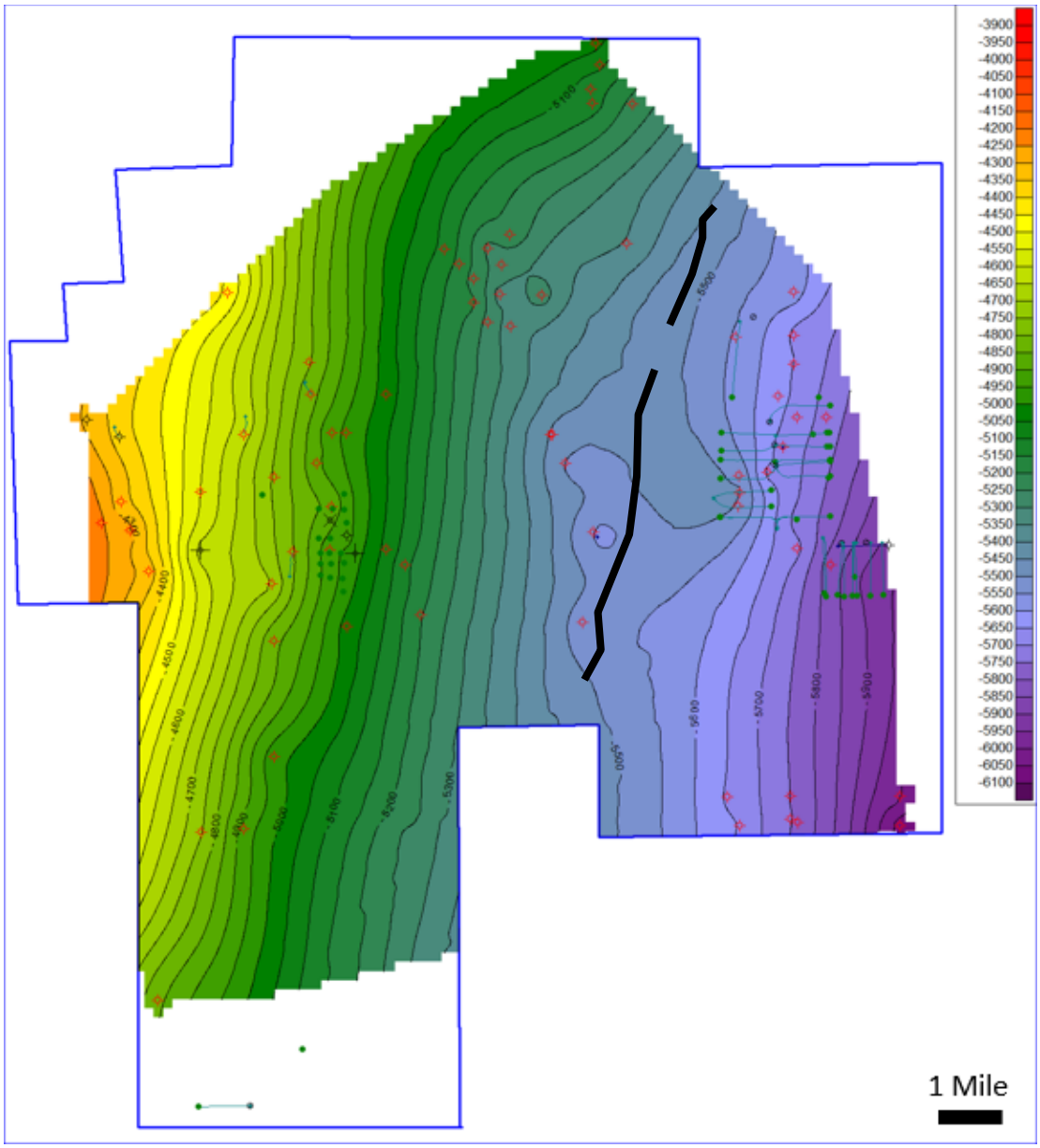

Figure 24: Structure map on the top of the Wolfcamp showing deepening of the basin to the southeast. SSTVD values range from -3900 to -6100 across the study area. The black lines represent an approximate N-S trending fault zone that was mapped from seismic in the area.

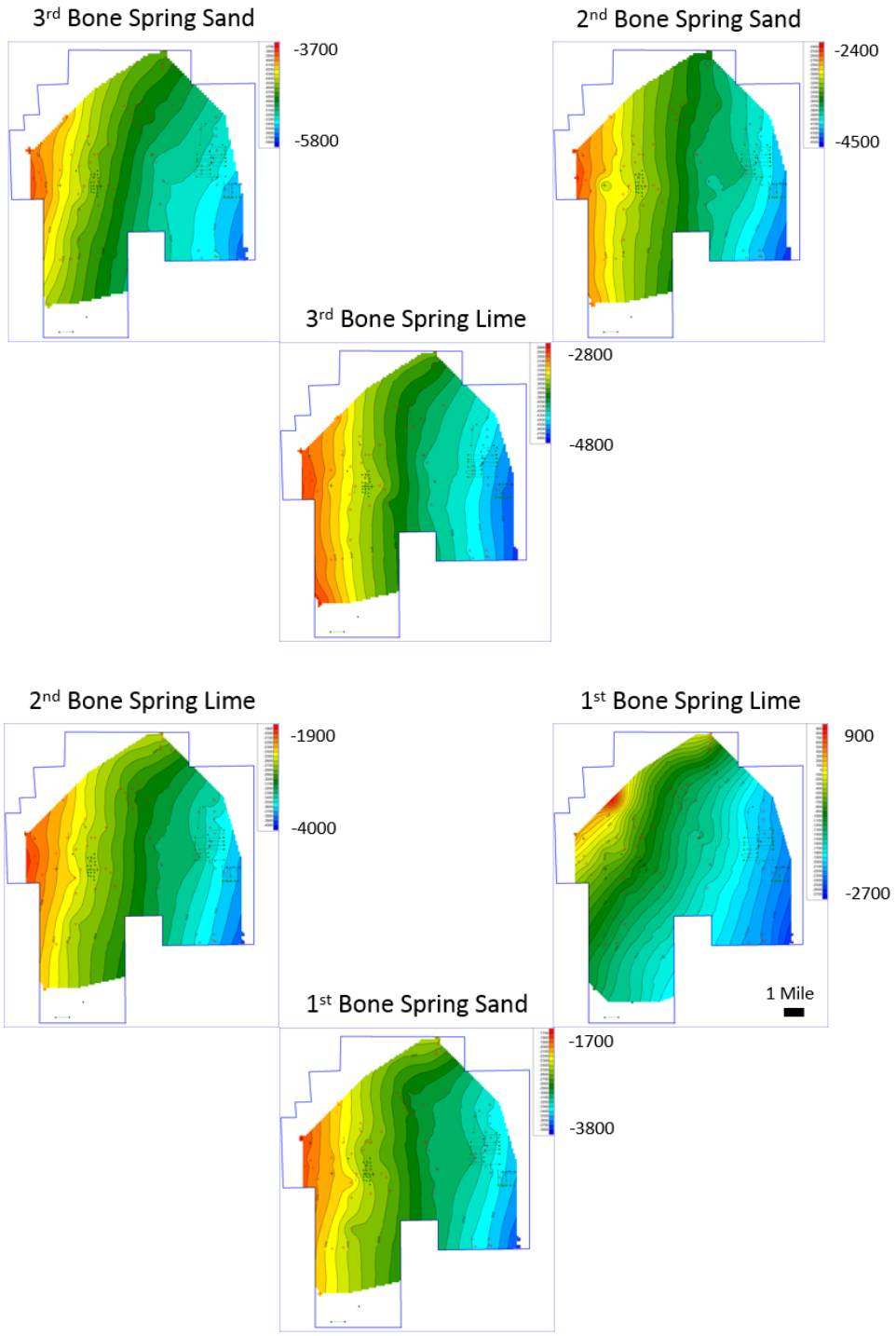

Figure 25: Structure maps on the top of the internal Bone Spring intervals in TVDSS. All intervals show the same general trend of deepening to the SE. Valley and ridge features are possible on the eastern side of the study area but are difficult to confirm with limited well density.

Figure 24 also shows in black the one major fault zone in the study area that was mapped using seismic data and appears to have exerted syndepositional influence. The

fault does not show a clean break on seismic data and instead shows a rollover feature that is prevalent up through most of the Bone Spring interval and caused a bathymetric high trending N-S through the study area with bathymetric lows on the east and west side of the fault. The fault appears to have been active during Bone Spring deposition due to the thinning of sediments over the structural high and thickening of sediments in the structural lows on either side of the fault.

Dip and Strike Cross Sections

Figure 26 is a map illustrating the location of the depositional dip and strike cross sections that are shown on the following figures (Figures 27 and 28 respectively). All the formations within the Bone Spring are broken out and colored by dominant lithology with blue representing carbonate intervals and yellow representing sand intervals. Although carbonate rich, the Wolfcamp is generally considered to be a shale and is colored grey. The dip cross section shows that all the formations generally dip to the southeast. Sediment packages up to the 1st Bone Spring Lime and Avalon series do not show drastic thickness changes from furthest updip to furthest downdip suggesting that they were deposited near the basin floor. However, carbonate packages in the 1st Bone Spring Lime, especially the upper 1st Bone Spring Lime thicken drastically towards the shelf/slope. The thickening of the carbonate packages suggests that by that time, the carbonate shelf had prograded much closer to the study area than it was during early Bone Spring deposition.

The depositional strike cross section shows that, with the exception of the 3rd Bone Spring Sand, the Bone Spring members vary drastically in thickness along strike. The variation in thicknesses suggests that local factors had a large impact on the deposition of the Bone Spring including active and inherited structures. Thin portions of

one formation tend to correlate with thick portions of the underlying formation and is interpreted to be due to compensational stacking patterns where thick deposition of mass transport deposits in one formation created a relative high that discourages the deposition of later flows.

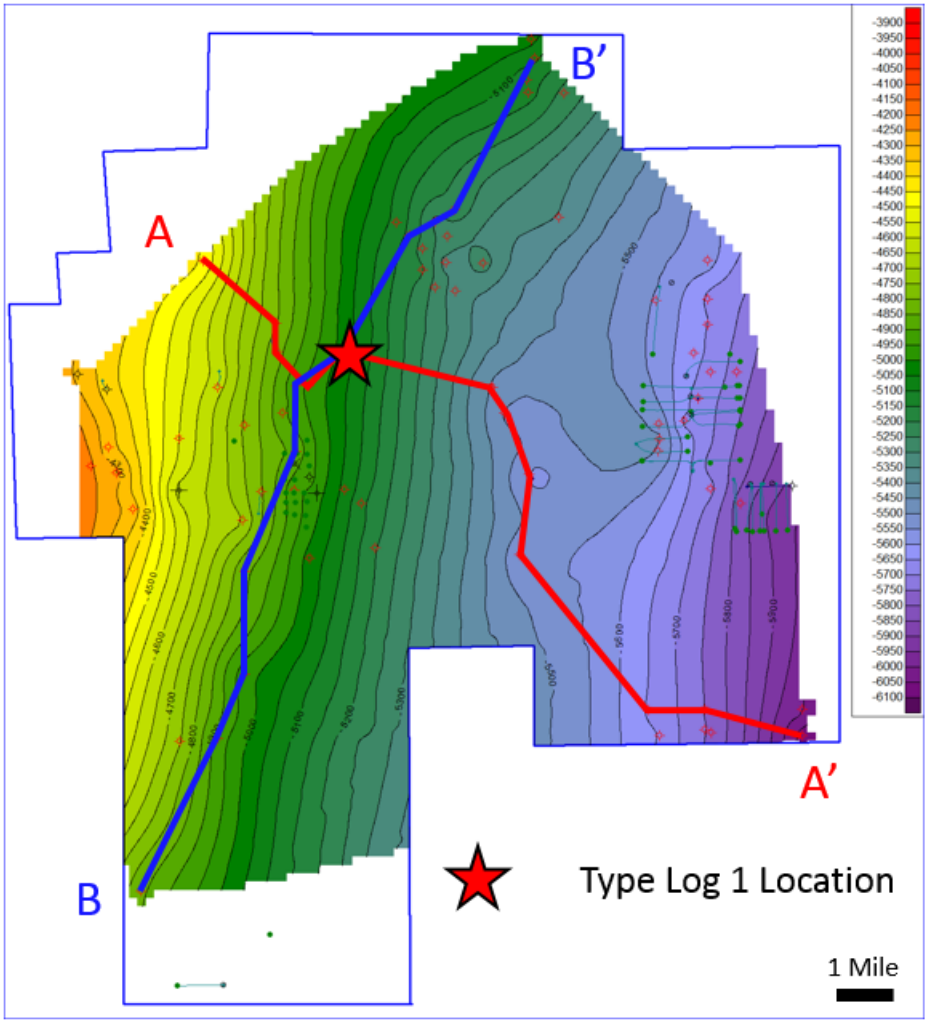

Figure 26: Cross section locator map showing the location of the following depositional dip cross section, A-A', and depositional strike cross section B-B'. Wolfcamp structure is shown for reference. The red star marks the location of Type Log 1 shown in Figure 20.

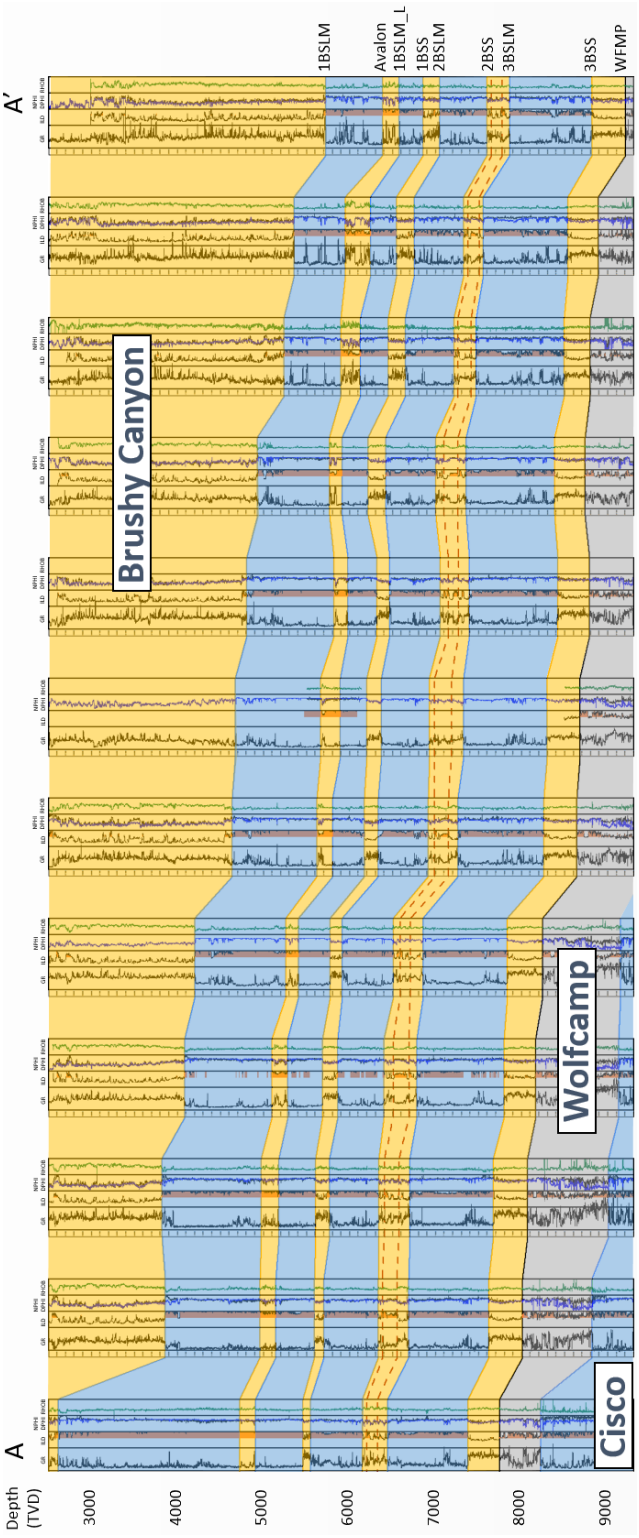

Figure 27: Depositional dip cross section A-A'. The Wolfcamp shale is colored grey and blue and yellow highlights through the Bone Spring interval represent carbonate dominated and sand dominated formations respectively. All formations generally dip toward the southeast.

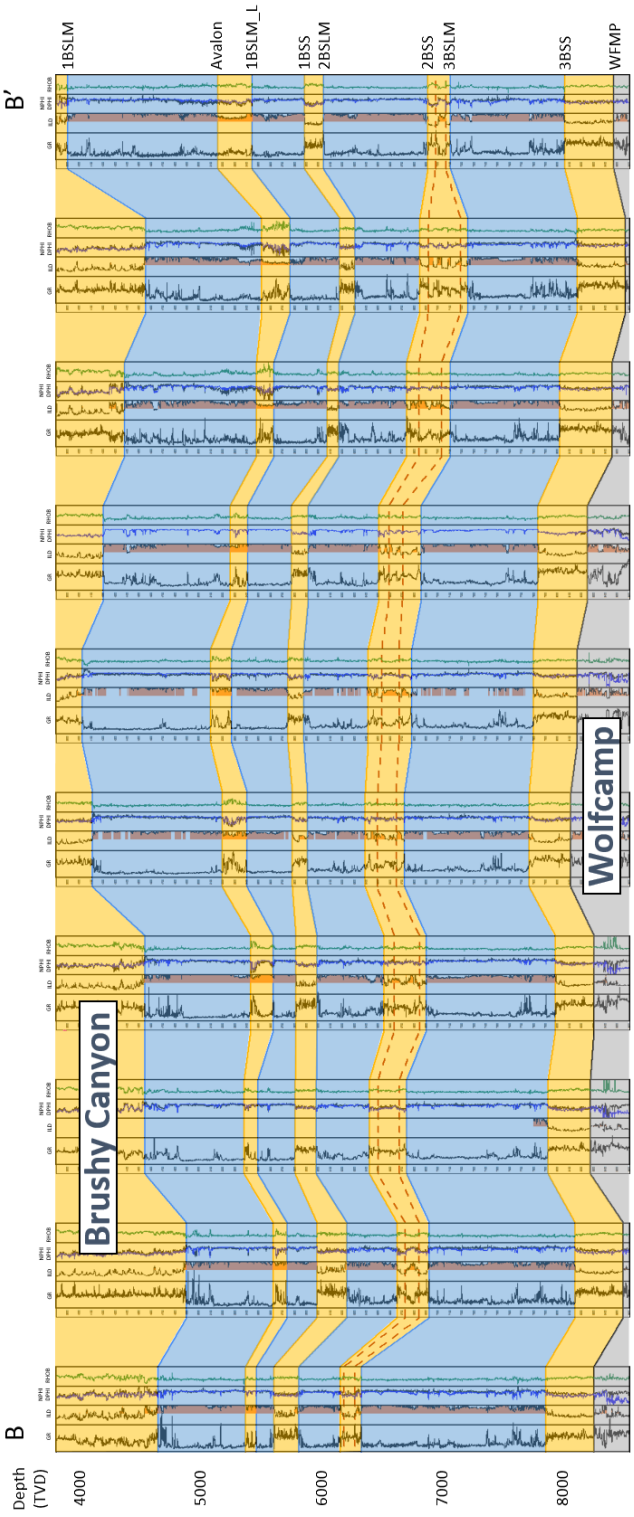

Figure 28: Depositional strike cross section B – B'. Formations are highlighted using the same colors as stated for the dip cross section.

Isopach Maps

Across the study area, the gross thickness of the Bone Spring increases to the Northwest and decreases fairly rapidly to the Southeast. Figure 29 shows a map of gross thickness of the Bone Spring from the top of the Bone Spring to the Wolfcamp. Maximum thickness in the study area is ~4800 feet to the northwest and the minimum thickness is ~3400 feet to the southeast. The buildup of shelf carbonates is the main driver for this increase in gross thickness to the NW. Throughout Leonardian time, shelf carbonates were generally prograding basinward although the progradation was not constant due to fluctuations in relative sea level. The progradation is seen in this study area especially in the 1st Bone Spring Lime which thickens substantially to the Northwest when compared to the other carbonate members.

By the end of Bone Spring deposition this study area was starting to see the influence of the prograding Victorio Peak and thicker, more proximal carbonate apron deposits. The overall gross thickness trend also shows the impact of these carbonate apron deposits with the gross thickness increasing with proximity to the slope. Siliciclastic sediments retain consistent thickness across the study area with smaller variations in thickness attributed to inherited topography causing accumulation of turbidite deposits and overall tilting and deepening of the basin to the east creating more accommodation space.

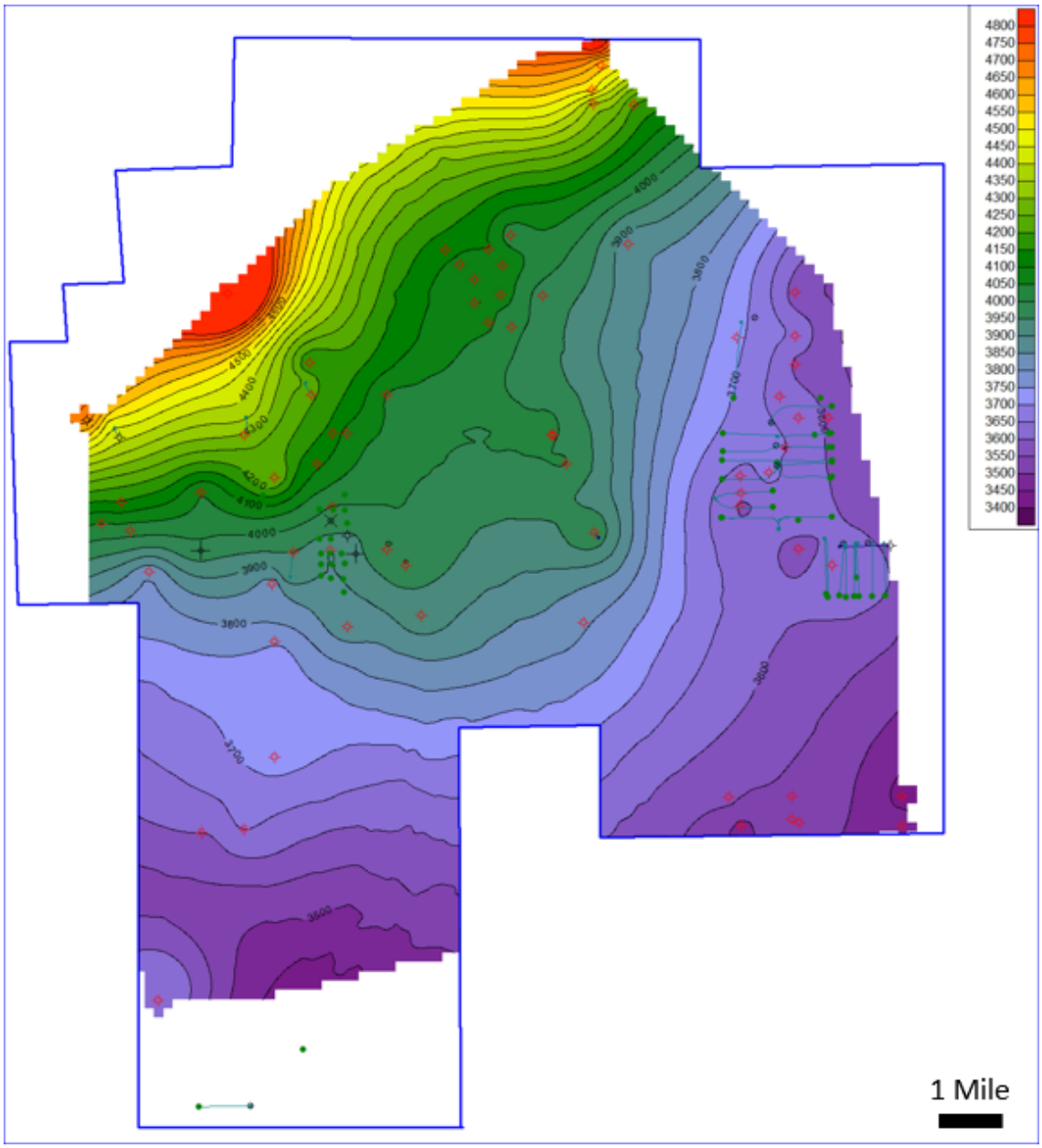

Figure 29: Gross Isopach map of the entire Bone Spring interval from the top of the Bone Spring to the top of the Wolfcamp. Thickness increases to the NW driven by the drastic thickening of carbonates intervals proximal to the slope and the progradation of the Victorio Peak seen within the 1st Bone Spring Lime.

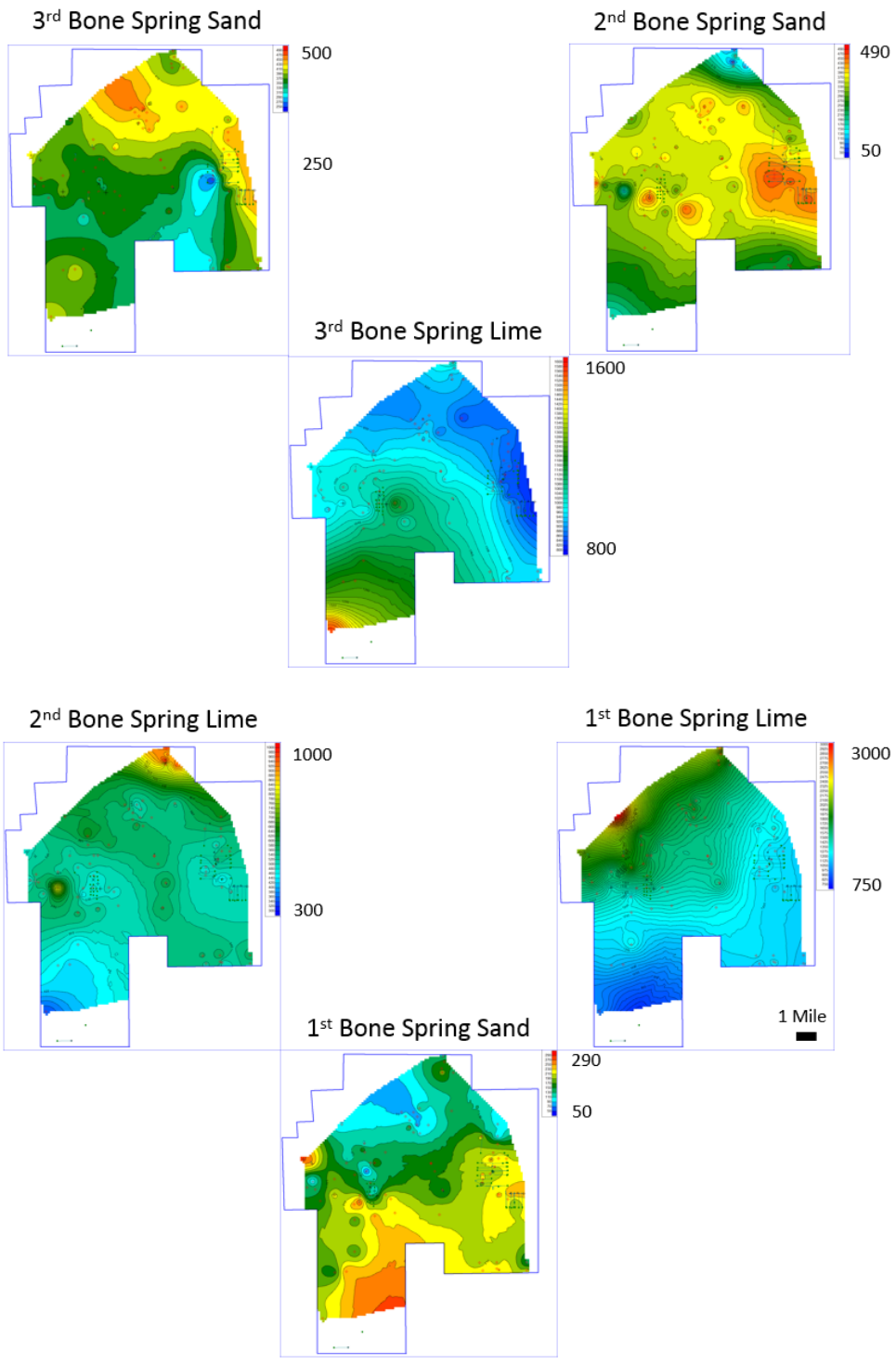

Figure 30: Gross Isopach maps of the internal Bone Spring intervals. Trends in gross thickness illustrate the impact of compensational stacking on Bone Spring deposition.

Figure 30 is a collection of isopach maps breaking the Bone Spring down into its respective formations starting with the base at the top left and moving to the top on the bottom right. The 3rd Bone Spring Sand has a relatively small change in thickness across the area with a range of thickness from 250 – 500 feet. Thinning of the package occurred over the relative structural high created by the N-S trending fault zone that runs through the eastern side of the study area. Thickening of the sand in the east and west of the study area also suggests that there could have been multiple sediment sources. The source to the east would have been the shelf that at this early period in Bone Spring deposition would have been further away than it was during later deposition. The distance from the shelf could explain why the 3rd Bone Spring Sand has relatively constant thickness as the fans would be more distal and laterally extensive. In his proximal study area, Crosby (2015) argues that the 3rd Bone Spring Sand also shows a thickness trend in line with the San Simon Channel. The channel is likely be the source of sediments that thicken on the eastern side of the fault in this study area.

The 3rd Bone Spring Lime is the first of the limestone intervals deposited in the Bone Spring. It is the only one of the three carbonate intervals that does not thicken to the northwest. This carbonate was therefore deposited before the carbonate shelf had fore stepped into the area and the facies would be those of a more distal carbonate apron. With that being said, there is a very slight thickening of the interval to the north that could be the beginning of carbonate shelf progradation into the area. The thickest part of the formation is about 1600 feet thick and occurs in the southwest part of the study area. The 3rd Bone Spring Lime also illustrates compensational stacking patterns with the thinner portions of the formation happening over thick 3rd Bone Spring Sand trends. All

of the Bone Spring is mass transport deposits and therefore this compensational stacking will show to be a major driver in deposition throughout the Bone Spring.

The 2nd Bone Spring Sand has a more variation in thickness than the 3rd sand with a range of 50 – 490 feet suggesting that the sand is being deposited in a more proximal environment where the turbidite fans are more localized. The thinnest portions of the 2nd Bone Spring Sand are deposited in the far north and southeast of the study area where the underlying limestone was the thickest again showing the importance of compensational stacking.

The 2nd Bone Spring lime has a range in thickness of 300 – 1000 feet with the thinnest portion of the formation occurring in the southwest. The thinning is consistent with thinning of the 2nd Bone Spring Sand suggesting that the thinning was still a compensational stacking effect due to thick deposition of the 3rd Bone Spring Lime in the area. In the north, the formation thickens to approximately 1000 feet illustrating the progradation of the carbonate shelf into the area that was only very minimal during deposition of the 3rd Bone Spring Lime.

The 1st Bone Spring sand thickens basinward and generally thins to the northwest toward the shelf. The thickening is consistent with siliciclastic turbidite deposits. Overall thickness of the sand is the thinnest of the sand formations with a thickness range of 50-290 feet. The thickest portion of the formation occurs in the southwest part of the study area where 2nd Bone Spring Lime and Sand deposits were the thinnest suggesting that by the end of deposition of the 2nd Bone Spring, the basin had finally filled in around the high created by thick sedimentation in the 3rd Bone Spring Lime due to compensational stacking. The filling in around this structural high caused the area to again become a structural low and created the accommodation space necessary for thick

1st Bone Spring Sand Deposition. Linear thickness trends in the western and northern portions of the study area suggest that the point sources associated with siliciclastic turbidite deposition could have been to the north and west of the study area. Subsequent study on the seismic data shows that these trends line up with structural lows that existed since the Wolfcamp suggesting that these valleys acted as a highway for sediment transport into the basin throughout most of the deposition of the Bone Spring.

Finally, thickness trends of the 1st Bone Spring Lime show the progradation of the carbonate shelf into or at least very close to the study area. The 1st Bone Spring Lime thickens to over 3000 feet in the far northwest portion of the study area along the trend of the carbonate shelf and thins to about 750 feet in the southwest portion of the study area where 1st Bone Spring Sand was the thickest. The thickness trend of the 1st Bone Spring Lime most closely resembles the shape of a carbonate apron when compared to the other limestone members of the Bone Spring also suggesting that the formation was deposited in closer proximity to the carbonate shelf.

3rd Order Sequence Stratigraphy

After analyzing the general thickness and structure trends using structure maps, cross sections, and isopach maps the next logical step was to verify that the accepted 3rd order sequences could be identified and correlated across the study area. As was stated earlier, it is generally accepted that during Bone Spring deposition carbonates were deposited at 3rd order highstands and sands were deposited at 3rd order lowstands. Therefore, the top of each carbonate a sequence boundary as discussed in chapter 3. Figure 31 below shows the location of cross section C – C' and type logs one and two in the study area. To verify 3rd order sequences, dip cross section C-C' was chosen. The

cross section and the type logs were chosen specifically because they are wells that have sonic logs and synthetic ties to the seismic to compare later to the seismic analysis.

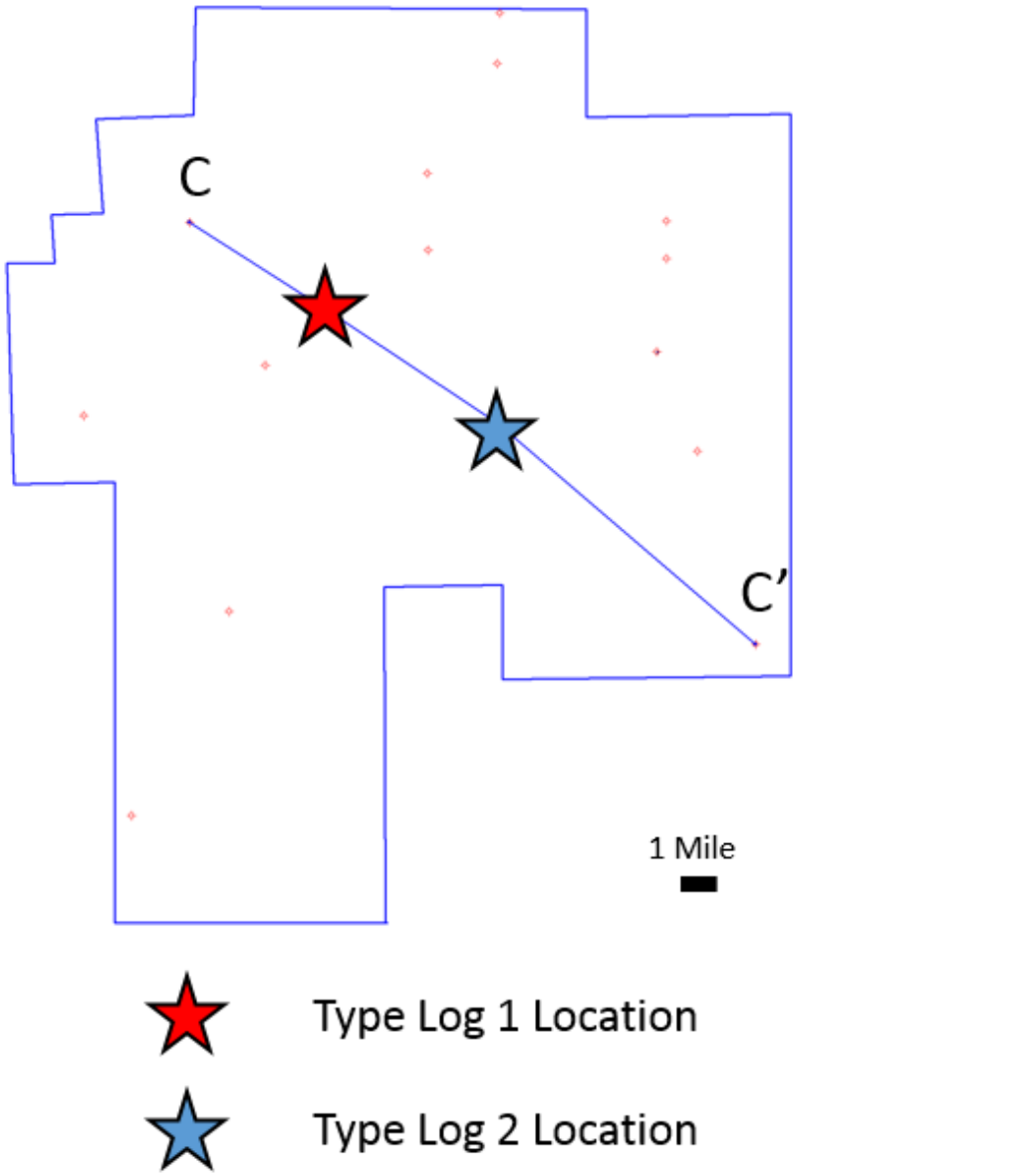

Figure 31: Locator map showing the locations of type logs 1 and 2 in the study area and cross section C – C'. These type logs and this dip cross section will be the focus of the remainder of the well log sequence stratigraphy study.

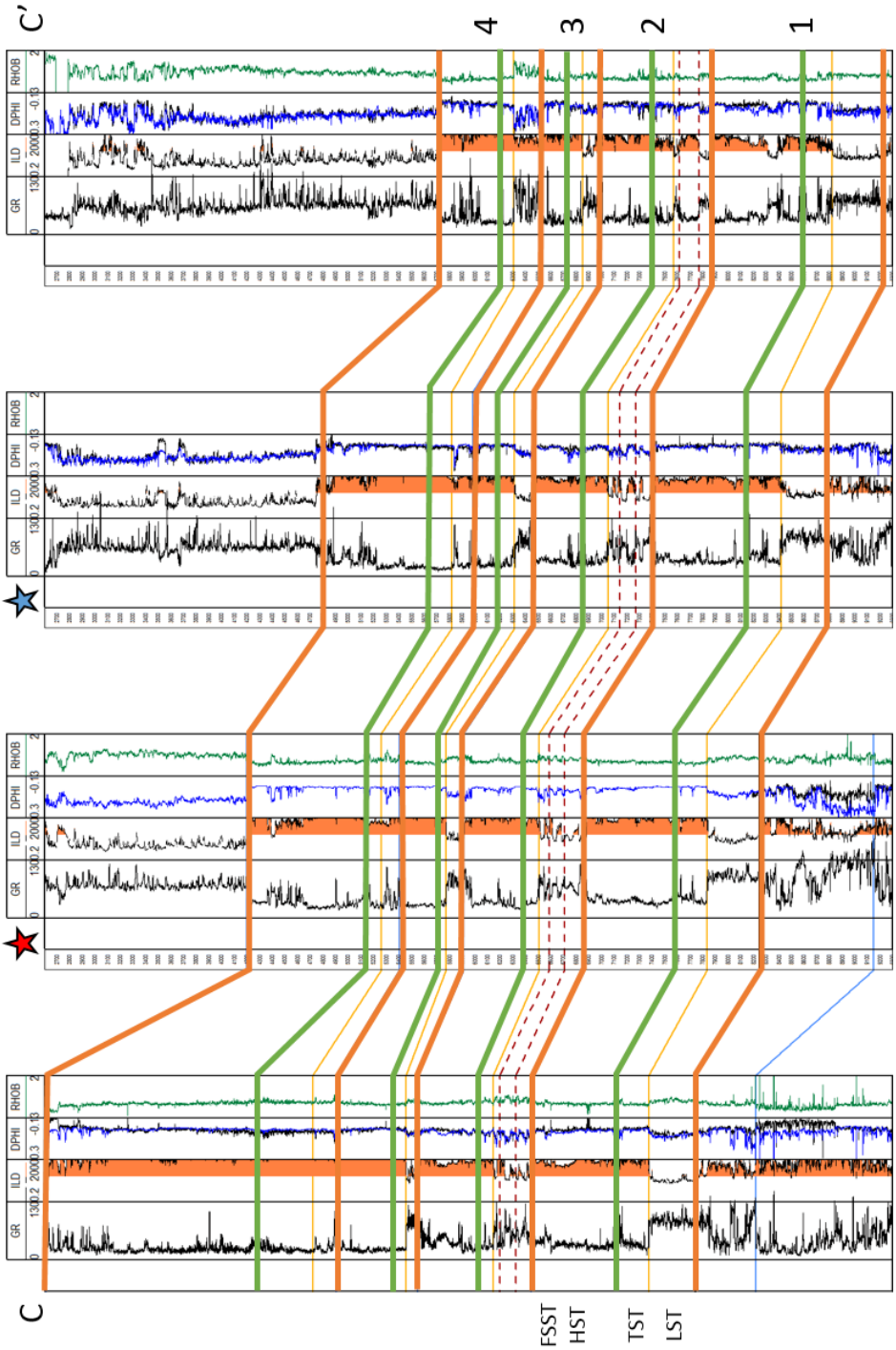

Figure 32: Cross section C – C' marking 3rd order sequence boundaries in orange and maximum flooding surfaces in green. Four 3rd order sequences were identified. Sequence 1 is the 3rd Bone Spring, sequence 2 is the 2nd Bone Spring, sequence 3 is the 1st Bone Spring Sand and Lower 1st Bone Spring Carbonate, and sequence 4 is the Avalon sand and Upper 1st Bone Spring Carbonate. An example of 3rd order parasequences is marked for sequence 1 but are correlatable through the other sequences as well.

On cross section C – C' (Figure 32) sequence boundaries were mapped which correlate to the tops of the four carbonate intervals within the Bone Spring. Maximum flooding surfaces were also mapped within the carbonate intervals. Usually these surfaces were marked by a thin shale flooding surface where sea level reached its maximum and the carbonate growth was still in catch up phase. The maximum flooding surface was followed by buildup and progradation of the carbonate shelf leading to more carbonate input into the basin in the form of carbonate mass transport deposits making up the HST. LSTs were marked by a drop in sea level, incision of the carbonate shelf, and the deposition of the sand intervals of the Bone Spring. The left of Figure 32 shows 3rd order parasequences in the 3rd Bone Spring suggesting that even though it is generally accepted that carbonates in the Bone Spring are deposited at highstands and sands are deposited at lowstands there is more complexity in the transition zones between these highstands and lowstands, namely the falling stage and transgressive systems tracts. However, when 3rd order sequences are shown on subsequent maps in this study, only the accepted HSTs and LSTs will be shown for simplicity and correlation with other studies but it is important to keep in mind that is a simplified version of the deposition.

4th Order Sequence Stratigraphy

Galloway motifs were applied to 4th order cycles and mapped out over select wells in the study area including many of the wells with seismic well ties and the wells that have core data. Figures 33 and 34 below are the 4th order adapted Galloway motif interpretations for the two type logs shown in the locator map in Figure 31. After identifying the trends on these two type logs the sequences were also identified for the other wells in cross section C – C' and correlated across the entire study area. After

correlating some of these wells it was immediately obvious that higher order cycles have an impact on Bone Spring deposition and their impacts are correlatable across the entire study area. Using a classic Galloway approach without correcting for lithology would make the correlation very difficult because of the complex nature of the Bone Spring. However, after correcting for lithology, 16 fourth order, regionally correlatable sequences were identified within the Bone Spring and these fourth order sequences have a significant impact on the petroleum system.

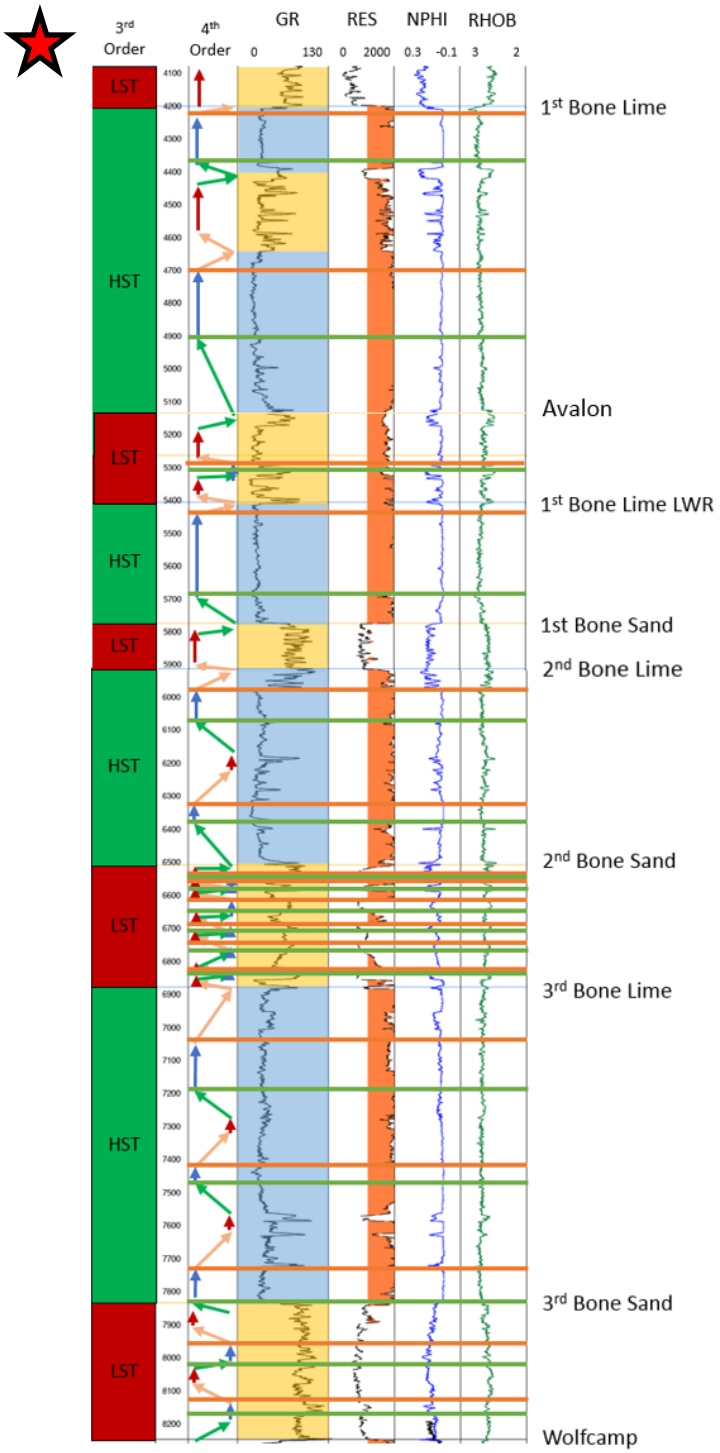

Figure 33: Type log 1 with 3rd order HSTs and LSTs marked. 4th order adapted Galloway motifs are shown in the next tract in the style described in chapter 3. Blue shading on the GR curve corresponds to dominantly carbonate intervals while yellow shading corresponds to dominantly san intervals. Orange lines represent sequence boundaries and green lines represent maximum flooding surfaces.

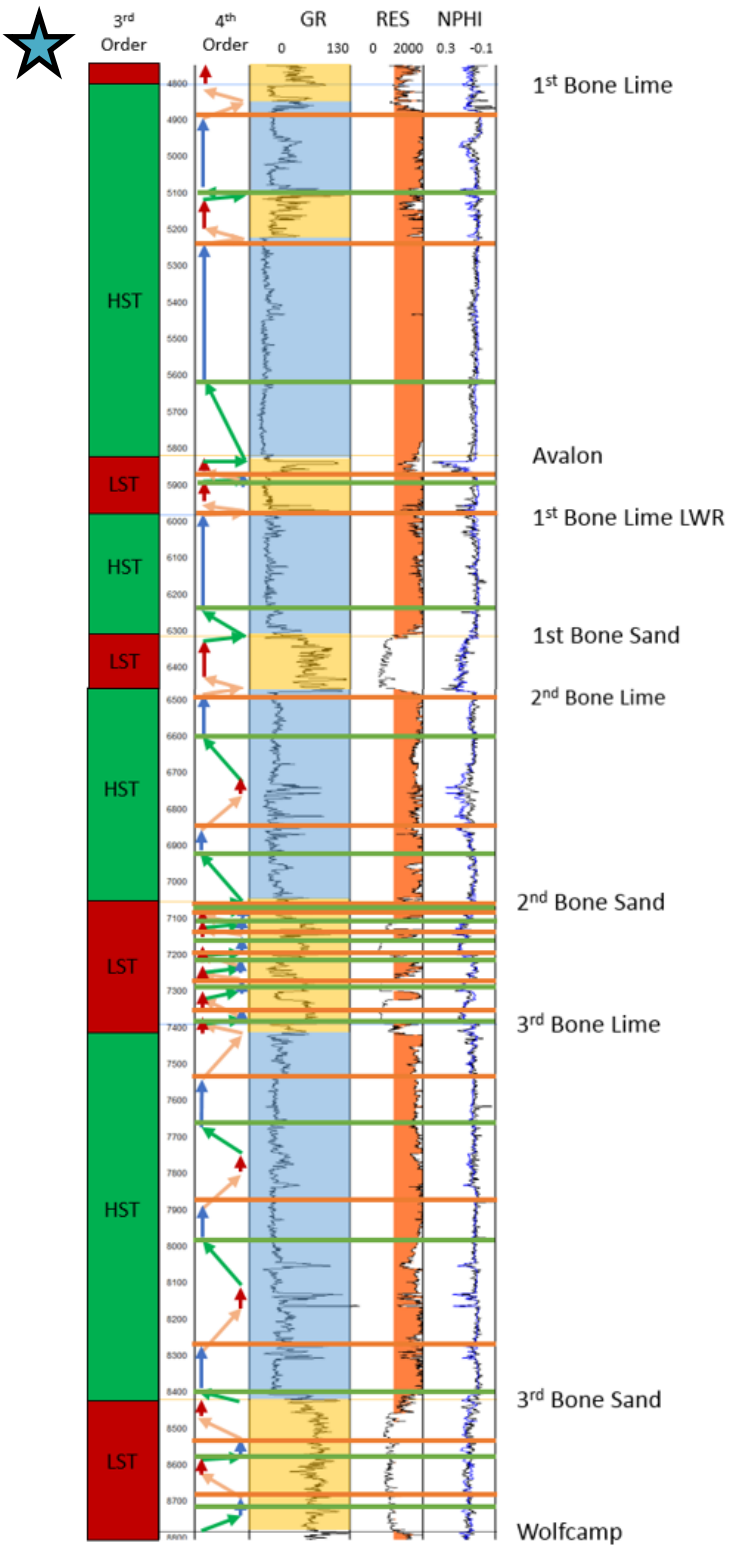

Figure 34: Type log 2 with 4th order adapted Galloway motifs. Displayed with the same style as described in Figure 33.

The fourth order sequences correlate very well between these two logs, so the following discussion will discuss both of the above type logs at the same time rather than going through them individually. While the sequences correlate it is important to note that facies can change within those sequences. The main difference between type logs one and two is that type log two is slightly more distal than type log one. Therefore, it can be observed from log character that the flooding surfaces on type log two are more prominent in the slightly deeper water.

Within the 3rd Bone Spring Sand, two full 4th order sequences were mapped out. The sand was deposited on the top of the Wolfcamp which is an unconformity and 2nd order sequence boundary. The first sediments deposited within the 3rd Bone Spring Sand were lowstand sands. Following those initial lowstand sand deposits there was transgression into a 4th order maximum flooding surface characterized within the sand intervals as gamma ray spikes that are likely attributed to silt or shale flooding surfaces. The flooding surface is overlain by a thin HST before regression into lowstand sands. After that sequence there was one more complete 4th order sequence within the 3rd Bone Sand and the sand is capped by transgression into higher gamma facies before continued transgression and a shift to dominantly carbonate deposition.

The transition from dominantly sand deposition to carbonate deposition at the 3rd Bone Spring Sand – 3rd Bone Spring Carbonate boundary marks the first reversal in Galloway motif interpretation. Within the carbonate, low gamma intervals are interpreted as cleaner carbonates deposited at highstands and higher gamma intervals are associated with more siliciclastic input at relative lowstands. Directly above the 3rd Bone Spring Sand is an almost 100-foot-thick clean, blocky carbonate interpreted as a 4th order highstand. Increasing gamma for the next ~100 feet suggests regression. Finally, gamma

readings get high enough that they are on par with what is seen in the sandstones below and resistivity readings go down suggesting more siliciclastic input. This is interpreted as a 4th order lowstand before transgression into another blocky carbonate. Another full 4th order sequence is interpreted above this sequence though the relative change in sea level is likely much less because the gamma ray readings are more consistent than in the previous sequence. Finally, increasing gamma at the top of the 3rd Bone Spring Lime suggests regression into the 2nd Bone Spring Sand.

The 2nd Bone Spring Sand is one of the dominant landing zones in the Delaware Basin for unconventional drillers and is also much more complex in nature than the 1st and 3rd sands. Increased resistivity readings suggest that carbonate input sporadically increased within the 2nd Bone Spring Sand. For these reasons, a more in depth look at the 2nd Bone Spring sand is taken in the next section with a suggestion for the nature of these increases in carbonate input. For now, it is important to note that 5 full 4th order sequences were identified within the 2nd Bone Spring Sand. The top of the sand is marked by transgression into high gamma silt and shale.

With the transition from siliciclastic to carbonate dominated deposition, the 2nd Bone Spring Carbonate begins with transgression into a relatively thin (~50 ft.) highstand carbonate before regression into higher gamma ray lowstand carbonate facies. Transgression back into another thin highstand carbonate interval follows before high amplitude regression forces another change from carbonate to siliciclastic deposition.

The 1st Bone Spring Stand is interpreted as being all deposited within one 4th order lowstand. Within these type logs the sand is only between 100-200 feet thick which is consistent, although on the thick end, of other 4th order LSTs interpreted. The gamma reading through the interval changes very rapidly between lower gamma sands

and higher gamma silts and shales. These high frequency changes could be due to higher order sea level changes. However, here it is interpreted that these fluctuations are attributed to individual turbidite flows and migrating channel patterns capped with shales deposited during periods of relative quiescence within this 4th order lowstand. There are also likely higher order cycles imprinted over this and it is possible that these higher order cycles triggered flows. Similarly, the Lower 1st Bone Spring Lime is interpreted to be largely deposited during one 4th order highstand interval underlain by a thin period of transgression.

The Avalon is a sand within the study area and was deposited at a third order lowstand within the 1st Bone Spring Lime. One full 4th order sequence is interpreted within the Avalon. Following a maximum flooding surface mid-way through the Avalon, additional lowstand sands were deposited before transgression began into the Upper 1st Bone Spring Lime.

After deposition of the Avalon sands, 3rd order transgression caused a shift back to carbonate deposition. The base of the upper 1st Bone Spring Lime is a fairly clean, blocky carbonate deposited at 4th order transgression and highstand. Following the highstand, 4th order regression seems to have increased the input of siliciclastic sediments marked by a decrease in resistivity and an increase in gamma ray reading. This is interpreted to be a 4th order lowstand before transgressing back into a 4th order highstand. The top 200 feet of the Upper 1st Bone Spring Lime is another clean carbonate capped by an abrupt change from carbonate to sand deposition. The abrupt change marks the top of the Bone Spring succession and is a 2nd order sequence boundary and unconformity.

Overall, these adapted Galloway motifs suggest that much of the internal character of the Bone Spring can be explained by 4th order sequence stratigraphy. These

4th order sequences imprinted over the 3rd order sequences that drove reciprocal sedimentation help to explain the complexity that is seen within these intervals. Figure 35 below show how these sequences correlate very well across the study area. Lithologies change within these sequences across the study area but the sequences help to correlate sediments that were being deposited at the same time. When mapping it is always tempting to see similar log signatures in nearby wells and assume that these represent connected units. However, in complex systems like the Bone Spring these units can be deposited at completely different times and can be completely compartmentalized. Compartmentalization is very important to consider when assessing reservoir rocks, especially today when operators are drilling extended laterals. It is important to know if the high-quality reservoirs observed are laterally connected and what type of changes to reservoir quality should be expected over the lateral length of the well. Furthermore, frac barriers such as carbonate rich intervals and thick shales are also important to map out laterally. It is important to characterize these barriers in order to optimally place wells, determine the correct number of wells to drill, and design completions to best develop the reservoir.

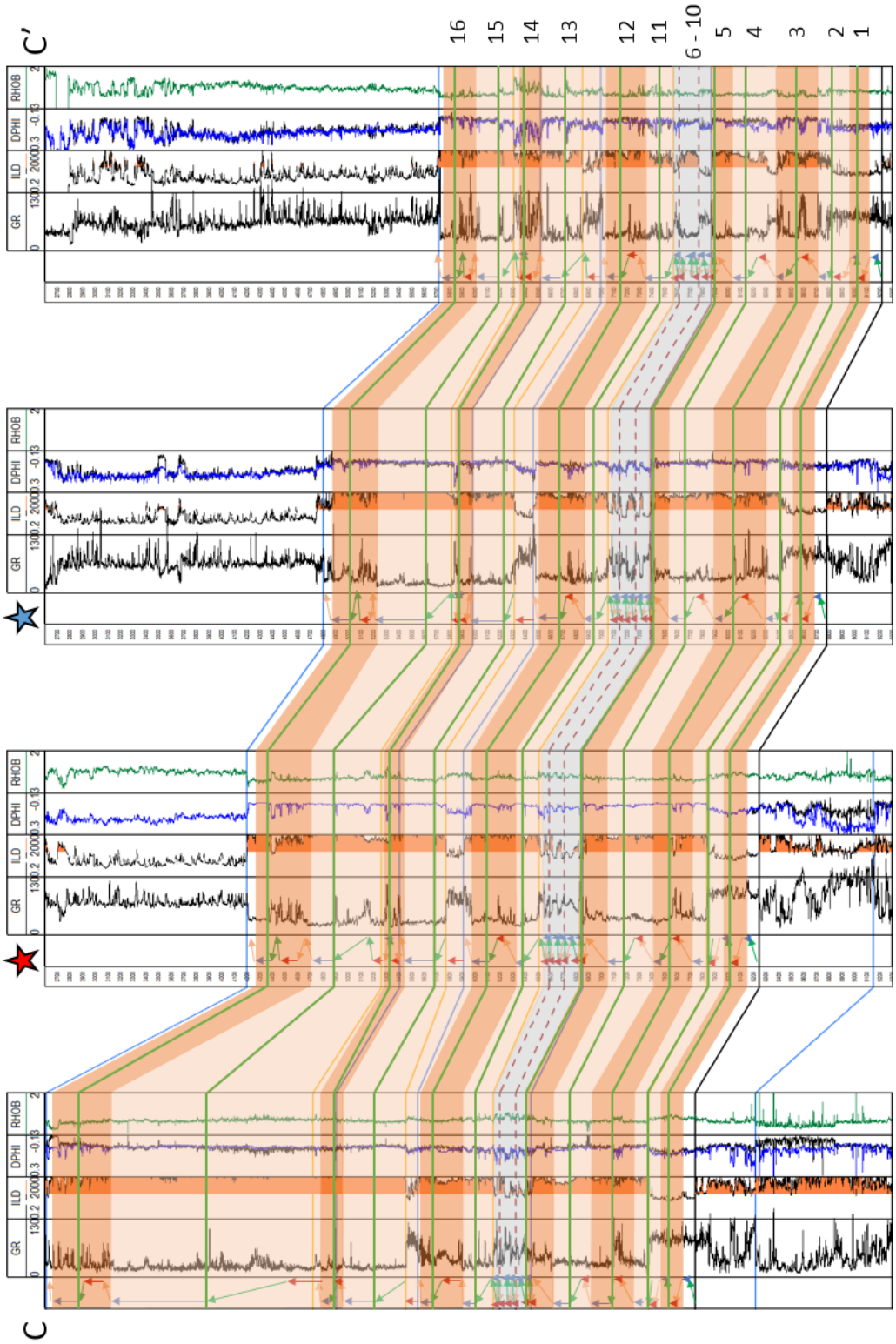

Figure 35: Cross section C – C' correlating 4th order adapted Galloway motifs across the study area. Orange highlights represent 4th order sequences. Green lines represent 4th order maximum flooding surfaces.

2nd Bone Spring Internal Stratigraphy

As was stated above, the 2nd Bone Spring is one of the most targeted sands in the Delaware Basin and is additionally the most internally complex of the Bone Spring sands. For these reasons, this study takes a more detailed look at the internal stratigraphy of the 2nd Bone Spring Sand and the impacts that stratigraphy has on reservoir quality and well planning.

Figure 36 shows cross section C – C' but is now zoomed in and focused on only the 2nd Bone Spring Sand. The logs show that the sand is much more complex than either the 1st or 3rd sands. While the internal character of those sands is generally just fluctuation between highstand silts and lowstand sands, the 2nd Bone Spring Sand also contains sporadic high resistivity intervals. These were interpreted as carbonate rich deposits within the 2nd Bone Spring Sand and this hypothesis will later be shown to be correct based on core analysis. Carbonate rich intervals within the sand are generally much lower porosity than the cleaner sands meaning it is essential to understand the depositional processes causing these carbonate rich beds. A full depositional understanding of these beds will help with predicting their occurrence in areas without a high density of well logs and also to predict their geometries so that operators can more accurately avoid these lower quality reservoir intervals to maximize well productivity.

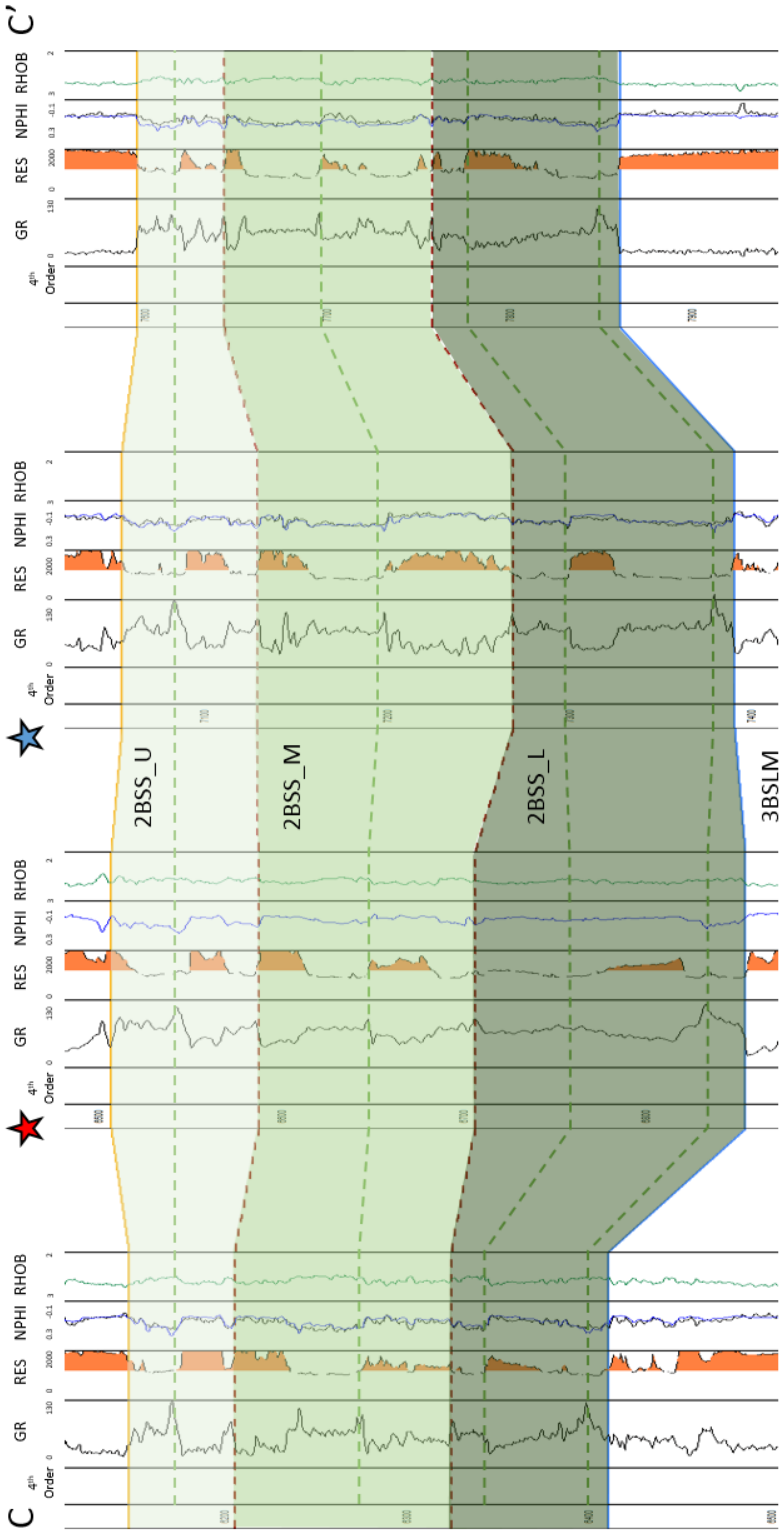

Figure 36: Cross section C – C' this time focused on the 2nd Bone Spring Sand and flattened on a flooding surface near the top of the sand. Six regionally correlatable flooding surfaces are shown with dashed lines. The dashed red lines were chosen to split the 2nd Bone Spring Sand into upper, middle, and lower members.

Six flooding surfaces were mapped regionally within the 2nd Bone Spring Sand. Of these 6 flooding surfaces, two were chosen to split the 2nd Bone Spring Sand into upper, middle, and lower members. A structural cross section of these internal members of the 2nd Bone Spring is shown in Figure 37 below. The structural cross section shows that the sand members show relatively constant thickness along dip with minor variations attributed to compensational stacking patterns. The upper and middle sands are generally thinner than the middle sand but also contain overall lower carbonate content than the middle sand making them the likely landing zones for horizontal wells. The thick, generally more carbonate rich middle sand could also act as a frac barrier between the upper and lower sands allowing for stacking or staggering of horizontal wells in the upper and lower landing zone.

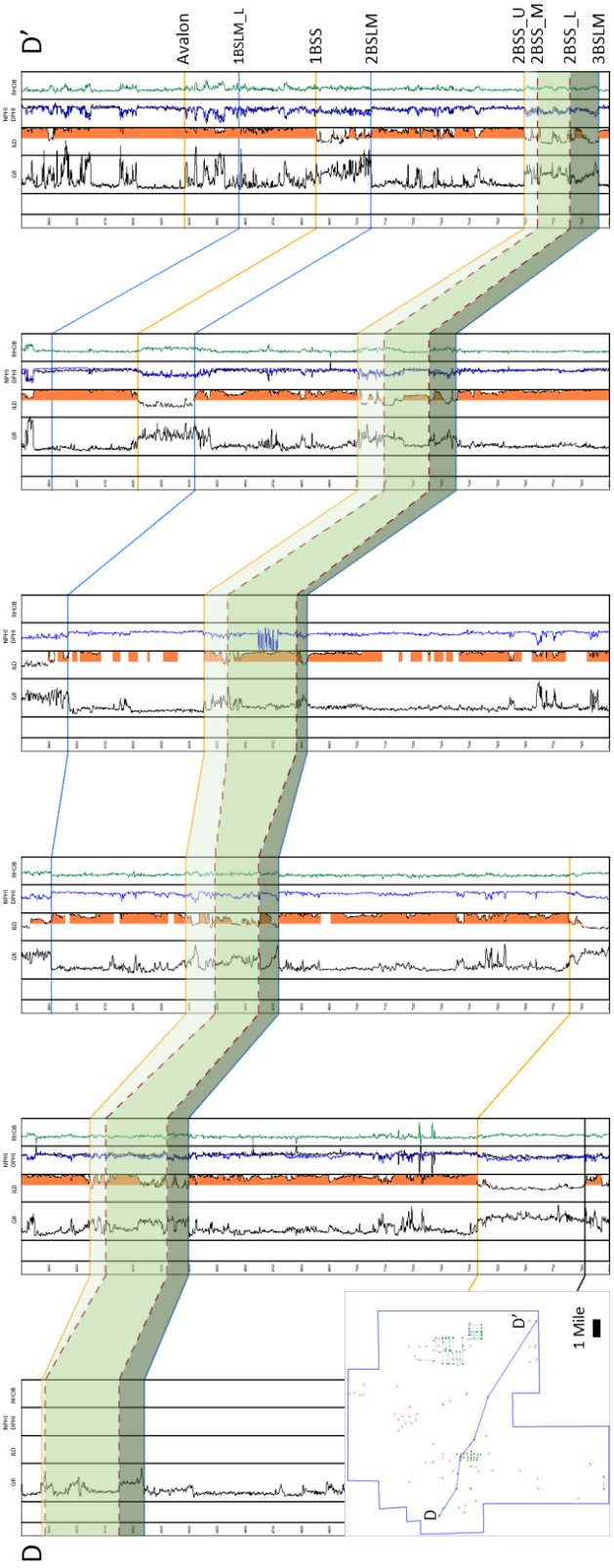

Figure 37: Structural cross section D – D' and locator map showing the internal upper, middle, and lower sands of the 2nd Bone Spring Sand.

Isopach maps of the internal sand members are shown in Figure 38. The lower sand shows a thickness trend that runs general NW to SE through the study area. The dominant source of the sand is to the northwest and this thickness trend is likely due to ponding of flows on inherited topography. The middle 2nd Bone Spring Sand shows a thickness trend that is almost the inverse of the lower sand suggesting that compensational stacking patterns played a major role in the deposition of these turbidite fan deposits. The thickest part of the upper sand lies in the eastern portion of the study area and is pooled up against the previously mentioned structural high created from the fault zone that runs through the area. The ponding of sediments on the eastern side of this structure suggests that the dominant sediment input direction may have shifted from the west to the east by the time the upper sand was being deposited. Crosby (2015) suggests that the San Simon Channel was a major source of sediment input during the 2nd Bone Spring. In the study area, it appears that sediment input dominated later in the deposition of the 2nd Sand while early sands were sourced off of the more proximal shelves to the northwest.

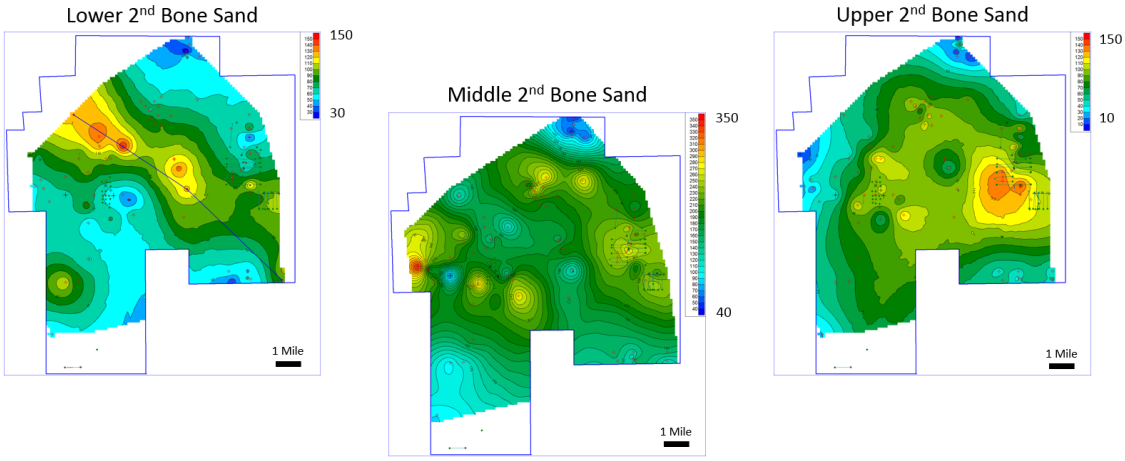

Figure 38: Isopach maps in feet of the lower, middle, and upper 2nd Bone Spring Sand intervals. Compensational stacking patterns play a significant role in controlling thicknesses.

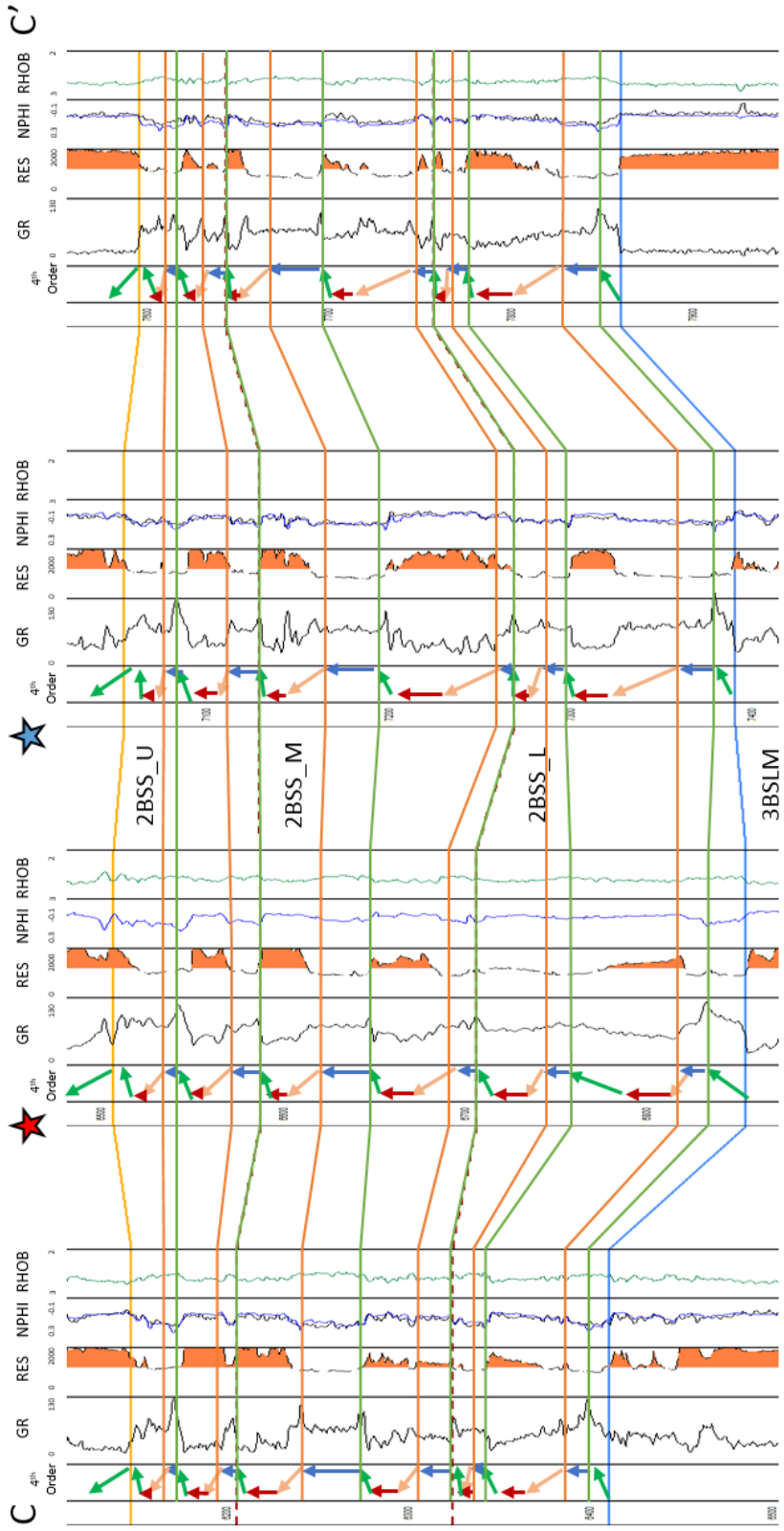

Figure 39: Cross section C – C' with 4th order sequences displayed within the 2nd Bone Spring Sand.

Figure 39 above shows the breakout of 4th order sequences within the 2nd Bone Spring Sand. Five full 4th order sequences were identified within the 2nd Bone Spring Sand and the 4th order parasequences that are identified correlate very well to observed well log facies that will be verified by core in the next section. Across the study area, 4th order highstands and transgressions tend to correlate to finer grained sands. Normally, finer grained sediments would suggest poorer reservoir quality because of lower porosity and permeability. However, the lowstand and falling stage coarser sands in the study area also correlate with higher carbonate content and lower porosities likely due to carbonate cementation. The correlation works very well across the study area but also is opposite to the 3rd order assumption that highstands cause increased carbonate input while lowstands cause increased siliciclastic input.

This investigation contends that during 4th order falling stage and lowstand systems tracts within 3rd order lowstand deposition, increased process energy, exposure of shelf/slope reefs, and erosion and incision of the shelf/slope led to increased basinal, reworked carbonate deposition. In addition, active carbonate growth at the time would have been forced downslope and moved carbonate sources closer to the basin floor. During transgression and highstand intervals, these slope reefs would have been drowned. The decrease in process energy would also lead to a reduction of erosion and incision into the shelf and slope reefs leading to decreased carbonate input into the basin and better preserved reservoir quality as observed today. An illustrative example of incision into shelf and slope reefs is shown in Figure 40 below.

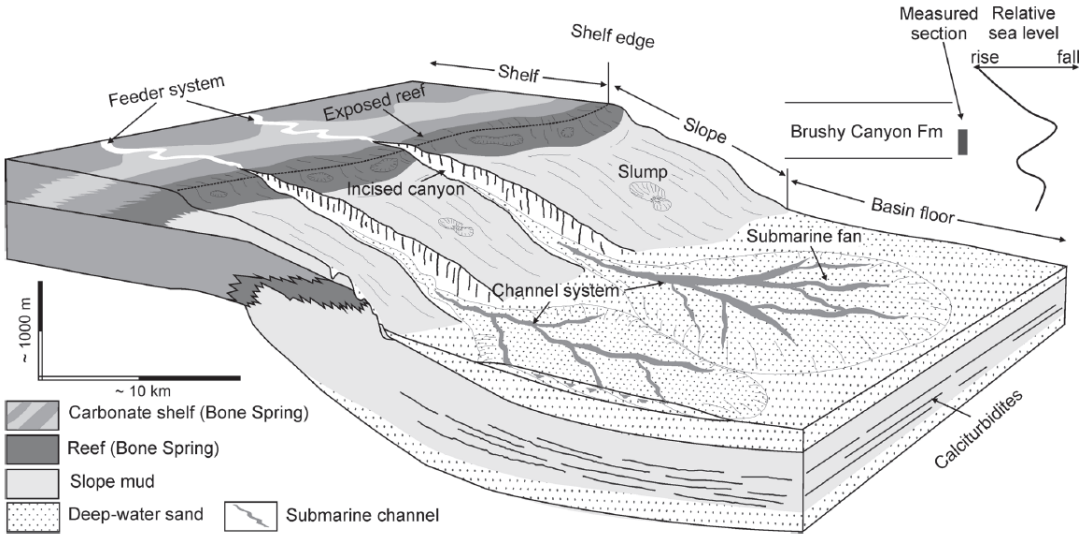

Figure 40: Illustrative example from Li et al. (2015) showing the incision and erosion of the carbonate shelf and slope during relative fall and lowstand in sea level. Incision and erosion would have caused more reworked carbonate to be deposited on the basin floor within turbite fan and channel systems.

While this study contends that falling stage and lowstand carbonate reworking is a likely mechanism for basinal carbonate deposition during a 3rd order lowstand, other explanations cannot be completely ruled out. First of all, a more traditional model of relative highstands creating more active carbonate growth cannot be completely ruled out. Some of these carbonate intervals have increased clay content as well suggesting that they could have been deposited at relative highstands in sea level. Additionally, tectonic activity associated with the major fault that runs through the study area could have triggered carbonate slope failures at any time during a sea level cycle. Therefore, this investigation argues that all of these mechanisms likely had an impact on transporting carbonates within the 2nd Bone Spring Sand. However, in this area the dominant mechanism appears to be reworking of carbonates during falling stage and lowstands in relative sea level.

The final question to be answered is why increased carbonate reworking at falling stage and lowstand systems tracts occurred during the 2nd Bone Spring Sand and was not as prevalent in the 1st or 3rd sands. Figure 41 below shows the relative sea level curve created by Li (2015). The relative sea level curve shows that the lowest relative sea level during Bone Spring deposition would have been around the time of 2nd Bone Spring Sand deposition while the 1st and 3rd sands would have been deposited at relatively higher sea level. The lower sea level would have created maximum exposure of the carbonate shelf during 2nd Bone Spring Sand deposition and therefore would have made the 2nd Bone Spring Sand more prone to carbonate reworking due to incision and erosion at 4th order falling stages and lowstands in sea level.

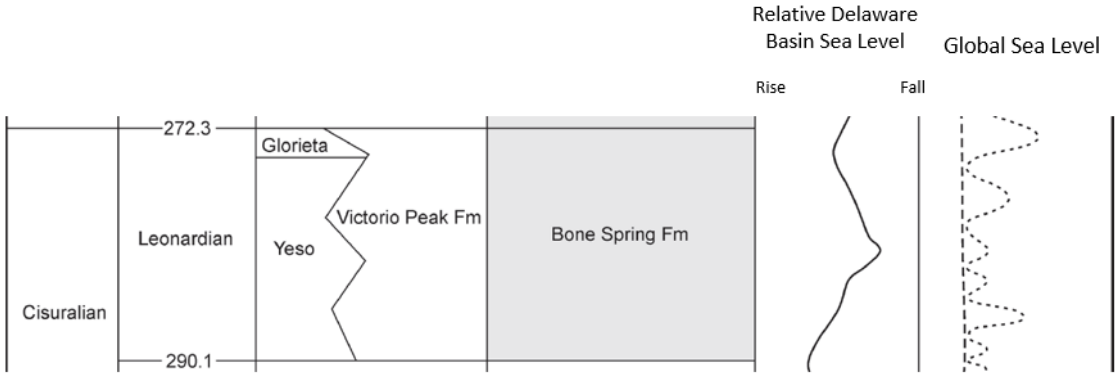

Figure 41: Relative sea level curve during Bone Spring deposition adapted from Li et al., 2015. 2nd Bone Spring Sand was deposited at the lowest relative sea level when compared to the 1st and 3rd Sands.

Using high resolution sequence stratigraphy, this study has attempted to identify high quality reservoirs and landing zones within the 2nd Bone Spring. The upper and lower members tend to have lower carbonate content and higher porosities and therefore are the higher quality landing zones. However, thickening and porosity reduction in the middle sand helps to create a frac barrier between the upper and lower members. In some areas this could lead to completely isolated reservoirs in the upper and lower sands and

suggests that stacking of horizontal wells in these areas could be justified. Identifying the mechanisms for carbonate transport into the basin also allows for more confident mapping of those lower quality reservoirs through the 2nd Bone Spring. Identification of the lower quality reservoir extents gives geologists more confidence when steering horizontal wells and they can better avoid drilling laterals in lower quality pay. More in depth analyses like this could also be done on the other formations within the Bone Spring in future studies.

As a whole, well log sequence stratigraphy using an adapted Galloway model that accounted for lithology allowed this study to create a more accurate sequence stratigraphic model of the Bone Spring in the study area than has previously been done. The improved model allows for more accurate mapping of the intervals within the Bone Spring and better identification and prediction of high-quality reservoir facies and frac barriers. As operators continue to develop the prolific 1st, 2nd, and 3rd Bone Spring Sand intervals in the Delaware Basin, this full understanding of 4th order depositional processes should help to better identify high quality landing zones for horizontal wells and help operators with more accurate development planning and prediction of the optimal number of wells needed per section in each landing zone for effective reservoir drainage.

Core Analysis

This investigations's core analysis constrains and verifies that the facies observed in core agree with the facies inferred from the previous well log study. Referring to Figure 21, the two cores used in this study are highlighted with yellow squares. The first core observed below cored the 2nd Bone Spring Sand and the top portion of the 3rd Bone Spring Lime. The second core cored most of the 1st Bone Spring Sand interval. The

remainder of this section displays selected intervals of the high-resolution core photography provided by Devon Energy with brief facies descriptions and discussion on how those facies tie with the sequence stratigraphic model created. For confidentiality reasons exact depths of the core photos are not provided.

2nd Bone Spring Sand

Figures 42 and 43 below shows some selected core photos with their position marked on the log. The first figure focuses on the high resistivity beds within the 2nd Bone Spring Sand and confirms that they are beds with higher carbonate content. Fourth order sequences are also illustrated for comparison to the core data. Core porosity data was available for this core and is displayed. The high resistivity carbonate beds correlate with sharp decreases in core porosity and therefore have much poorer reservoir quality than the lower resistivity sand intervals.

Sample A comes from the base of the core and is within the 3rd Bone Spring Lime. It is a lime wackestone to mudstone consistent with the assumed carbonate apron style of deposition during relative highstands. Sample B is deposited during falling stage systems tract and is characterized as a debris flow. Large allochthonous carbonate blocks are observed in a lime mudstone matrix. The debris flow is capped with a shale suggesting a period of quiescence between debris flows and confirms that during falling stage systems tracts, debris flows were being initiated and transporting eroded carbonate blocks into the basin along with carbonate mud sourced from the slope.

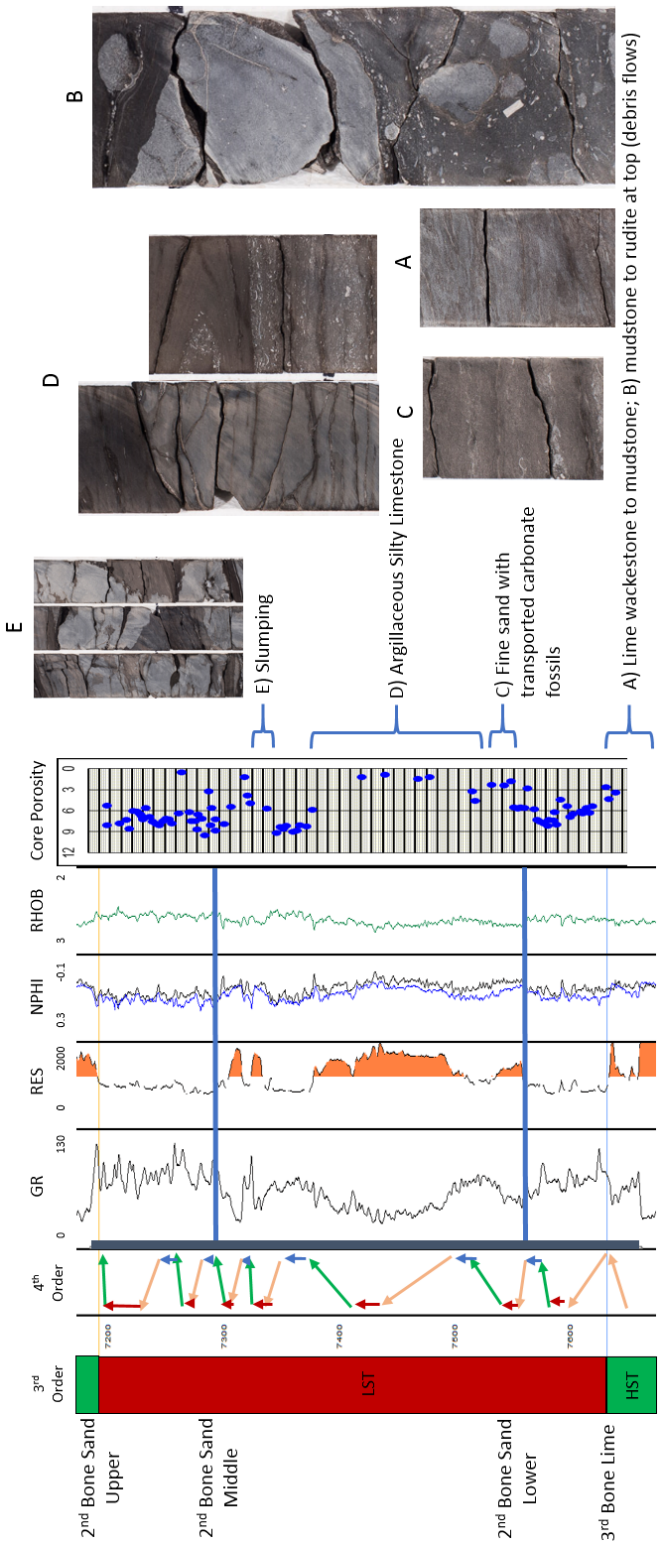

Figure 42: 2nd Bone Spring Sand high resistivity carbonate bed core analysis. Selected core photography illustrating position on the log and within 4th order sequences.

Sample C comes from the middle 2nd Bone Spring Sand and is another higher resistivity bed interpreted to be deposited at a falling stage and lowstand in sea level. The facies is described as fine sand with transported carbonate fossils in the form of carbonate shells. Given that most of the interval is characterized as very fine to silt sized sand, the larger grain size is consistent with deposition at a higher process energy during a relative lowstand in sea level. Transported carbonate fossils are consistent with inferred erosion from the slope and shelf and deposition on the basin floor.

Sample D is a selected sample from the thick high resistivity interval within the middle 2nd Bone Spring Sand. This interval is generally described as an argillaceous, silty limestone. Transported carbonate shells are also visible over the interval in higher abundance than in sample C. Folded beds and soft sediment deformation are common. Debris flows capped by silt to shale beds are also common. All of the transported carbonate material was clearly eroded from the slope and redeposited on the basin floor in agreement with the theory that these beds were deposited during falling stage and lowstand in sea level when erosion of the carbonate shelf and slope would be at a maximum. Beds with increased clay content also appear to be mass transport deposits suggesting that they are reworked sediments from the underlying highstand in sea level.

Sample E rounds out the high resistivity beds. These two carbonate rich beds at the top of the middle 2nd Bone Spring Sand are clearly slump deposits with very large transported carbonate blocks in a mud matrix. These slumps were likely triggered at lowstand times or early rise in sea level and is consistent with the proposed sequence stratigraphic model.

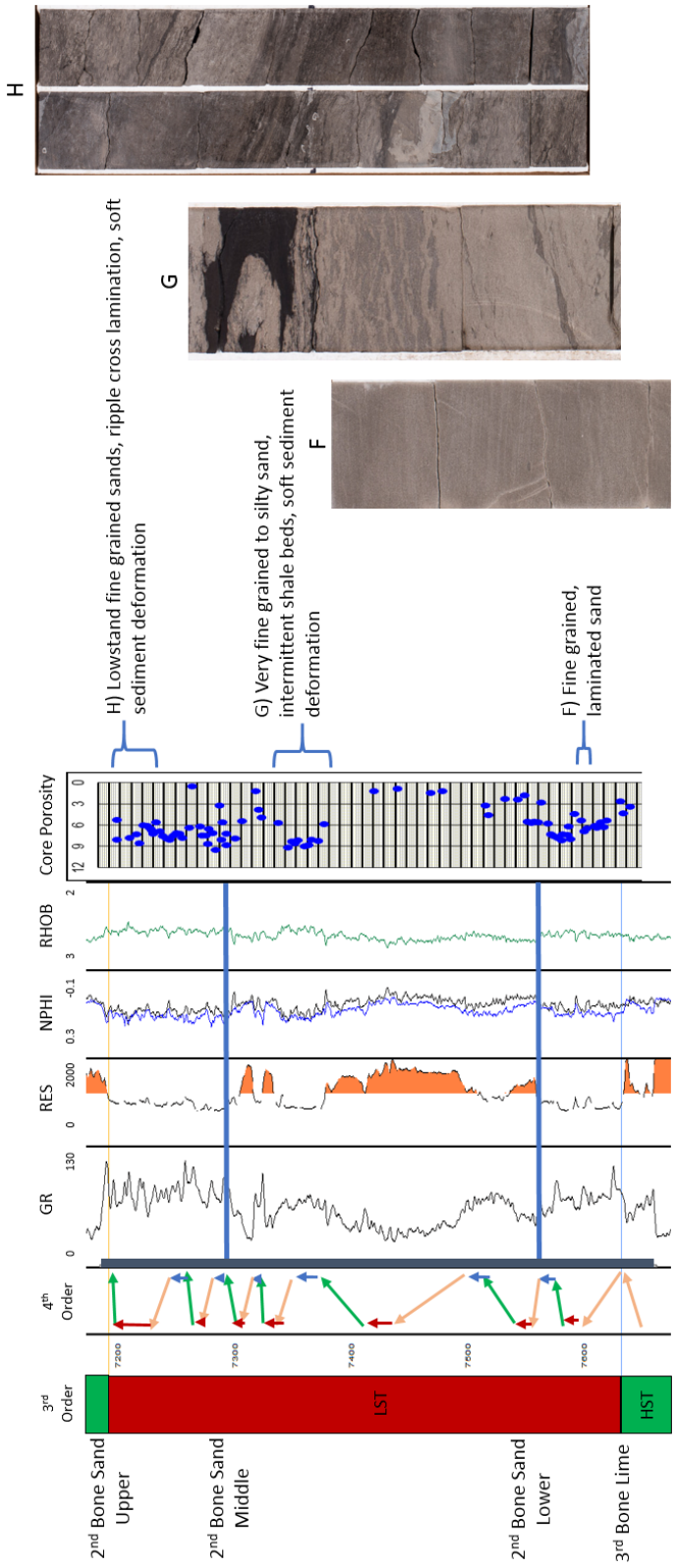

Figure 43: Selected core photos from the low resistivity sand beds within the 2nd Bone Spring Sand shown in the same format as figure 42.

Figure 43 above shows core samples F-H taken from the lower resistivity sandy intervals with the 2nd Bone Spring Sand. Sample F is taken from the lower 2nd Bone Spring Sand and is characterized by fine grained, laminated sand deposited at lowstand times. Increased carbonate content is not observed in the area during this particular lowstand allowing for the preservation of porosity.

Sample G is taken from a transgressive to highstand sand interval within the middle 2nd Bone Sand. The sample is described as very fine grained to silty sand with intermittent shale beds and soft sediment deformation. The decrease in overall grain size is consistent with the argument that these cleaner sands were deposited during relatively higher sea level than the coarser grained sands with higher carbonate content.

Finally, sample H was taken from a 4th order lowstand interval in the Upper 2nd Bone Spring Sand. The sample is fine grained sand with ripple cross lamination consistent with deposition under the higher process energy of a relative lowstand in sea level.

Overall, core analysis within the 2nd Bone Spring confirms that resistivity spikes are associated with higher carbonate input. Carbonate beds with coarser associated sand grain sizes are consistent with a model suggesting they were deposited at a relative lowstand in sea level. Lowstand sands that do not show an increase in carbonate content and transgressive to highstand sands show higher porosity and are therefore better reservoir targets. Not all lowstands correlate with an increase in carbonate content suggesting that the fans of increased carbonate content are localized and sporadic consistent with a mass transport style of deposition. The magnitude of these 4th order changes in sea level also likely played a role in carbonate reworking with larger amplitude changes leading to more erosion and incision and more carbonate reworking.

The localization of these fans also means that a clean reservoir sand can laterally grade into a sand with higher carbonate content and lower porosity making it all the more important to effectively map out these intervals before drilling wells.

1st Bone Spring Sand

The facies associated with 4th order parasequences in the 1st Bone Spring Sand are remarkably consistent throughout the interval. Therefore, Figure 44 below shows just two examples from the core. Sample I is a regression to lowstand sand facies showing millimeter scale laminations and very fine to fine grained sand with black mudcaps. These sands are generally finer grained than the lowstand sands of the 2nd Bone Spring Sand and is consistent with the theory that the 2nd Bone Spring Sand was deposited at an overall lower relative sea level than the 1st Bone Spring Sand. Thin laminations capped with mud suggest high frequency of flow events during the 1st Bone Spring Sand. Sample J is taken from one of the transgression/highstand intervals and is a black siltstone with dark grey planar to wavy laminations and pyrite nodules. The facies is consistent with the assumed facies deposited at relative highstands in sea level. These interbedded silts and shales in the 1st Bone Spring have a higher TOC content and could have acted as source rocks within the 1st Bone Spring Sand sourcing the more porous sand intervals. However, these thick shales can also act to isolate the reservoir sands from each other. Therefore, when developing the 1st Bone Sand operators should design stimulations to overcome these barriers, land wells in staggered landing zones, or purposely drill up section through the shales in order to connect to the most reservoir.

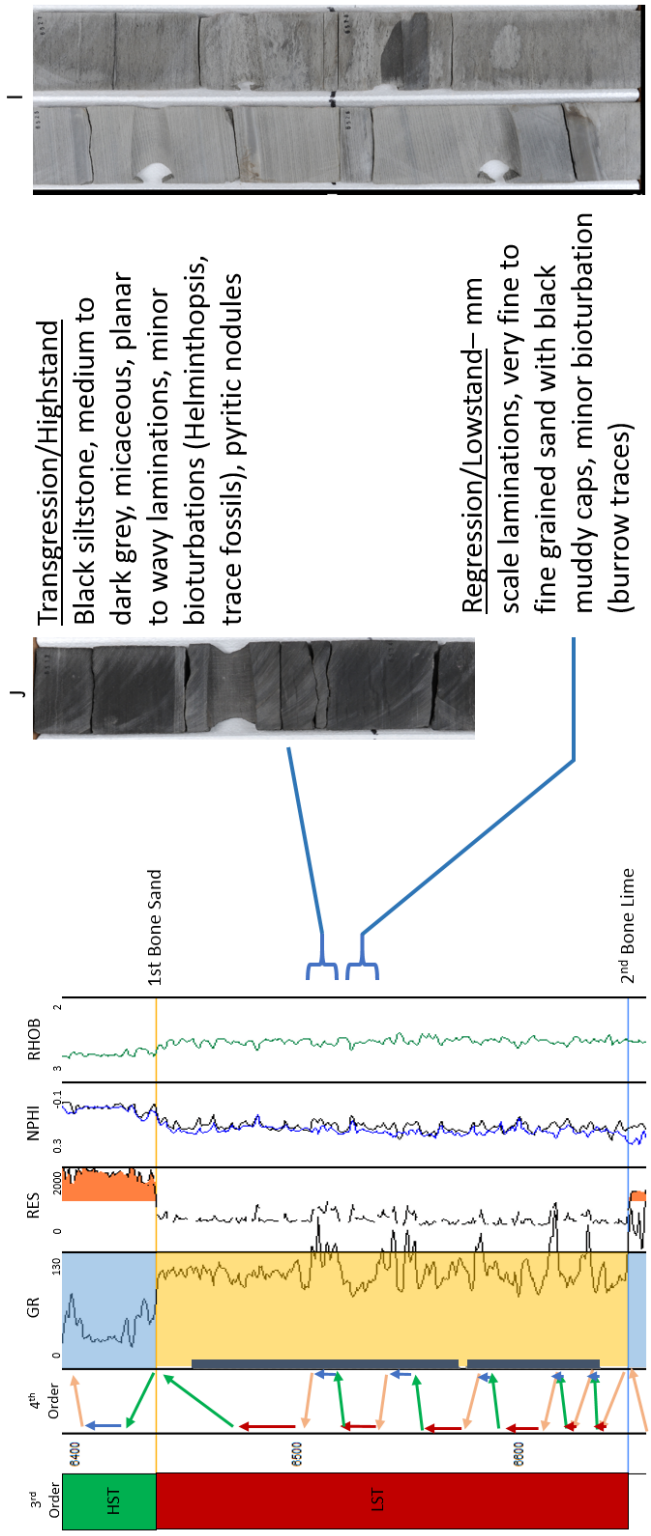

Figure 44: Core samples from the 1st Bone Spring Sand core highlighting transgressive/highstand shales and regressive/lowstand sands.

Seismic Analysis

The final pillar of this study focuses on the seismic data that was provided. Over the last two sections a solid foundation has been built using well logs and core data. These data types by nature provide better vertical resolution than seismic data can provide. Well logs and core data have helped to analyze the vertical stacking patterns within the Bone Spring and helped to build a sequence stratigraphic model that gives a good idea of the facies present throughout the Bone Spring. Now, seismic analysis attempts to look at a much more detailed lateral picture given that its horizontal resolution is much higher than could ever be achieved using well logs or core data. This section will walk through the picking of relevant horizons within the Bone Spring, the creation of time structure and isochron maps, the seismic stratigraphic analysis that was done, and will finish with an attempt to tie the adapted Galloway sequence stratigraphic motifs to the seismic.

Horizons, Time Structure Maps, and Isochrons

Before any horizons could be picked, the first step in the seismic analysis was to complete synthetic well ties across the study area. Figure 21 shows the locations of the sonic logs that were used to create synthetic ties. The high density of synthetic ties allowed for very accurate interpretation of the horizons relevant to Bone Spring deposition. Additionally, before interpreting horizons the seismic was checked for major structures that could impact horizon picking. Small faults are observed throughout the survey, but most are too small to impact horizon picking. However, one major fault zone was identified and mapped along the eastern side of the study area which has been shown in map view earlier and is also shown on Figure 45 below.

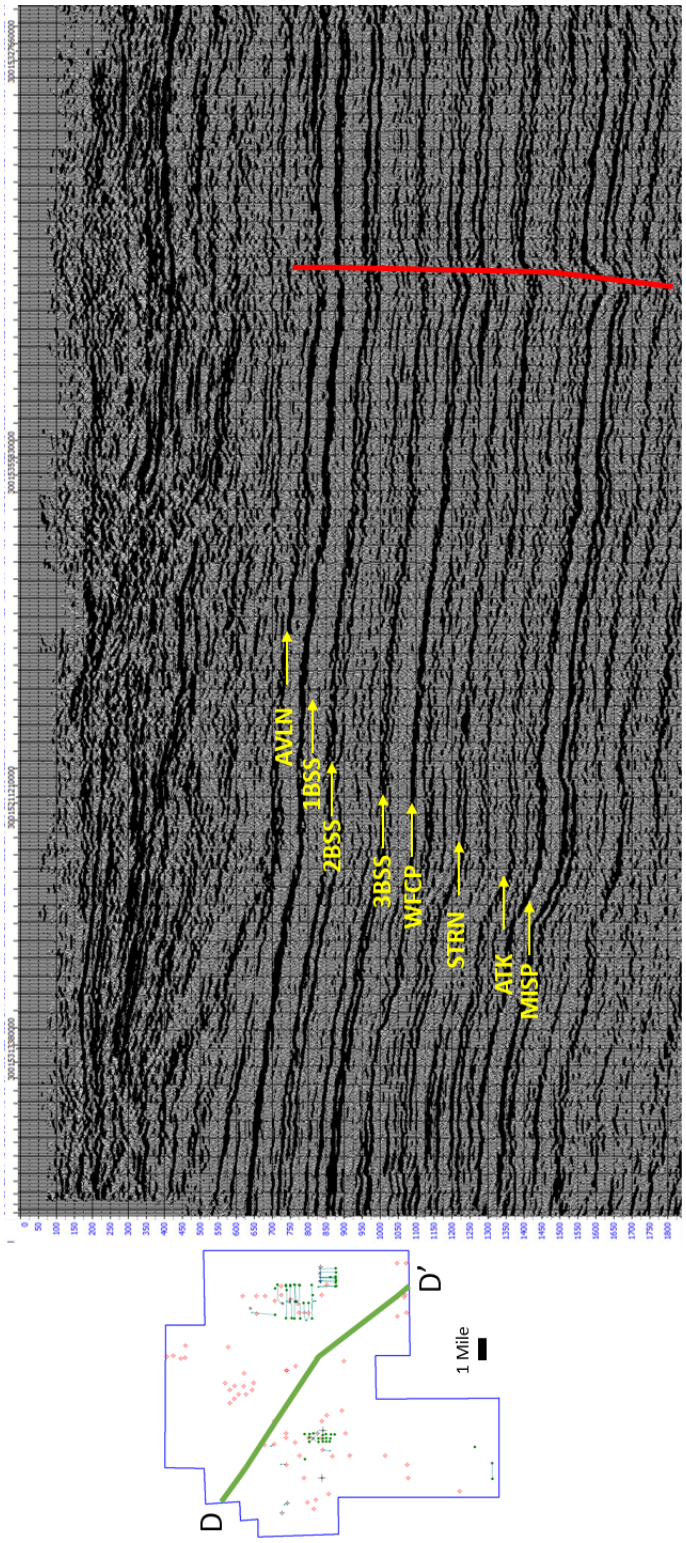

Figure 45: Arbitrary dip line D – D' through the study area. The data is European polarity convention. Some relevant reflectors are identified. The red line marks the position of the major N – S trending fault.

Figure 45 shows some of the immediately obvious reflectors that stand out within the survey. Below the Bone Spring, the Wolfcamp, Strawn, Atoka, and Miss Lime reflectors are obvious. Within the Bone Spring reflectors marking the top of each change in dominant lithology can be interpreted. These interpreted horizons along with the overlain synthetic well ties are shown in Figure 46. The 1st Bone Spring Sand is so thin that it is only one reflector thick on seismic. Therefore, a horizon representing the top of the 1st Bone Spring Sand and 2nd Bone Spring Lime is picked and that is what is used to create the isochron and time structure maps. However, an approximate 2nd Bone Spring Sand interpretation was estimated and added in on most of the subsequent arbitrary lines.

Arbitrary line D – D' follows a very similar to the dip cross section C – C' that was used in the well log section and allows for comparison of the two dip lines. The two cross sections are shown to be very similar, however the seismic version gives a much clearer picture of the bed dips and structural changes that occur across the study area. For example, the fault zone is immediately obvious on seismic and its impact on deposition can be seen. Mapping the fault would be nearly impossible with the level of well density that was provided for this study. However, the internal thicknesses and general trends within the formations are very similar leading to the conclusion that the synthetic ties are correct and the correct horizons were interpreted. Additionally, the seismic data reveal that by the time of deposition of the 1st Bone Spring Lime, the Victorio Peak Reef is beginning to prograde into the study area.

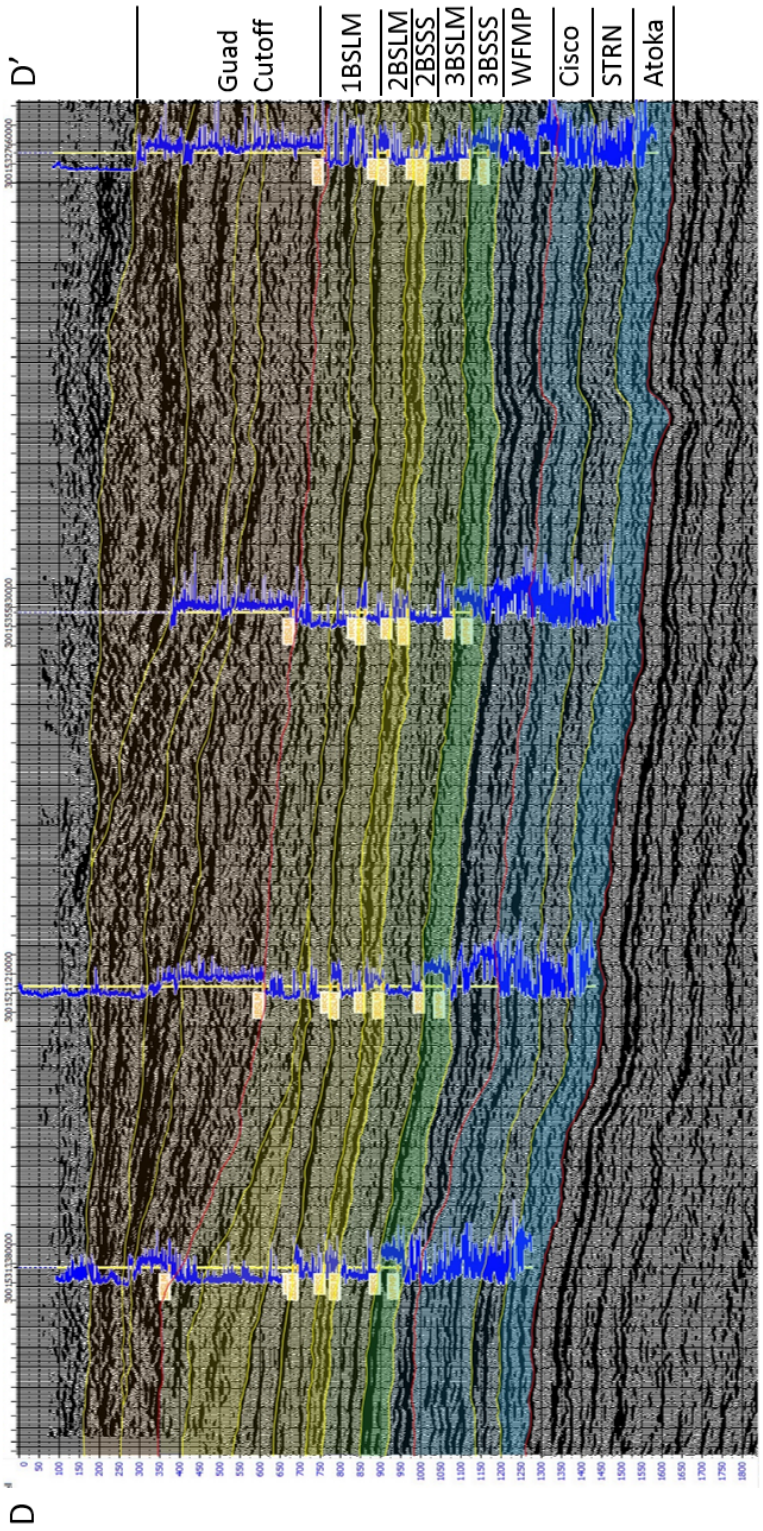

Figure 46: Arbitrary Line D – D' with all relevant horizons interpreted and synthetic well ties with tops overlain. Formations are colored and labeled along the right side.

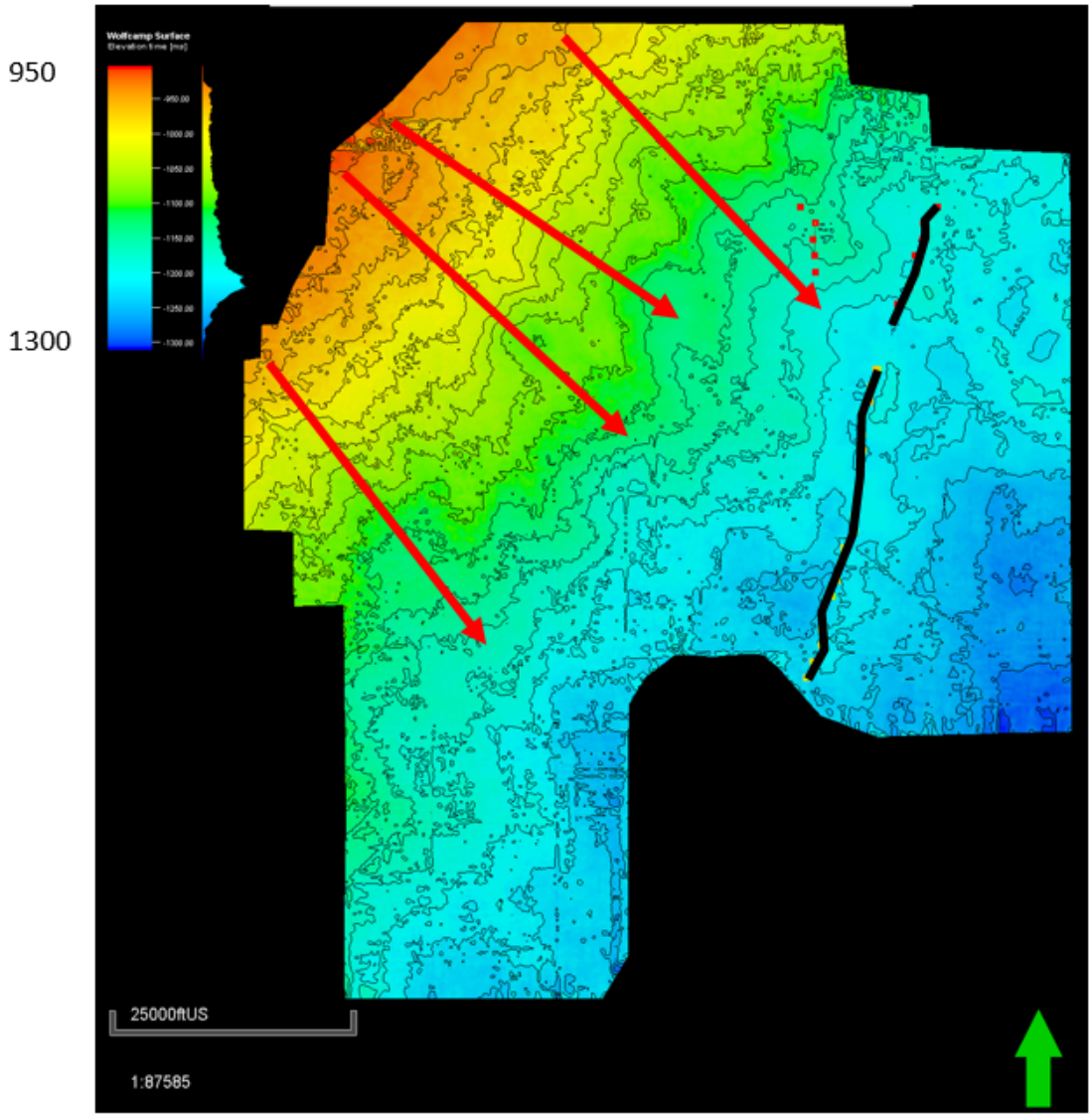

Figure 47: Time structure map in two way travel time in ms on the top of the Wolfcamp. This surface represents the base of the Bone Spring and is therefore very important because it is the surface that the Bone Spring was deposited onto. The four red arrows represent potential valleys that could have acted as incised canyons feeding sediment into the basin. The black line to the left illustrates the picked fault zone.

Figure 47 above shows a time structure map on the top of the Wolfcamp. The major fault zone running through the study area is highlighted in black and valley like structures running perpendicular to depositional dip are highlighted with red arrows. Structure mapping using well logs previously showed far less detail than what is shown

above. It was postulated from those well log structure maps that potential valleys could be seen running perpendicular to depositional dip that would have acted as sediment pathways for sediment flows. The Wolfcamp time structure map shows these incised valleys in much more detail. Four major valleys can be seen on the structure map separated by ridges. Subsequent isochron maps will show that inherited topography from the top of the Wolfcamp had a significant impact on Bone Spring deposition. The valleys observed at the Wolfcamp level seem to carry through the other time structure maps as well. Although they migrate slightly, it is evident that these valleys were active sediment pathways throughout Bone Spring deposition. Crosby (2015) contended that these valleys were likely influenced by the natural spur and grove topography of the shelf carbonates with incised valleys preferentially forming in the carbonate groves. This study corroborates Crosby's theory with the seismic maps showing the incised valleys in more detail.

The local structural high and offsetting local structural lows created by the major fault that runs through the area are also seen in more detail on the time structure map than on the well log structure maps. The structural high runs through the study area in an approximate N-S orientation on the east side of the study area. The local high that is formed separates two structural lows on either side of the fault. Subsequent isochrons will show that this was an important depositional feature throughout Bone Spring deposition suggesting that the fault was active during deposition. Sediments thin over the structural high created and thicken to the east and west where relative structural lows were formed.

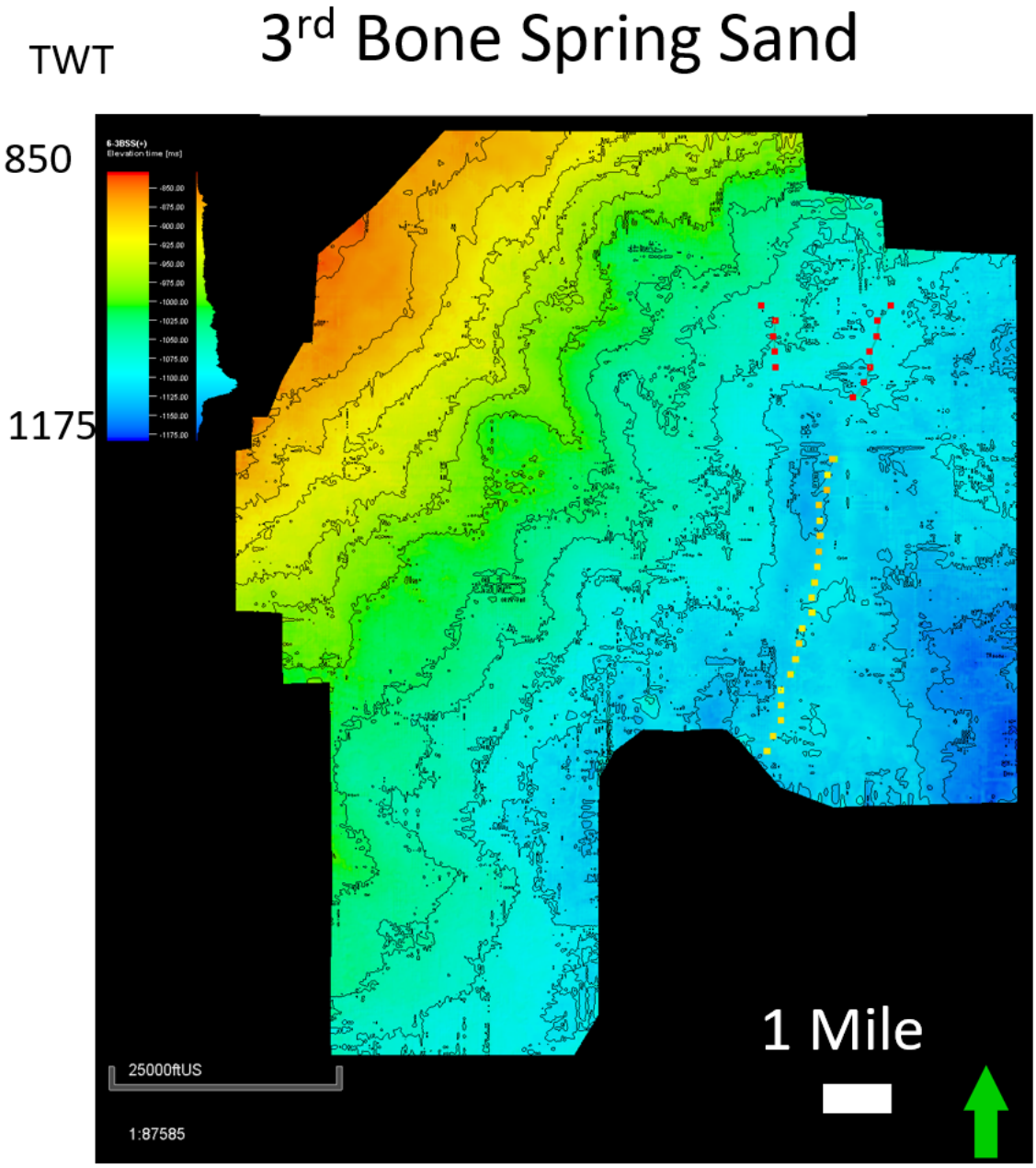

Figure 48: Time structure map (TWT in ms) on the top of the 3rd Bone Spring Sand.

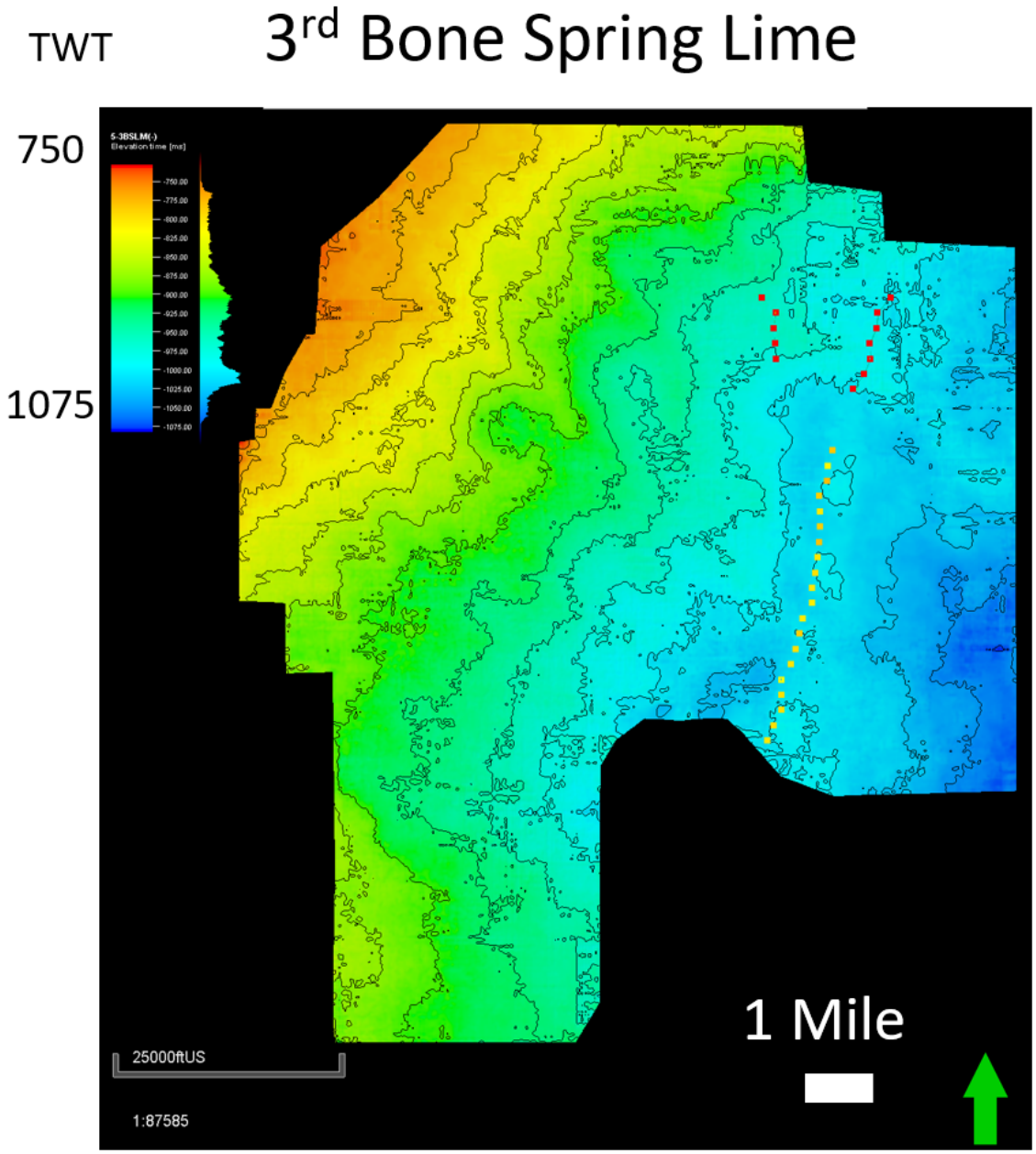

Figure 49: Time structure map on the top of the 3rd Bone Spring Lime.

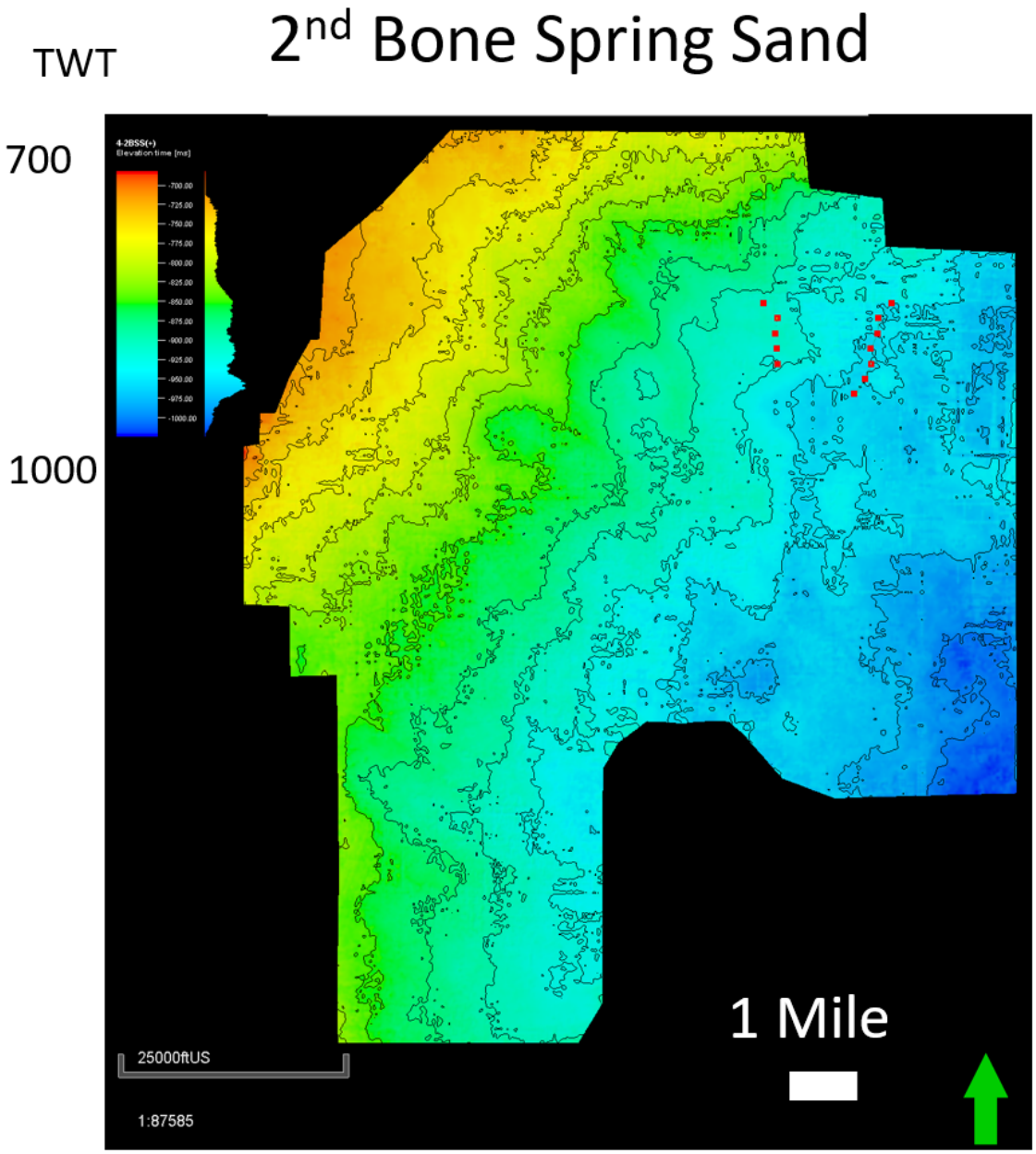

Figure 50: Time structure map on the top of the 2nd Bone Spring Sand.

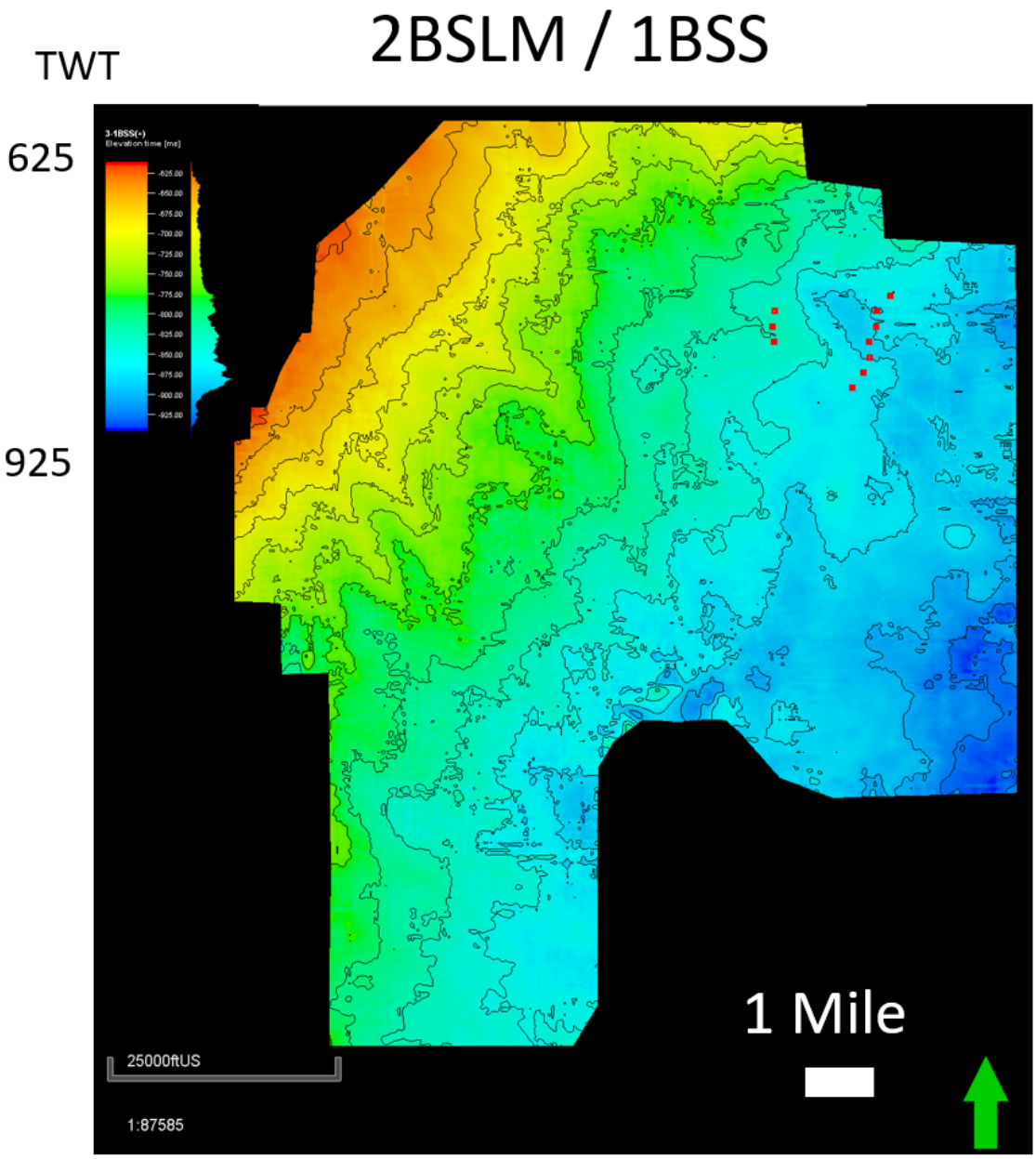

Figure 51: Time structure map at the 2nd Bone Lime/1st Bone Sand horizon.

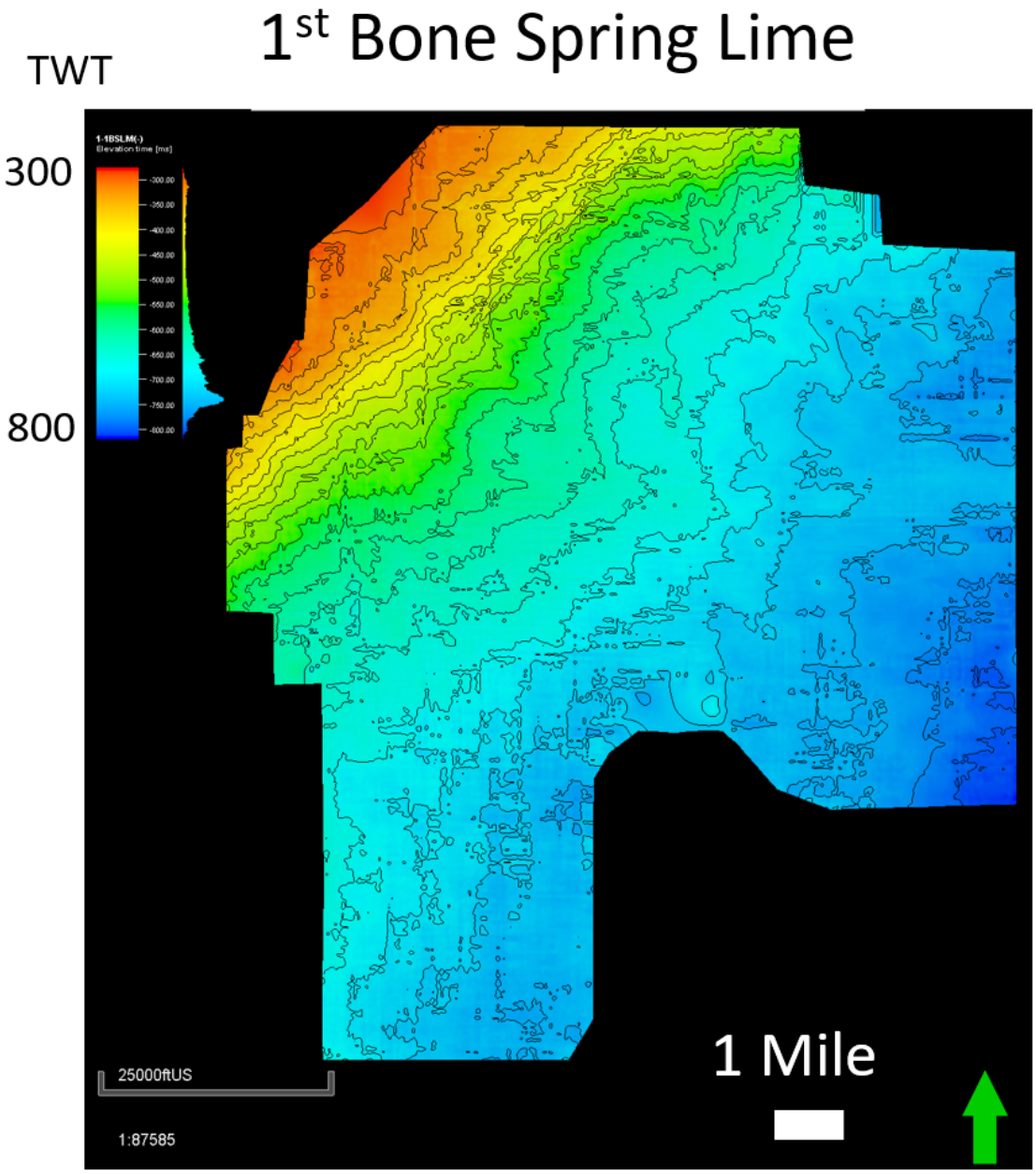

Figure 52: Time Structure map on the top of the 1st Bone Spring Lime.

Figures 48-52 above show the internal time structure maps on the tops of the prominent Bone Spring horizons that were picked. The incised valleys mentioned above can be shown to carry through the maps with only slight migration over time. Additionally, the major fault system on the eastern side of the study area can be seen to

carry through early Bone Spring deposition only dying out by approximately the 1st Bone Spring 3rd order sequence.

Figures 53-57 below shows the isochron maps made from these internal Bone Spring horizons. The isochrons represent the same intervals as the isopach maps shown earlier except for the 2nd Bone Spring Lime and 1st Bone Spring Sand being combined. However, because the 1st Bone Spring Sand is so thin, major thickness trends on this map are associated with the 2nd Bone Spring Lime. The thick portions of the 3rd Bone Spring Sand on the isochron map line up very well with the isopach maps with the thickest portions being to the far southwest and southeast of the study area. However, significant thinning occurs to the northwest toward the shelf whereas the isopach maps show a subtle thickening trend in that direction that is believed to be due to the well density being much lower in the northwest corner of the study area. Many vertical wells in the northwest corner of the study area targeted the 2nd Bone Spring Sand and therefore do not drill through the third Bone Spring Sand. Some of the sporadic thickness trends in the area are likely observed in well logs and due to the low well density these contours extend to the edge of the study area rather than showing the true thinning of sediments onto the shelf. The isochron model is also more consistent with what would be expected of lowstand siliciclastic fan deposition.

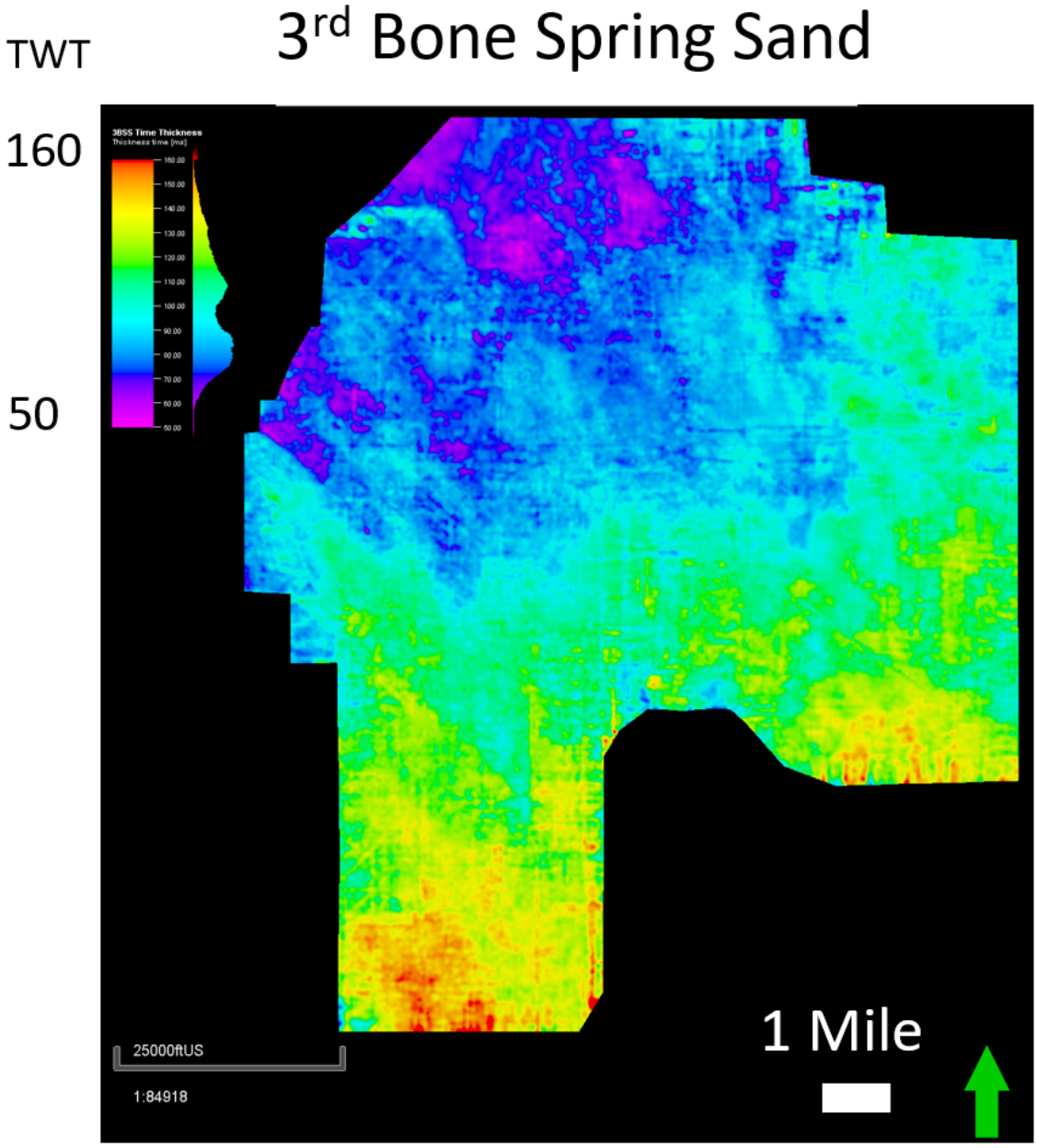

Figure 53: Isochron map (TWT in ms) of the 3rd Bone Spring Sand.

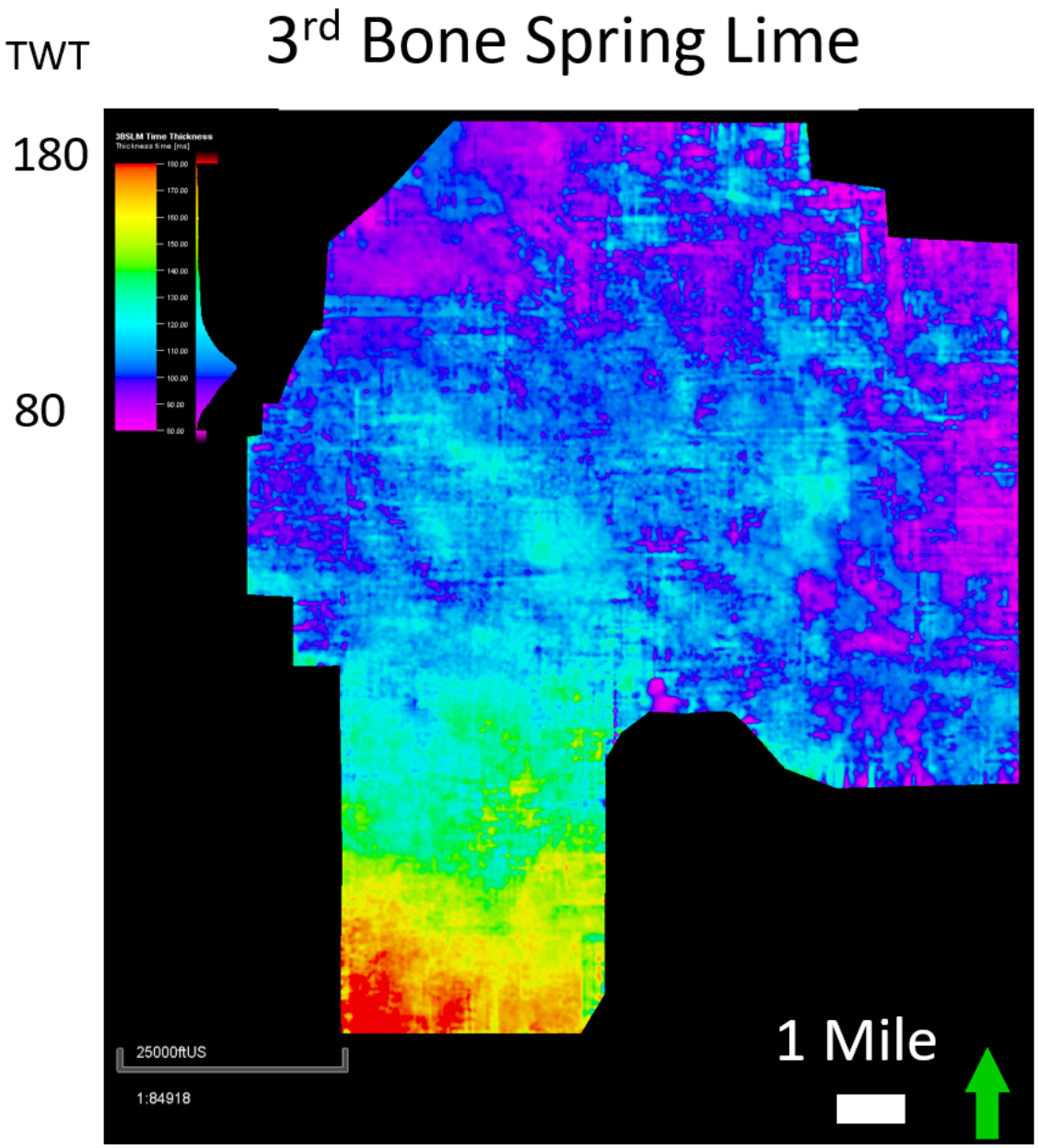

Figure 54: Isochron of the 3rd Bone Spring Lime.

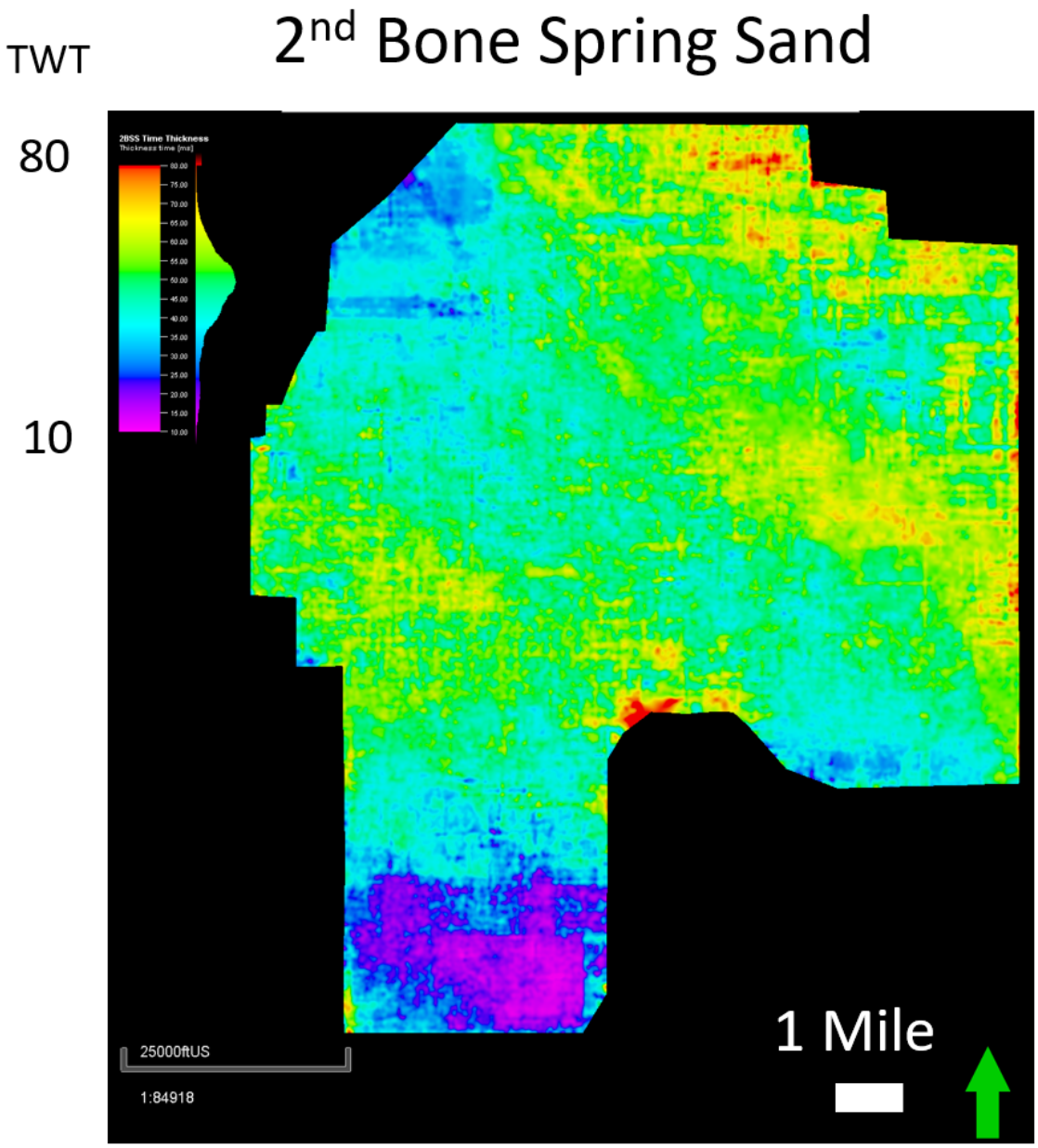

Figure 55: Isochron map of the 2nd Bone Spring Sand.

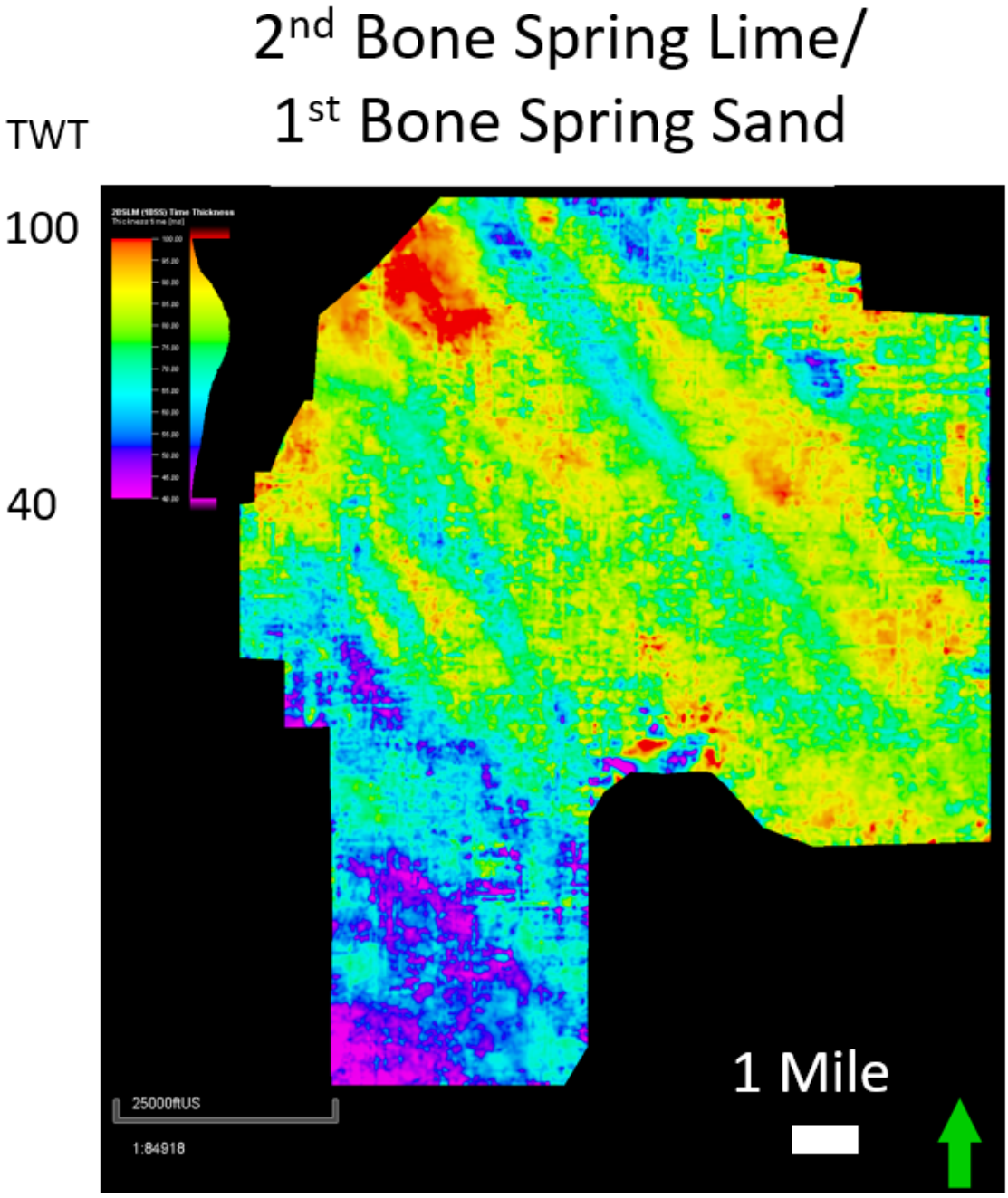

Figure 56: Isochron map of the 2nd Bone Spring Lime/1st Bone Spring Sand.

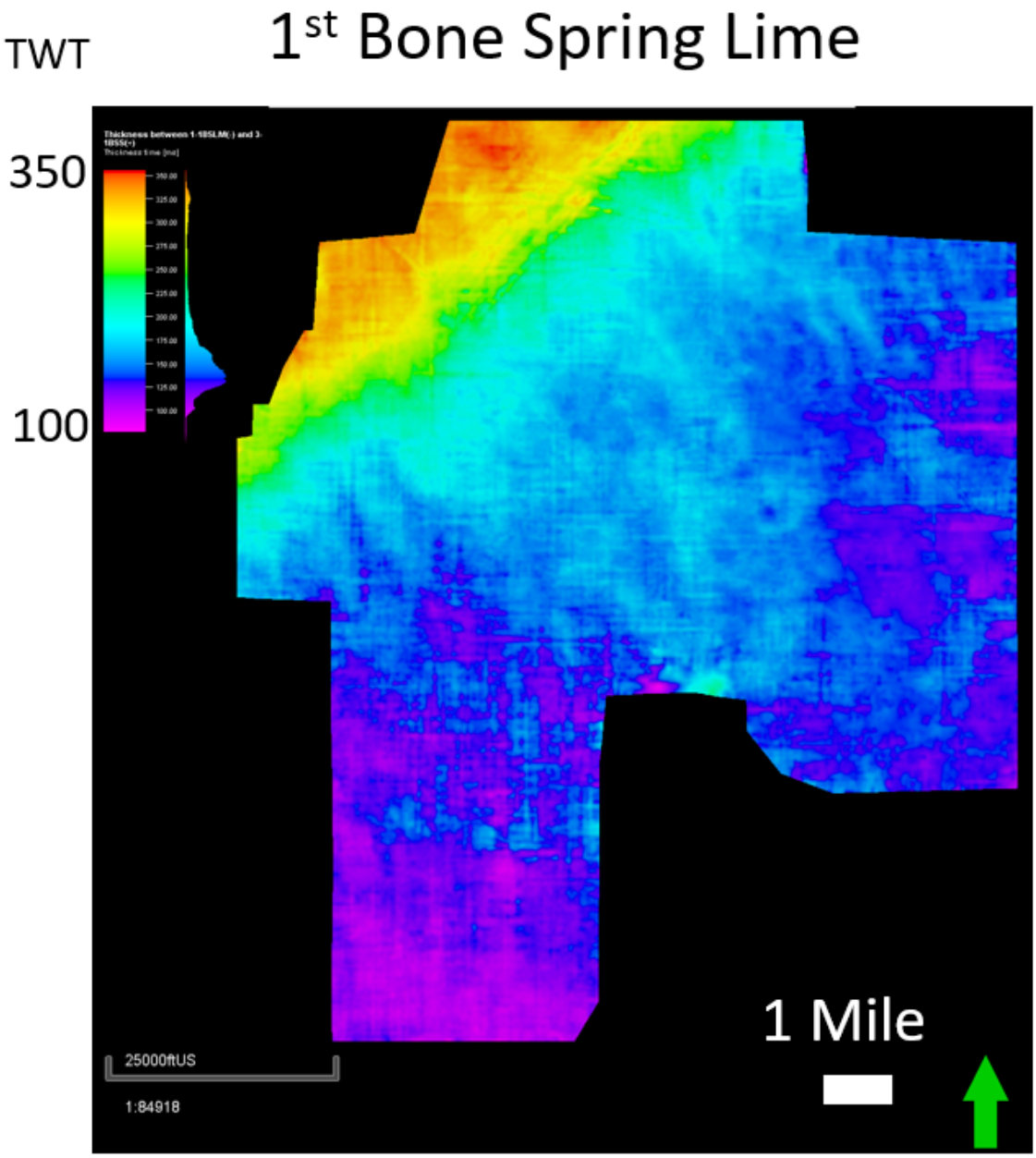

Figure 57: Isochron map of the 1st Bone Spring Lime.

The isochron of the 3rd Bone Spring Lime agrees with the isopach map shown earlier and confirms that at the time of deposition the carbonate shelf had not forestepped

into the study area. The thickest trends in the carbonate occur in the southwest portion of the study area implying that these sediments were deposited as a more distal carbonate apron shedding off of the slope in the west. The 3rd lime thins rapidly across the major fault in the area suggesting that these flows coming from the west were confined to the west side of the fault and did not breach the relative high formed by the structure.

The 2nd Bone Spring Sand also shows a similar thickness pattern to the isopach maps though more detail can be seen. The thickness trend on the eastern side of the fault agrees with the isopach map and the theory that the San Simon channel could have been a sediment source for these flows in the 2nd Bone Spring Sand. Another thick trend on the western side of the fault was likely sourced from the western shelf/slope. The thinnest portion of the 2nd Sand occurs in the southwest corner of the study area where the 3rd lime was the thickest confirming that compensational stacking patterns were a major driver in Bone Spring deposition.

The 2nd Bone Spring Lime isochron map shows much more detail than the previous isopach map although the same general trends can be observed. Thickening of the carbonate to the north and northwest imply that the carbonate shelf is forestepping closer to the study area at this time. The thinnest area of the 2nd lime is also in the southwest corner of the study area confirming that sedimentation had not yet completely overcome the relative high created by the 3rd Bone Spring Lime. Linear thickness trends running perpendicular to depositional dip are also more obvious on the isochron map than on the isopach. These trends will be discussed in more detail later but are interpreted as linear carbonate fans being shed off the shelf/slope to the northwest.

Finally, the isochron of the 1st Bone Spring Lime confirms that by this point in Bone Spring deposition, the shelf had prograded very close to if not into the study area as

is shown by drastic thickening of the interval to the northwest. However, the isochron map shows carbonate apron deposits being shed off the reef in much more detail. Lobe shaped thickness trends coming off the shelf are consistent with a carbonate apron style of deposition. In addition, thinner parts of the carbonate shelf to the northwest line up with the previously interpreted incised valleys that continue down through the stratigraphic section all the way to the Wolfcamp which provides additional evidence for the theory that these incised valleys originated at grooves formed from carbonate spur and groove topography.

Figure 58 below is an interpreted view of the 3rd Bone Spring Sand isochron side by side with the lowstand turbidite sand depositional model proposed by Li et al. (2015). The red arrows on the map are the same red arrows marking the positions of incised valleys on the Wolfcamp structure map above. These valleys tend to line up with thickness trends in the 3rd Bone Spring Sand implying that these valleys were active sediment transport mechanisms to move siliciclastic sediments through the shelf reef and onto the basin floor. The most active of these channels during 3rd Bone Spring deposition based on the thickness of sediments seems to be the incised valley furthest to the south.

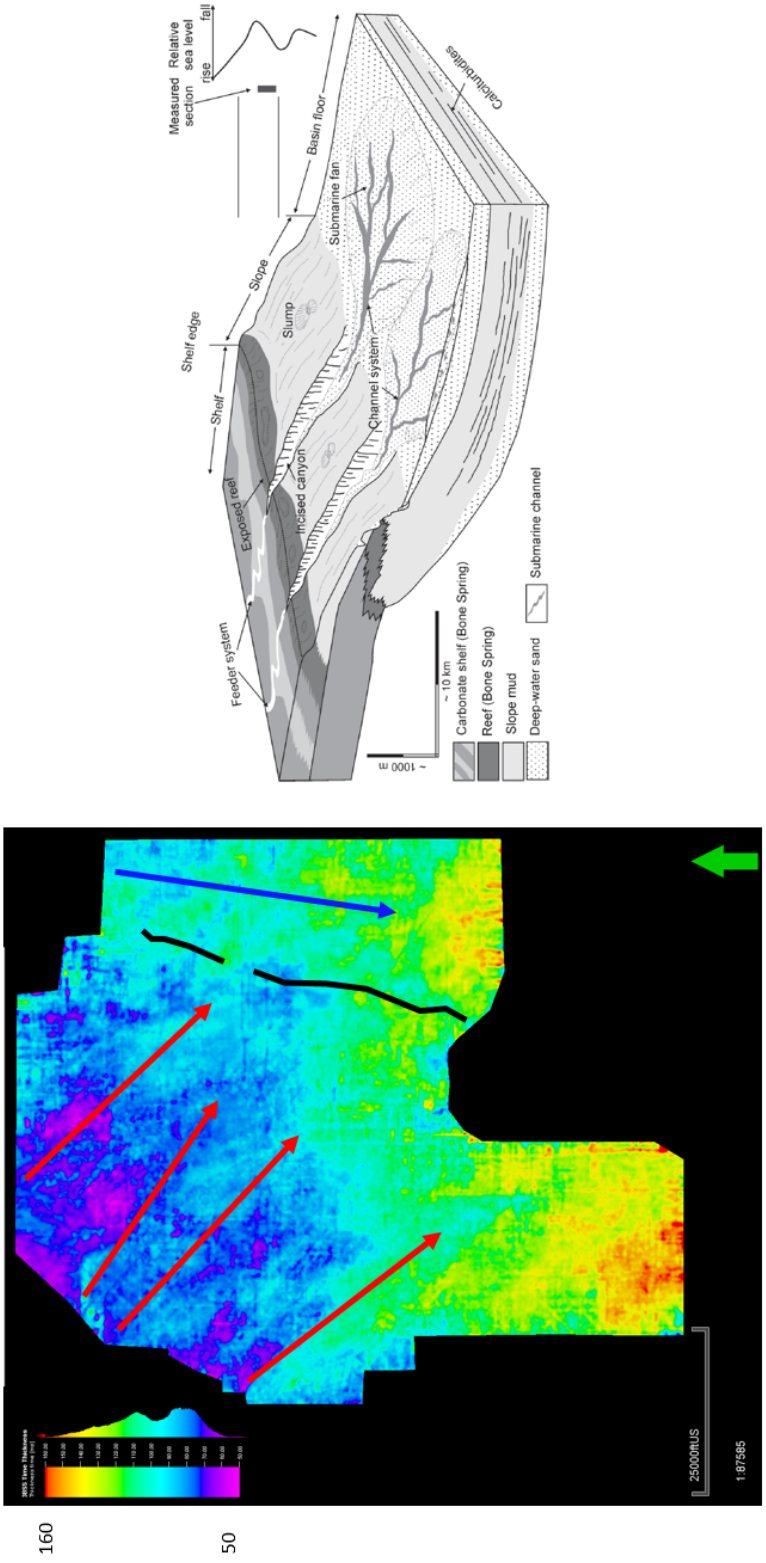

Figure 58: Detailed and interpreted isochron map of the 3rd Bone Spring Sand and the assumed depositional model illustrating the controls on deposition of these sands (Li et al., 2015).

The depositional model shown above also agrees with the observed isochron map because siliciclastic sediments are shown to thin onto the slope. The thickest portions of the sand are either within the submarine incised valleys or at the base of the valleys where the sediment flows spread out into basin floor fans. Additionally, the major fault running through the area appears to have had a major impact on 3rd Bone Spring Sand deposition. Thickness trends on either side of the fault and a relative thinning of the sediments over the structural high created by the fault show that the fault was active during deposition. Additionally, a thickness trend moving to the north on the eastern side of the fault implies a potential second sediment source coming from the north or northeast. These could have been sediments being shed off the northern shelf/slope or they could have also been sourced from the San Simon Channel to the northeast as is proposed by Crosby (2015).

Figure 59 is similar to Figure 58 but now shows the 2nd Bone Spring Lime isochron with the same interpreted valley features and fault system. The illustrative model of highstand deposition during the Bone Spring created by Li et al. (2015) is also shown. The 2nd Bone Spring Lime isochron shows much more linear flows than is shown in the siliciclastic basinal turbidites of the 3rd Bone Spring Sand. These flows are consistent with Li's (2015) model of linear carbonate fans being shed off of the slope during relative highstands in sea level. Additionally, these fans also seem to be sourced from the same incised valley features observed in the 3rd Bone Spring Sand confirming that inherited topography from the Wolfcamp had a significant impact on Bone Spring deposition and helped to control sediment sources throughout Bone Spring deposition.

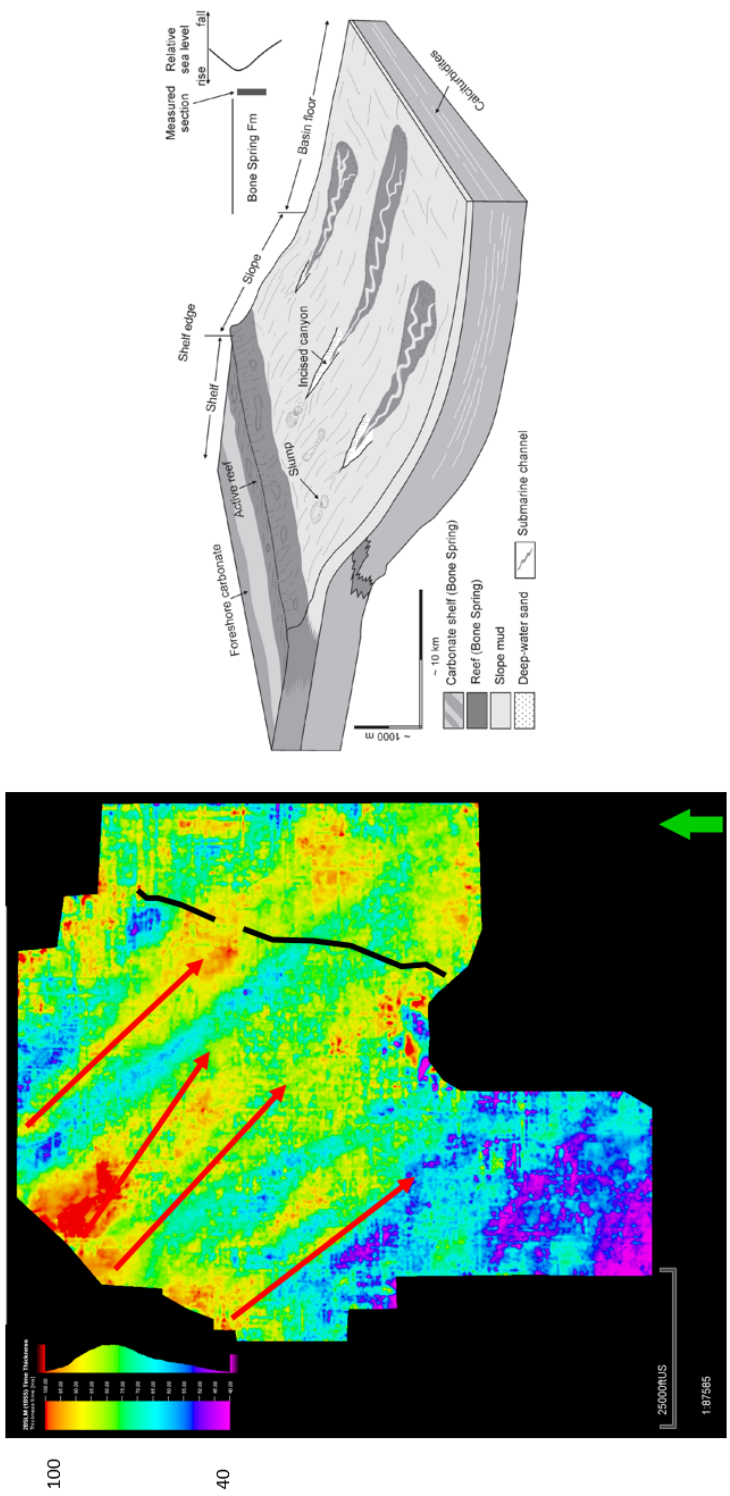

Figure 59: Isochron of the 2nd Bone Spring Lime with red arrows representing locations of valleys consistent with the previous figures. Also shows an illustrative model done by Li et al. (2015) representing highstand deposition during the Bone Spring.

Another interesting aspect of these flows is how they seem to interact with the fault running through the study area. The linear flow furthest to the north seems shows a thickness trend on the western side of the fault, thinning over the local high caused by the fault, and then another thickness trend in the local low on the eastern side of the fault. These thickness trends suggest that this flow or amalgamation of flows was large enough to fill in the structural relief on the western side of the fault, breach the structural high, and continue filling the structural low to the east.

Overall these two examples help to confirm the depositional model for the Bone Spring with siliciclastic basin floor fan deposits at 3rd order lowstands and linear carbonate flows and carbonate apron deposition during 3rd order highstands in sea level. Throughout Bone Spring deposition the carbonate shelf is prograding closer to the study area and likely reaches the far northwestern portion of the study area by 1st Bone Spring deposition meaning that later facies are more consistent with more proximal portions of carbonate and siliciclastic mass transport deposition.

Seismic Stratigraphy

With the depositional model confirmed and refined using seismic time structure maps and isochron maps, seismic stratigraphic analysis was performed with the goal of tying the well log sequence stratigraphy to the seismic data. In order to do this, terminations were picked across the study area confirming the assumed 3rd order sequence boundaries determined from well logs could be picked on seismic as well. These terminations and sequence boundaries are shown on the seismic in Figure 60 below.

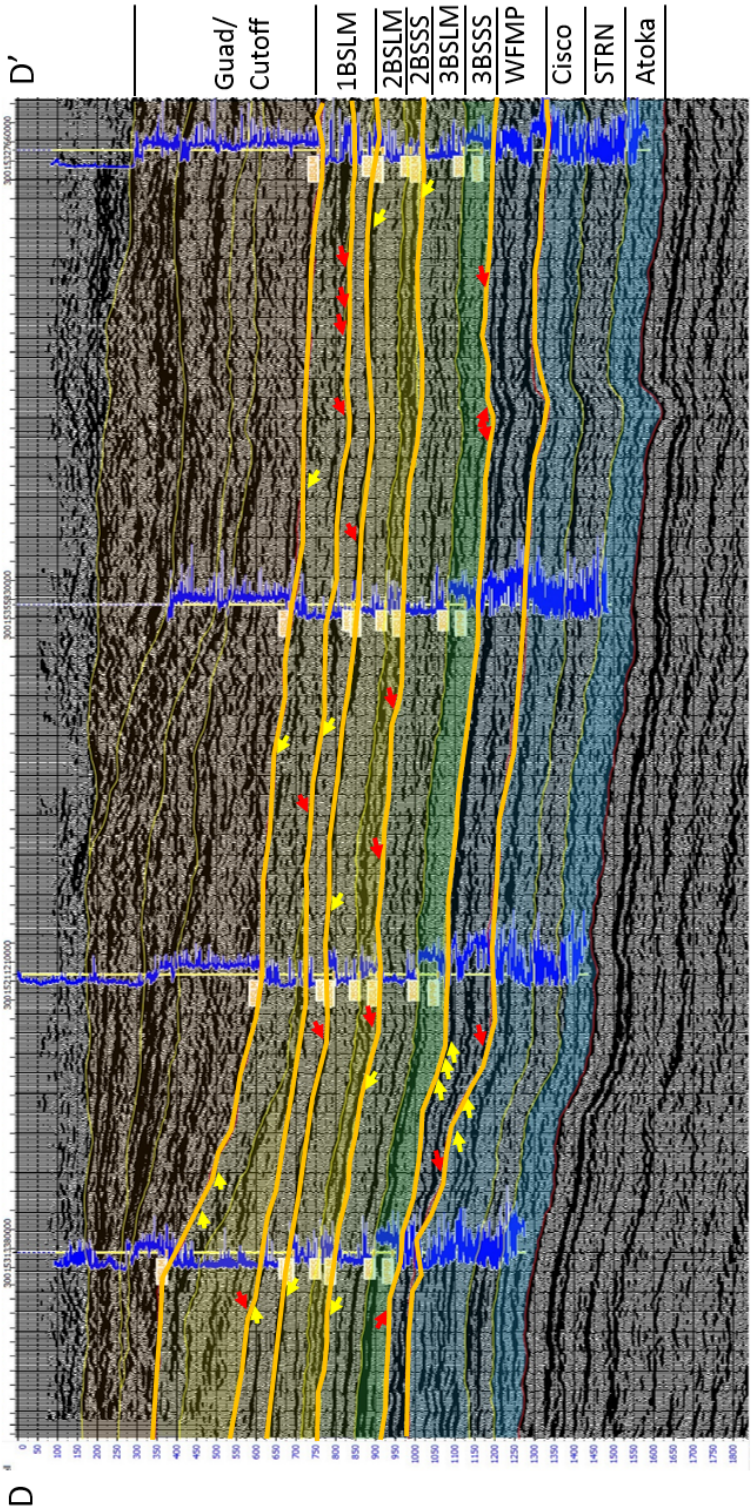

Figure 60: 3rd order seismic sequence boundaries overlain on arbitrary line D – D'. Yellow arrows represent top terminations while red arrows represent bottom terminations.

Terminations can be much more difficult to pick with onshore data than with offshore data not only because of the seismic data quality but because onshore seismic lines are usually much shorter than offshore lines which means less of the overall depositional system is seen. However, upon close analysis, upper and lower terminations can be picked identifying the four 3rd order sequences of the Bone Spring. As long as multiple top and bottom reflectors terminate into another reflector, this horizon can be interpreted as a sequence boundary. As expected, the sequence boundaries within the Bone Spring interval line up with the tops of highstand carbonates.

Within the Bone Spring interval top and bottom terminations are mostly associated with toplap and downlap given that these successions are relatively conformable. However, the sequence boundaries marking the base and top of the Bone Spring interval are 2nd order unconformities and therefore are expected to be more erosional than the contacts within the Bone Spring. Top terminations associated with erosional truncation are observed at both the top Wolfcamp sequence boundary and the top of the Bone Spring sequence boundary. In many places, seismic downlap and onlap are observed in a pattern that is consistent with mass transport deposition and are likely showing the extents of amalgamated basin floor fan systems in the lowstand sand intervals. With this analysis confirming the four third order sequences within the Bone Spring observed using well log sequence stratigraphy, an attempt to compare higher order sequence stratigraphy was carried out.

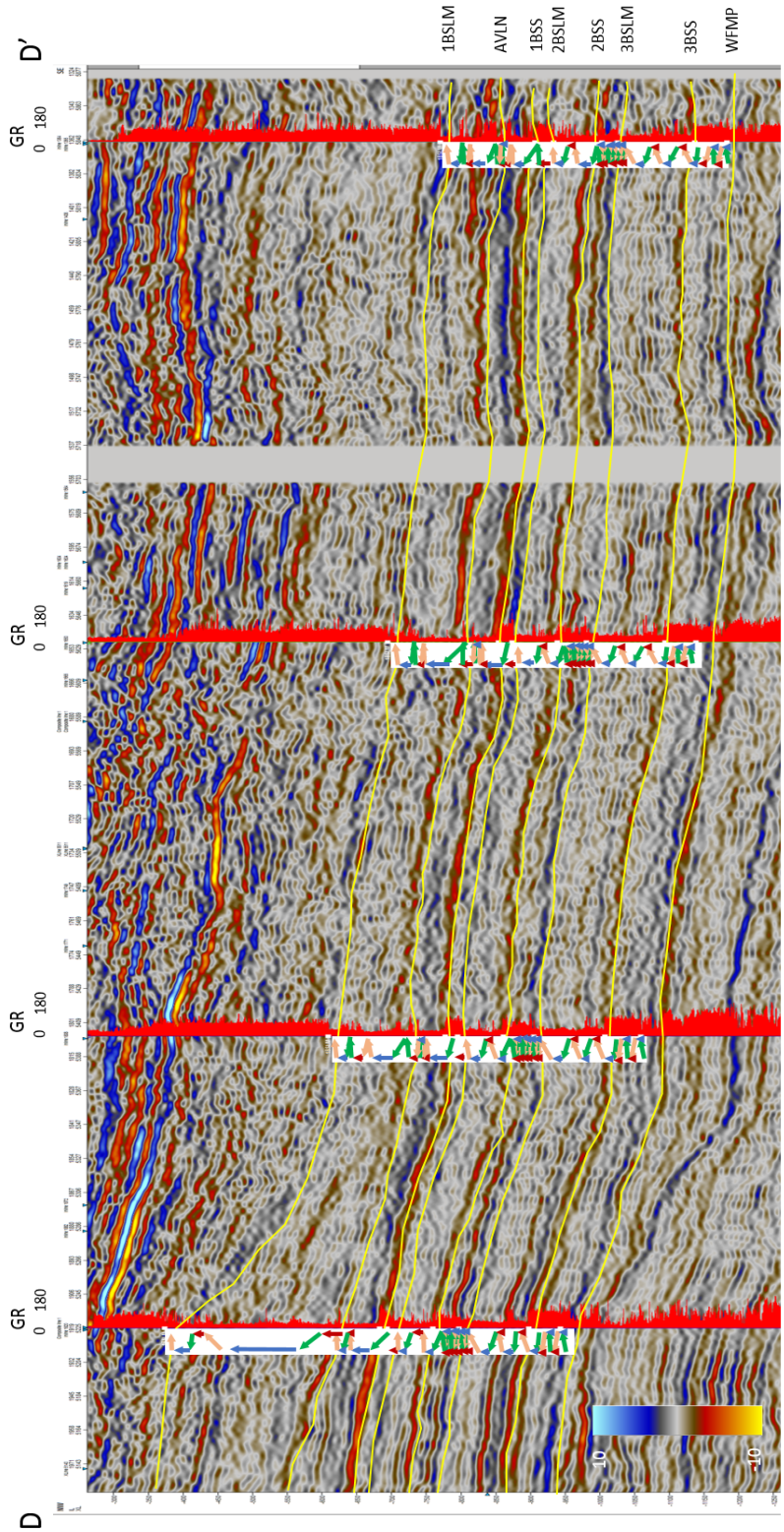

Figure 61: Arbitrary line D – D'. Yellow lines represent the picked horizons within the bone spring interval. Overlain arrows are the adapted Galloway motifs determined from well logs. Red logs are GR logs.

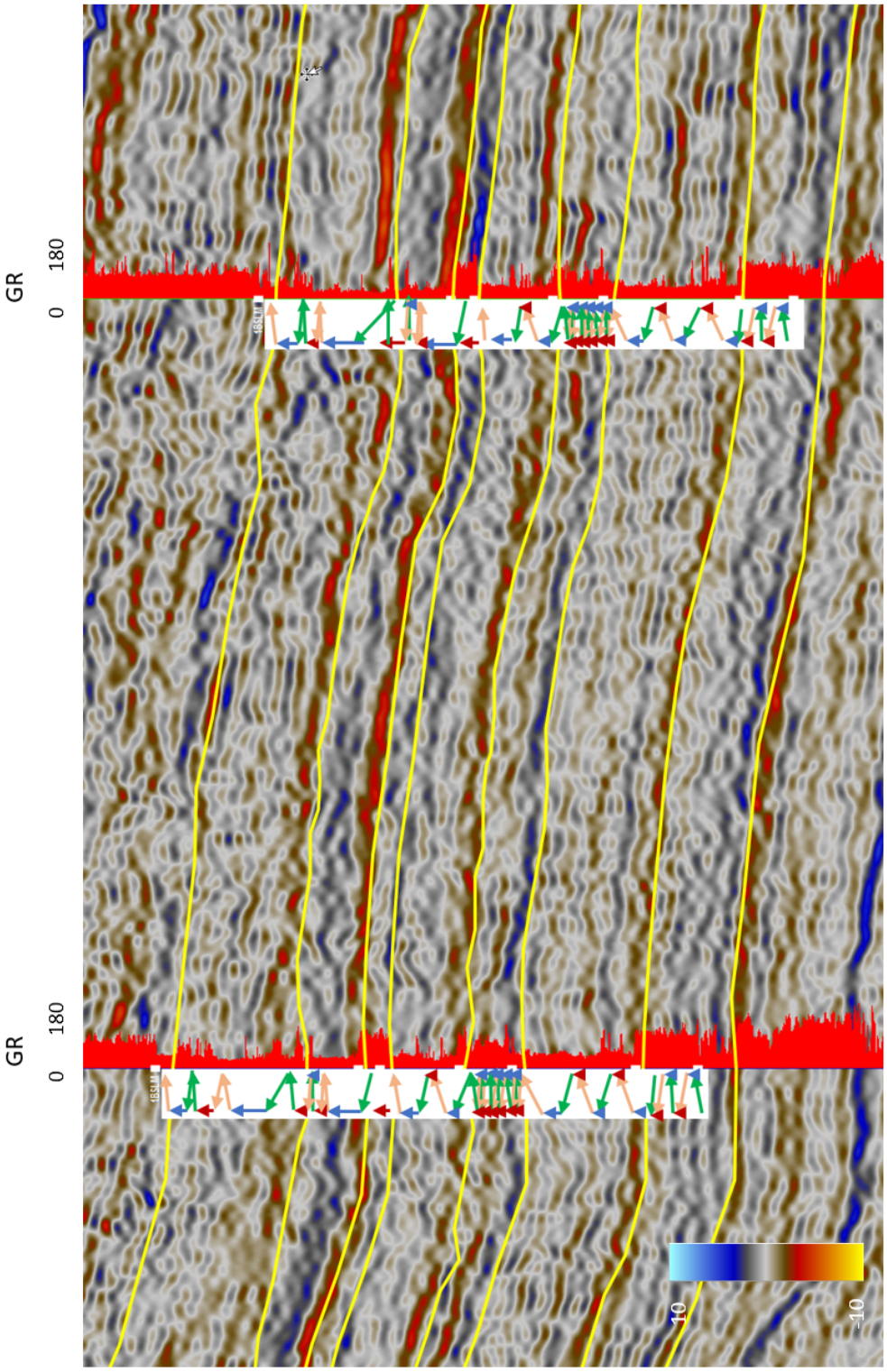

Figure 62: Zoomed in version of middle two wells in Figure 61 to give a more detailed view of the overlain adapted Galloway motifs.

Figures 61 and 62 above illustrate an attempt to overly adapted Galloway sequence stratigraphic motifs with the seismic. Yellow lines on the seismic represent the major internal Bone Spring horizons picked across the survey. The overlay was created manually by matching up the adapted Galloway motifs that were determined earlier from well logs with the synthetically tied wells shown on the seismic. The red logs shown here are gamma ray logs allowing an accurate translation of these motifs to the seismic. Overall, these overlain motifs allow for a more accurate interpretation of the internal reflectors within the Bone Spring intervals. While these reflectors generally look fairly chaotic due to the mass transport style of deposition, the overlain Galloway motifs help to act as a guide to give meaning to some of these reflectors.

Many of these 4th order parasequences can be seen much more clearly using these overlain Galloway motifs. Immediately obvious is the thick 4th order highstand carbonate parasequences of the 1st Bone Spring Lime. The carbonate thins rapidly into the basin and these motifs can help guide where that interpretation should occur. Additionally, maximum flooding surfaces within the sands generally tie with the same reflectors from well to well. While these reflectors represent a package of sediment, it can be useful to map these reflectors out for well planning purposes to see where one might expect to encounter these beds between well logs. The same mapping can be carried out for the carbonate beds within the 2nd Bone Spring as is shown below.

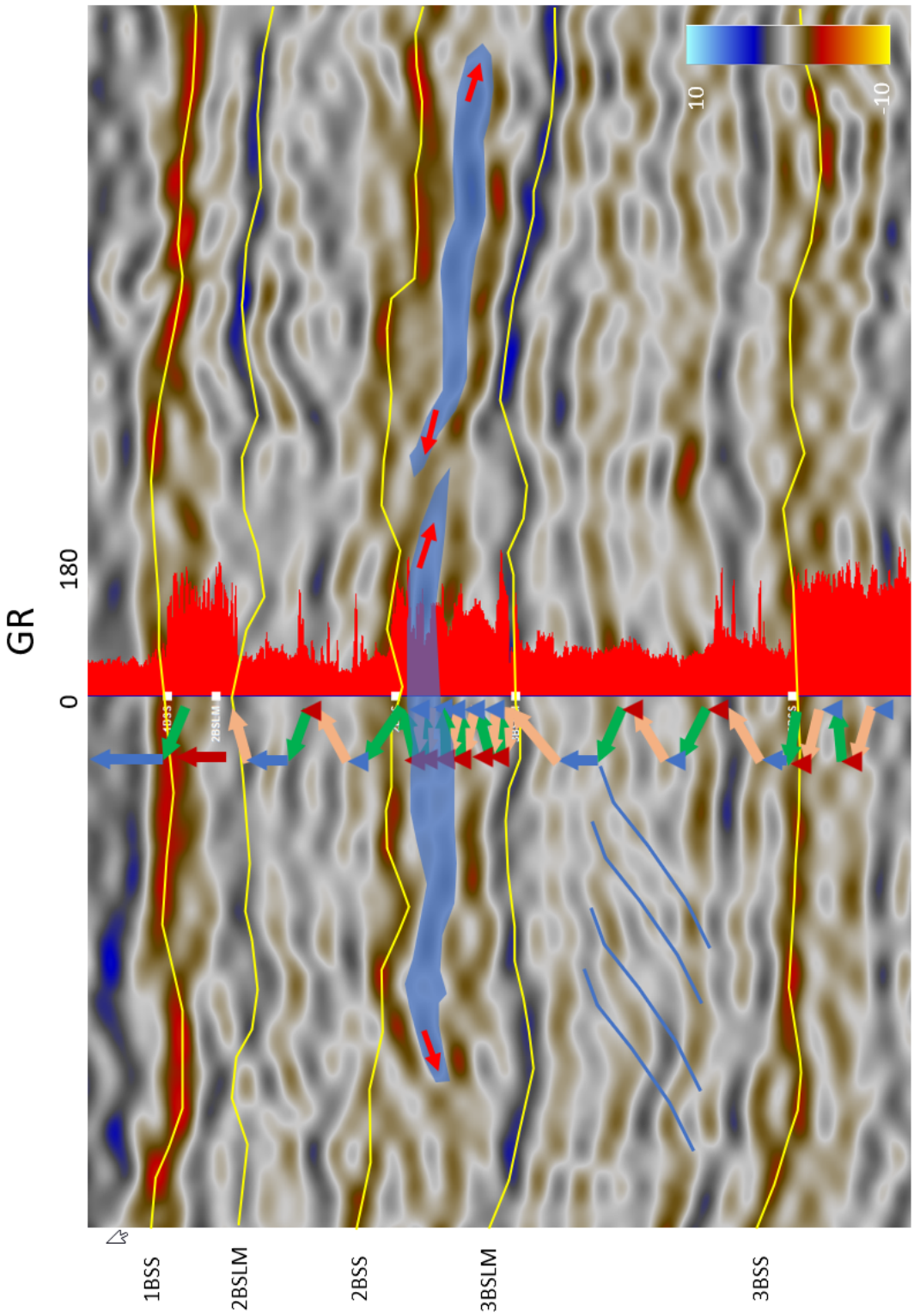

Figure 63: Zoomed in version of Figure 62 focused on one well over the 1BSS – 3BSS interval. Blue packages are interpreted as carbonate fan deposits within the 2nd Bone Spring Sand. Blue lines are interpreted as toe thrusts within the 3rd Bone Spring Lime due to the creep of carbonate muds down the slope.

Figure 63 above shows a zoomed in version of figure 62 focused on one well over the 1st Bone Spring Sand down to the top of the 3rd Bone Spring Sand. When looking in detail at the 2nd Bone Spring Sand, it is observed that the thickest 4th order lowstand deposit, earlier interpreted as a carbonate rich flow within the 2nd Bone Spring Sand, correlates with a blue peak reflector as would be expected. The increased carbonate content within the bed should cause a positive impedance change and create a blue positive reflection on the seismic. Tracing this reflector laterally shows that the reflector terminates laterally in both directions. The reflector is then interpreted as a carbonate rich flow or amalgamation of flows that was deposited within the 2nd Bone Spring. Moving away from the wellbore, there is another blue reflector that terminates in both directions and seems to stack laterally to the first fan. This reflector is interpreted as an additional carbonate flow deposit that is compensationally stacked on the previous fan. Blue lines within the 3rd Bone Spring Carbonate represent likely toe thrusts due to the creep of carbonate muds down the slope. These thrusts have been observed by the author in Bone Spring outcrops in and around the Guadalupe Mountains. Being able to interpret these features on seismic also helps with well planning and serves as a reminder of the complex nature of Bone Spring deposition.

Using this method of comparing 4th order sequences to the seismic, interpretations can be made about internal Bone Spring reflectors both within synthetic well control and expanded out to the surrounding areas. More work could be done and is currently being done to map out more of these internal characteristics of the Bone Spring using this sequence stratigraphic model as a guide. Attribute and inversion work is also being done in order to more clearly delineate these features and tie them to the seismic stratigraphic model and 4th order adapted Galloway motifs.

Overall, the seismic analysis done in this study was able to refine the depositional model of the Bone Spring largely because the horizontal resolution of the seismic is better than could ever be achieved using well logs alone. The structure and isochron maps created shed more light on the depositional processes occurring during Bone Spring deposition and the location of sediment sources around the study area. In addition, seismic stratigraphic analysis helped to confirm the 3rd order sequence boundaries observed within the Bone Spring. Additionally, comparison of the seismic data to 4th order adapted Galloway motifs allows for more detailed interpretation of depositional features shown on the seismic.

Chapter 7: Conclusions

Conclusions

Using well logs, core data, and seismic data this study has laid out a stratigraphic depositional model of the Bone Spring that incorporates the high vertical resolution of well log and core data and the high horizontal resolution of seismic data. Only by using all of the available data is it possible to create a coherent model of the complex Bone Spring formation. Sequence stratigraphy from well logs allowed for the identification of 3rd and 4th order sequences within the Bone Spring. The 4th order sequences were picked using a lithology corrected adapted Galloway technique that is unique to this study and more accurately maps out sequences within the mixed siliciclastic and carbonate Bone Spring system. Core analysis showed that within the 1st and 2nd Bone Spring sands, facies agreed with their assumed position within 4th order sequences. Finally, seismic analysis confirmed the 3rd order sequences identified from well logs and seismic mapping using time structure maps and isochrons helped to refine the depositional model and identify sediment supply pathways and structural controls on deposition. A combination of the 4th order sequences determined from well logs with the seismic data proves the concept that a combination of these tools allows for a more detailed interpretation of the seismic data and will help with well planning in areas with lower well control. Below is a summary of some of the major findings of this study.

- 3rd order sequences in the study area were mapped using well logs and seismic data and were determined to agree with the industry accepted model that 3rd order highstands correlate with dominantly carbonate deposition and 3rd order lowstands correlate with dominantly siliciclastic deposition.

- More detailed analysis using adapted Galloway motifs determined that 16 4th order sequences can be identified within the Bone Spring interval that help to explain the complex changes observed within 3rd order sequences. Explaining these complex changes will have impacts on well planning and development of the Bone Spring because it helps to identify sequence stratigraphic drivers on facies observed within the Bone Spring. The model leads to more accurate facies prediction and helps to identify the lateral extents of high-quality reservoirs and potential frac barriers.
- Adapted Galloway motifs that account for changes in lithology were successfully used to map out these 4th order sequences and more accurately predict these 4th order sequences than the classic non-lithologically corrected method.
- Core data confirmed the lithologies predicted from well logs and verified that they fit well within the stratigraphic model created.
- Within the 2nd Bone Spring Sand, carbonate rich beds were deposited during falling stage and lowstand parasequences and is interpreted to be because erosion and incision of the carbonate shelf was at a maximum during this time and led to more reworked carbonate being deposited within basin floor fans. Additionally, active carbonate growth would have moved closer to the basin floor also accounting for some of this increase in carbonate deposition.
- Overlying the interpreted 4th order sequences with the seismic data helps to better interpret the internal complexities observed within the Bone Spring intervals. For example, carbonate fans within the Bone Spring can be mapped out leading to better well planning in order to avoid these lower quality reservoirs.

- Seismic time structure and isochron maps have much higher horizontal resolution than the isopach maps used in this study and previous studies. The higher horizontal resolution allowed for more accurate mapping of incised submarine valleys within the study area that acted as sediment transport mechanisms throughout deposition of the Bone Spring. Individual flows or amalgamations of flows can also be observed proving that compensational stacking had a major impact on Bone Spring deposition.

Overall, this investigation provides a sequence stratigraphic depositional model of the Bone Spring with immediate impacts on development of the study area and conceptual impacts for mapping out other development areas within the Bone Spring. The depositional model created within this study can help operators to better plan development of the Bone Spring interval and will serve as a launching point for further study of the Bone Spring.

Recommendations for Future Work

Even with all of the work still ongoing in this study area, the shear amount of data provided for this study lends itself to even more studies. Some recommendations are:

- Stratigraphic analysis could be done for each individual Bone Spring formation. This study looked more in depth at the 2nd Bone Spring Sand but a similar study could be done for each interval within the Bone Spring.
- Seismic facies analysis and inversion can be done in order to better utilize the seismic data and map out individual flows.
- An in depth look at the stratigraphy of the 1st Bone Spring Lime and the transition into the Guadalupian sands would be a fascinating study given the complex stratigraphy observed on seismic in that shallow portion of the study.
- Although not developed in the study area, the Wolfcamp is a major producer in the Delaware Basin. This dataset contains high quality seismic data of the more proximal facies of the Wolfcamp. An in-depth study of the Wolfcamp could help to define the depositional controls of the Wolfcamp and have far reaching impacts on oil and gas production from this prolific interval.

References

Adams, J.E., 1965, Stratigraphic-Tectonic Development of Delaware Basin: Bulletin of the American Association of Petroleum Geologists, v. 49.11, p. 2140-2148.

Bachmann, Joseph, Philip Stuart, Brian Corales, Blake Fernandez, Peter Kissel, Holly Stewart, David Amoss, Blaise Angelico, Alonso Guerra-Garcia, K. Blake Hancock, Richard Roberts, and Bill Sanchez, 2014, The "New" Horizontal Permian Basin. < *https://docplayer.net/15628065-The-new-horizontal-permian-basin.html*> Accessed June 21, 2019

Brown, A. R., 2011, Interpretation of Three-Dimensional Seismic Data Seventh Edition: AAPG Memoir 42, p. 48

Catuneanu, O., W.E. Galloway, C.G.St.C Kendall, A.D. Miall, H.W. Posamentier, A. Strasser, and M.E. Tucker, 2011, Sequence Stratigraphy: Methodology and Nomenclature: Newletters on Stratigraphy, v. 44/3, p. 173-245.

Catuneanu, O., V. Abreu, J.P. Bhattacharya, M.D. Blum, R.W. Dalrymple, P.G. Eriksson, C.R. Fielding, W.L. Fisher, W.E. Galloway, M.R. Gibling, K.A. Giles, J.M. Holbrook, R. Jordan, C.G.St.C. Kendall, B. Macurda, O.J. Martinsen, A.D. Miall, J.E. Neal, D. Nummedal, L. Pomar, H.W. Posamentier, B.R. Pratt, J.F. Sarg, K.W. Shanley, R.J. Steel, A. Strasser, M.E. Tucker, and C. Winker, 2009, Towards the Standardization of Sequence Stratigraphy: Earth-Science Reviews, v. 92.1-2, p. 1-33.

Crosby, C. B., 2015, Depositional History and High Resolution Sequence Stratigraphy of the Leonardian Bone Spring Formation, Northern Delaware Basin, Eddy and Lea Counties, New Mexico. University of Oklahoma Master's Thesis

Crosby, Charles B., John D. Pigott, and Kulwadee L. Pigott, 2017, Bone Spring Formation High Resolution Sequence Stratigraphy, Northern Delaware Basin, Eddy and Lea Counties, New Mexico, AAPG Annual Convention & Exhibition, Houston, TX.

EIA, 2017, U.S. Crude Oil and Natural Gas Proved Reserves, 2017: <*http://www.eia.gov/naturalgas/crudeoilreserves/?src=home-b1*> Accessed June, 2019.

Galloway, W., E., 1989, Genetic stratigraphic sequences in basin analysis; 1, Architecture and genesis of flooding-surface bounded depositional units, AAPG bulletin, 73,125-142.

Haq, B. U., and S. R. Schutter, 2008, A Chronology of Paleozoic Sea-Level Changes: Science, v. 322, p. 64-68

Hardage, B. A., J. L. Simmons, V. M. Pendleton, B. A. Stubbs, and B. J. Uszynski, 1998, 3-D Seismic Imaging and Interpretation of Brushy Canyon Slope and Basin Thin-bed Teservoirs: Geophysics, v. 63.5, p. 1507.

Hart, B.S., 1997, New Targets in the Bone Spring Formation, Permian Basin: Oil & Gas Journal, p. 85-88.

Henderson, C. M., V. I. Davydov, B. R. Wardlaw, and O. M. Hammer, 2012, Chapter 24: The Permian Period, in F.M. Gradstein, ed., The Geologic Time Scale 2012: 1st ed. Oxford: Elsevier, 2012. P. 654-677

Hill, C.A., 1996, Geology of the Delaware Basin, Guadalupe, Apache, and Glass Mountains, New Mexico and West Texas: Society for Sedimentary Geology, Albuquerque, New Mexico, v. 96-39.

Hills, J.M., 1984, Sedimentation, Tectonism, and Hydrocarbon Generation in Delaware Basin, West Texas and Southeastern New Mexico: AAPG Bulletin, v. 68.3, p. 250-267.

Keller, G.R., J.M. Hills, and R. Djeddi, 1980, A Regional Geological and Geophysical Study of the Delaware Basin, New Mexico and West Texas: New Mexico Geological Society Guidebook, p. 105-111.

Kocurek, G. and B.L. Kirkland, 1998, Getting to the Source: Aaeolian Influx to the Permian Delaware Basin Region: Sedimentary Geology, v. 117.3-4, p. 143-149.

Li, Shunli, 2015, The role of sea level change in deep water deposition along a carbonate shelf margin, Early and Middle Permian, Delaware Basin: Geologica Carpathica, p. 99-116.

May, Jeff, 2018, Well Log Sequence Stratigraphy: Applications to Exploration and Production. 2018. Unpublished Nautilus Lecture Notes

Mazzullo, S.J., 1995, Permian Stratigraphy and Facies, Permian Basin (Texas-New Mexico) and Adjoining Areas in the Midcontinent United States *in* P.A. Scholle, T.M. Peryt, and D.S. Ulmer-Scholle, eds., The Permian of Northern Pangea, Berlin: Springer-Verlag, v. 2, p. 41 58.

Mccullough, B.J., 2014, Sequence-Stratigraphic Framework and Characterization of the Woodford Shale on the Southern Cherokee Platform of Central Oklahoma: Master's thesis, University of Oklahoma, Norman, Oklahoma, 210 p.

Montgomery, S.L., 1998, The Permian Bone Spring Formation, Delaware Basin: Petroleum Frontiers, v. 14.3, p. 1-89.

Mullins, H.T., and H.E. Cook, 1986, Carbonate Apron Models: Alternatives to the Submarine Fan Model for Paleoenvironmental Analysis and Hydrocarbon Exploration: Sedimentary Geology, v. 48.1-2, p. 37-79.

Pigott, J.D., 2016, GPHY 5613: Introduction to Seismic Stratigraphy. Fall 2016. Unpublished Lecture Notes.

Pigott, J.D., 2015, GEOL 5363: Carbonate Geology. Fall 2015. Unpublished Lecture Notes.

Pigott, John D., Esra Yalcin, Kulwadee L. Pigott, and Michael Williams, 2015, 3D Delaware basin model: Insight into its heterogeneous petroleum system evolution as a guide to new exploration, West Texas Geological Society Convention, Midland, Tx.

Shumaker, R.C., 1992, Paleozoic Structure of the Central Basin Uplift and Adjacent Delaware Basin, West Texas: AAPG Bulletin, v. 76.11, p. 1804-1824.

ShaleExperts, 2019, Permian Basin: <https://www.shaleexperts.com/plays/permian-basin/Overview?menu> Accessed June 21, 2019

Slatt, R.M., 2013 GEOL 5970: Reservoir Characterization I. Fall 2016. Unpublished Lecture Notes.

Slatt, R. M., 2006, Stratigraphic Reservoir Characterization for Petroleum Geologists, Geophysicists, and Engineers, v. 10, Elsevier.

Sloss, L.L., 1963, Sequences in the Cratonic Interior of North America: Geological Society of America Bulletin, v. 74.2, p. 93-113.

Sloss, L.L., 1988, Chapter 3: Tectonic Evolution of the Craton in Phaerozoic Time, in L.L. Sloss, ed., Sedimentary Cover – North American Craton: U.S.: The Geology of North America: The Geological Society of America, p. 25-41.

Ross, C.A. and J.R.P. Ross, 1995, Permian Sequence Stratigraphy in P.A. Scholle, T.M. Peryt, and D.S. Ulmer-Scholle, eds., The Permian of Northern Pangea: Berlin: Springer-Verlag, v. 1, p. 98-113.

Ruppel, Stephen C., and W. Bruce Ward, 2013, Outcrop-based Characterization of the Leonardian Carbonate Platform in West Texas: Implications for Sequence-stratigraphic Styles in the Lower Permian: AAPG Bulletin, v. 97.2, p. 223-250.

Saller, A.H., J.W. Barton, and R.E. Barton, 1989, Slope Sedimentation Associated with a Vertically Building Shelf, Bone Spring Formation, Mescalero Escarpe Field, Southeastern New Mexico: SEPM Special Publication, v. 44, p. 275-288.

Silver, B.A. and R.G. Todd, 1969, Permian Cyclic Strata, Northern Midland and Delaware Basins, West Texas and Southeastern New Mexico: AAPG Bulletin, v. 53.11, p. 2223-2251.

USGS, 2018, USGS Announces Larges Continuous Oil Assessment in Texas and New Mexico: <https://www.usgs.gov/news/usgs-announces-largest-continuous-oil-assessment-texas-and-new-mexico> Accessed June 21, 2019.

Vail, P. R., 1987, Seismic Stratigraphy Interpretation Using Sequence Stratigraphy: AAPG Studies in Geology 27, volume 1:Atlas of Seismic Stratigraphy.

Veevers, J. J., and C.M. Powell, 1987, Late Paleozoic Glacial Episodes in Gondwanaland Reflected in Transgressive-regressive Depositional Sequences in Euramerica: Geological Society of America Bulletin, v. 98.4, p. 475-487.

Williams, Michael T., John D. Pigott, and Kulwadee L. Pigott, 2014, Delaware Basin Evolution: Preliminary Integrated 1D,2D, And 3D Basin Model for Petroleum System Analysis, 2014, AAPG Annual Convention & Exhibition, Houston, Tx.

Yang, K.M. and S.L. Dorobek, 1995, The Permian Basin of West Texas and New Mexico: Tectonic History of a "Composite" Foreland Basin and Its Effects on Stratigraphic Development: SEPM Special Publication, v. 52, p. 149-174

Zhou, Y., 2014, High Resolution Spectral Gamma Ray Sequence Stratigraphy of Shelf Edge to Basin Floor Upper Capitan Permian Carbonates, Guadalupe Mountains, Texas and Delaware Basin, New Mexico: Master's thesis, University of Oklahoma, Norman, Oklahoma, 131 p.